Report No. MCR-74-88
NAS9-13570
DRL T-914, Item 2
DRD MA-378T

DISSIMILAR METALS JOINT EVALUATION

FINAL REPORT

APRIL, 1974

MICHAEL E. WAKEFIELD
LESLIE E. APODACA

PREPARED BY

PROPULSION ENGINEERING, RESEARCH & DEVELOPMENT
MARTIN MARIETTA CORPORATION
P.O. BOX 179, DENVER, COLORADO 80201

ABSTRACT

Dissimilar metals tubular joints between 2219-T851 aluminum alloy and 304L stainless steel were fabricated and tested to evaluate bonding processes. Joints were fabricated by four processes: inertia (friction) welding, where the metals are spun and forced together to create the weld; explosive welding, where the metals are impacted together at high velocity; co-extrusion, where the metals are extruded in contact at high temperature to promote diffusion; and swaging, where residual stresses in the metals after a stretching operation maintain forced contact in mutual shear areas. Fifteen joints of each type were prepared and evaluated in a 6.35 cm (2.50 in.) O.D. size, with 0.32 cm (0.13 in.) wall thickness, and 7.6 cm (3.0 in.) total length .

The joints were tested to evaluate their ability to withstand pressure cycle, thermal cycle, galvanic corrosion and burst tests. Leakage tests and other non-destructive test techniques were used to evaluate the behavior of the joints, and the microstructure of the bond areas was analyzed.

Joints were successfully produced by each of the four processes. The general resistance of each type to the test series was good to excellent, although most of the coextruded joints were not available in time for submittal to the complete test program.

The feasibility of manufacturing joints up to 43 cm (17 in.) diameter by these techniques is evaluated, and estimated costs are included.

LIST OF ILLUSTRATIONS

		Page
1.	Joint Configuration - Inertia Welded, Explosive Welded, Coextrusion Bonded	6-1
2.	Joint Configuration - Swaged Construction	6-2
3.	Coextrusion Process	7-1
4.	Inertia Welded Parts Arrangement	8-2
5.	Inertia Welding 2219 to 6061 Aluminum During Development	8-3
6.	Inertia Welded Tensile Specimens 2219 to 6061	8-4
7.	Inertia Welding 2219 to 6061 Aluminum for Preliminary Joints	8-4
8.	Refacing of 6061 After Inertia Welding	8-5
9.	Inertia Welding 2219 to 6061 Aluminum for Production	8-6
10.	Inertia Welding 304L Stainless to 2219/6061 Aluminum for Production Joints	8-7
11.	Final Machining of Inertia Welded Joint	8-7
12.	Section of Explosive Welded 304L Stainless Steel to 2219-T851 Aluminum	9-1
13.	Explosive Bond Joint Method #1 Setup	9-2
14.	Explosive Bond Joint Method #2 Stainless to Silver/ Aluminum	9-3
15.	Explosive Bond Joint Method #3 Silver/Aluminum to Stainless	9-4
16.	Explosive Bond Joint Production Silver to Aluminum	9-5
17.	Explosive Bonding Parts	9-6
18.	Setup for Explosive Bond Joint Production Stainless to Silver/Aluminum	9-7
19.	Explosive Bonded Joint Following Detonation	9-7
20.	Configuration of Commercial Swaged Joint	10-1
21.	Ferrule Installation Tool	10-1
22.	Initial Concept for Welded End Fittings	11-4
23.	Concept for Aluminum End Fitting Weld Using Tubular Cap	11-5
24.	Coextruded Joint	11-9

LIST OF ILLUSTRATIONS
(Continued)

		Page
25.	Explosive Welded Joint	11-9
26.	Inertia Welded Joint	11-10
27.	Swaged Construction Joint	11-10
28.	Yield Determination Test Vessel	11-11
29.	Yield Determination and Burst Test Results	11-12
30.	Operating Pressure Leakage Test Setup	11-15
31.	Thermal Cycle Test Fixture	11-16
32.	Pressure Cycle Test Fixture	11-17
33.	Typical Joints Being Subjected to Pressure Cycle	11-18
34.	Fatigue Failure of Inertia Welded Joint	11-19
35.	Fatigue Failure of Swaged Joint	11-20
36.	Section of Swaged Construction Joint	11-20
37.	Corrosion Test Fixture	11-22
38.	Inertia Welded Joint After Corrosion and Burst Test - View of Stainless Surface at Interface	11-22
39.	Inertia Welded Joint After Corrosion and Burst Test - View of Aluminum Joint Half O.D. at 2219/6061 Interface	11-23
40.	Explosive Welded Joint Burst Failure	11-25
41.	Explosive Welded Joint Burst Failure After Separation	11-26
42.	Hoop Mode Failure of Explosive Welded Joint	11-26
43.	Inertia Welded Joint Burst Failure	11-27
44.	Swaged Construction Joint Burst Failure	11-27
45.	Singular Occurrence of Axial Shear Failure of Swaged Construction Joint	11-28
46.	Coextruded Joint Burst Failure	11-28
47.	One-Atmosphere Helium Leakage Test	11-31
48.	Ultrasonic Test Setup	11-32
49.	EDM Flaw Depth - Ultrasonic Reference Joints	11-33

LIST OF ILLUSTRATIONS
(Continued)

		Page
50.	Ultrasonic Inspection Readout of Inertia Welded Reference Joint	11-36
51.	Ultrasonic Inspection Readout of Inertia Welded Joint 9	11-36
52.	Ultrasonic Inspection Readout of Inertia Welded Joint 10	11-37
53.	Ultrasonic Inspection Readout of Inertia Welded Reference Joint (At Reduced Sensitivity)	11-37
54.	Ultrasonic Inspection Readout of Inertia Welded Joint 9 (At Reduced Sensitivity)	11-38
55.	Ultrasonic Inspection Readout of Inertia Welded Joint 10 (At Reduced Sensitivity)	11-38
56.	Ultrasonic Inspection Readout of Inertia Welded Reference Joint (Adjusted Post-Pressure Cycle)	11-39
57.	Ultrasonic Inspection Readout of Inertia Welded Joint 9 (Post-Pressure Cycle)	11-39
58.	Ultrasonic Inspection Readout of Inertia Welded Joint 10 (Post-Pressure Cycle)	11-40
59.	Ultrasonic Inspection Readout of Explosive Welded Reference Joint (Low Sensitivity)	11-40
60.	Ultrasonic Inspection Readout of Explosive Welded Reference Joint (High Sensitivity)	11-41
61.	Ultrasonic Inspection Readout of Explosive Welded Joint 5, Pre-Thermal Cycle (Low Sensitivity)	11-41
62.	Ultrasonic Inspection Readout of Explosive Welded Joint 5, Pre-Thermal Cycle (High Sensitivity)	11-42
63.	Ultrasonic Inspection Readout of Explosive Welded Joint 5, (Post-Thermal Cycle)	11-42
64.	Micrograph of Typical 304L Stainless Steel/6061 Aluminum Inertia Weld	12-2
65.	Micrograph of Typical 6061 Aluminum/2219 Aluminum Inertia Weld	12-2
66.	Micrograph of Typical Explosive Bond Between 304L Stainless Steel and 2219 Aluminum, Using Silver Intermediate Material	12-3

LIST OF ILLUSTRATIONS
(Continued)

		Page
67.	Micrograph of Typical Single Wave Pattern of Stainless Steel Explosively Bonded to Silver	12-4
68.	Micrograph of Typical Wave Pattern of Silver Explosively Bonded to Aluminum	12-5
69.	Micrograph of Silver/Aluminum Explosive Bond Showing Voids and Inclusions	12-6
70.	Electron Microprobe Scan of 6061/2219 Inertia Weld . . .	12-8
71.	Electron Microprobe Scan of 6061/2219 Inertia Weld . . .	12-8
72.	Electron Microprobe Scan of 304L/6061 Inertia Weld . . .	12-8
73.	Electron Microprobe Scan of 304L/6061 Inertia Weld . . .	12-8
74.	Electron Microprobe Scan of 6061/Ag Explosive Bond . . .	12-9
75.	Electron Microprobe Scan of 304L/Ag Explosive Bond . . .	12-9
76.	Electron Microprobe Scan of 304L/Ag Explosive Bond . . .	12-9
77.	Baseline Joint Configuration - Large Joint Evaluation .	13-1
78.	Large Explosive Joint Mandrel	13-5
79.	Large Explosive Joint Silver Bond Concept	13-5
80.	Large Explosive Joint Stainless Bond Concept	13-6

LIST OF TABLES

		Page
1.	Comparative Weights of Selected Joints	5-2
2.	Tensile Data, Inertia Welded 2219 to 6061 Aluminum . . .	8-3
3.	Preliminary Inertia Welded Joints 6061 Dimensions	8-5
4.	Test Matrix for Inertia Welded, Coextruded and Explosive Welded Joints	11-2
5.	Test Matrix for Swaged Joints	11-3
6.	Receiving Inspection Results	11-6
7.	Operating Pressure Leakage Test Results	11-14
8.	Thermal Cycle Test	11-16
9.	Pressure Cycle Test Results	11-16
10.	Burst Test Results	11-24
11.	Dye Penetrant Test Results	11-30
12.	One Atmosphere Helium Leakage Test Results	11-31
13.	Joint Type Suitability	14-1

DEFINITIONS

The definition of frequently used words or abbreviations, as used in this report, follows:

Joint	A test specimen prepared under this program, consisting of a 6.35 cm (2.50 in.) diameter tubular section 7.6 cm (3.0 in.) long, with one end of 2219-T851 aluminum and the other of 304L stainless steel.
Dissimilar Metals	Metals which exhibit significant difference in physical and/or metallurgical properties. For this report, 2219 aluminum is considered dissimilar to 304L stainless steel.
NDT	Non-destructive test
MSLD	Mass Spectrometer Leak Detector
O.D.	Outside Diameter
I.D.	Inside Diameter

SUMMARY

Dissimilar metals tubular joints between 2219-T851 aluminum alloy and 304L stainless steel were fabricated and tested to evaluate bonding processes. Joints were fabricated by four processes: inertia (friction) welding, where the materials were spun and forced together to create the weld; explosive welding, where the materials were impacted together at high velocity; coextrusion, where the materials were extruded in contact at high temperature to promote diffusion; and, swaging, where residual stresses after a stretching operation maintained forced contact in mutual shear areas. Fifteen joints of each type were fabricated in a common configuration, and were subjected to a series of environmental and structural tests. The joints were 6.35 cm (2.50 in.) in diameter with a 0.32 cm (0.13 in.) wall thickness, and were approximately 7.6 cm (3.0 in.) long. A thicker welding boss was provided at the aluminum end of each joint to allow for strength degradation during welding. The theoretical yield pressure of the joints based on the yield strength of the stainless steel portion of the joint in hoop stress was 2590 N/cm^2 (3750 psig). The theoretical ultimate pressure of the joints based on the ultimate strength of the aluminum portion of the joint in hoop stress was 4200 N/cm^2 (6100 psig).

The joints were subjected to a series of tests. First, a determination of the yield pressure and burst pressure of each joint type was made by monitoring the volume growth vs internal pressure during a hydrostatic burst test. This allowed the proof and operating pressure level of each joint type to be established so that subsequent test levels could be determined. All joints responded similarly, so a common proof pressure of 2200 N/cm^2 (3200 psig) was established. This allowed an operating and leak test pressure of 1450 N/cm^2 (2100 psig) to be used. Thermal cycling from 78K (-320°F) to 375K (+212°F) was performed, followed by burst tests. Pressure cycling from 430 N/cm^2 (620 psig) to 2140 N/cm^2 (3100 psig) was performed to determine fatigue life. Galvanic corrosion resistance was evaluated by exposure to a $NaCl/H_2O$ electrolyte solution, followed by burst tests. Other burst tests were performed on joints not exposed to adverse environments, and an evaluation of adaptability of the joints to NDT was made by subjecting them to NDT before and after the other environments.

An evaluation of the feasibility and costs of adapting the various joint types to 20 cm (8 in.), 30 cm (12 in.) and 43 cm (17 in.) diameters was made. The manufacturing techniques are described, and special tooling requirements are identified. An evaluation of the suitability of each joint type for use in the larger sizes is presented, based on manufacturing, test, and service criteria.

RESULTS

The purpose of this program was to develop the production technique for 6.35 cm (2.50 in.) diameter bimetallic transition joints from 2219-T851 aluminum to 304L stainless steel by four methods, and to compare their relative performance through a series of tests. Also, an evaluation was made of the costs and constraints of applying the production methods to larger joints up to 43 cm (17 in.) diameter.

A total of twenty-one joints were fabricated by inertia welding (friction welding) using a Caterpillar Tractor Co. welder. The joints were manufactured by Interface Welding Company of Carson, California. Attempts were made to weld the 2219 directly to the 304L by exploring all adjustable machine parameters, by using different configurations, and by using both T851 and T351 tempers. This resulted in developing a poor quality bond, so it was elected to provide an intermediate layer of 6061-T6 aluminum, which is more readily weldable to each of the other materials. The production process which evolved welded the 6061-T6 to 2219-T851, then welded the refaced 6061 to 304L. The completed joint was artifically aged to recover 6061-T6 aluminum properties in the thin intermediate layer.

A total of eighteen joints were fabricated by explosive welding. They were manufactured by Martin Marietta Corporation, Denver Division. The configuration chosen featured a scarf angle at the interface in order to provide more bond area to dissipate stresses. The joints used an intermediate layer of sterling silver bonded to the T851 condition aluminum, with the 304L stainless steel then bonded to the silver. No ageing or stress relieving operations were performed during assembly of these joints.

Fifteen joints were fabricated by coextrusion bonding. To fabricate a joint, the 2219 aluminum was placed in intimate contact with the 304L stainless steel within an extrusion billet. After heating, the billet was extruded to promote the diffusion between the aluminum and stainless steel. After preliminary machining, the joint was solutionized and quenched, subjected to 1 to 3% cold deformation, and artificially aged to bring the aluminum to T851 condition.

Fifteen joints were prepared by swaged construction. They were manufactured by Metal Bellows Corporation of Chatsworth, California. The joint was formed by mechanically swaging a cylindrical section of 304L stainless steel within a serrated 2219 aluminum collar. The sharp edges of the serrations were held in intimate contact with the opposing piece due to the high residual stresses following swaging (tensile in the aluminum and compressive in the stainless).

Tests were performed to compare the structural integrity and leakage resistance of the four joint types. Tests consisted of proof, leakage, NDT, thermal cycle, pressure cycle, galvanic corrosion, burst, and metallographic inspection.

The overall results of the test program were excellent. Each joint type (in at least one phase of testing) exhibited an advantage over the other joint types, when all test results were compared. Thus, one fabrication technique could prove to be more suitable than the others for a given application. The detailed test results are shown in Tables 6 thru 12. A brief summary of these results follows: All joint types exhibited good mechanical strength. All joint types were essentially leak-free except for the swaged construction and some of the explosive welded joints. All joint types exhibited a yield pressure of from 2100 N/cm^2 (3000 psig) to 2800 N/cm^2 (4000 psig) and a burst pressure of approximately 5000 N/cm^2 (8000 psig). All joint types withstood exposure to thermal cycling without apparent degradation and exhibited reasonable life when subjected to pressure cycling. The inertia welded joints showed the best resistance to pressure cycling (at a stress level equivalent to that produced by proof pressure), surviving to about 170,000 cycles, and failed in the parent aluminum material. The galvanic corrosion test, while harsh (items unprotected while immersed in a $NaCl/H_2O$ bath), indicated that the swaged construction and explosive welded joints exhibited a reasonable resistance to galvanic corrosion. Of all joint types, the inertia welded joints were more severely attacked.

Unfortunately, manufacturing problems forced delivery of most of the co-extruded joints too late for complete evaluation under this test program.

CONCLUSIONS

The following determinations were made with respect to the 6.4 cm (2.5 in.) O.D. joints produced by inertia welding:

1. A weld between 2219-T851 and 304L could not be made without an intermediate material.
2. A layer of 6061-T6 is a suitable intermediate material between 2219-T851 and 304L.
3. The process was found to be consistent and reliable, as critical parameters are controlled by machinery rather than by personnel.
4. The joints exhibited excellent fatigue strength when compared to the parent 2219 aluminum.
5. The joints exhibited poor galvanic corrosion resistance compared to the explosive welded and swaged construction joints, when submerged in a $NaCl/H_2O$ electrolyte.
6. The joints exhibited excellent thermal cycle resistance when cycled between 78K (-320°F) and 375K (+215°F).
7. The joints exhibited excellent leakage resistance.
8. The joints failed axially at the 304L/6061 bond interface when hydroburst, with little apparent ductillity.
9. The 2219/6061 and 6061/304L bonds were found to have metallurgical diffusion.

The following determinations were made with respect to the 6.4 cm (2.5 in.) O.D. joints produced by explosive welding:

1. The process is more subject to inconsistency when compared with inertia welding or swaged construction, as several critical parameters are controlled by workmanship of personnel.
2. A tubular weld between 2219-T851 and 304L can be successfully made on a scarf angle, using a sterling silver intermediate layer.
3. The joints exhibited about 20% of the fatigue strength of the parent 2219 aluminum.
4. The joints exhibited galvanic corrosion resistance between inertia welded and swaged construction joints when submerged in a $NaCl/H_2O$ electrolyte.
5. The joints exhibited good thermal cycle resistance when cycled between 78K (-320°F) and 375K (+215°F).
6. The joints exhibited good leakage resistance when once verified leak free after manufacture.
7. The joints failed in an axial shear mode partly in the 304L/Ag bond, and partly in the aluminum parent metal when hydroburst.

8. The 304L/Ag and Ag/2219 bonds were found to have metallurgical diffusion.

The following determinations were made with respect to the 6.4 cm (2.5 in.) O.D. joints produced by swaged construction:

1. A tubular joint may be made between 2219-T851 and 304L, but additional development is necessary.
2. The joints exhibited about 40% of the fatigue strength of the parent 2219 aluminum.
3. The joints exhibited better galvanic corrosion resistance than inertia welded or explosive welded joints when submerged in a $NaCl/H_2O$ electrolyte. This resistance is due to anodization of the aluminum portion prior to assembly, which is not feasible on the other joint types.
4. The joints exhibited excellent thermal cycle resistance when cycled between 78K (-320°F) and 375K (+215°F).
5. Most of the joints were not leak free. It is felt that the leakage could be remedied thru development.
6. The joints failed in an axial shear mode in the stainless portion, or by the joint pulling slightly apart, but always in a leak-before-burst mode.

The following determinations were made with respect to the 6.4 cm (2.5 in.) O.D. joints produced by coextrusion:

1. A joint between 2219-T851 and 304L, although possible, presents serious problems during fabrication, particularly during the heat treatment portion of the process.
2. The joint tested exhibited excellent thermal cycle resistance when cycled between 78K (-320°F) and 375K (+215°F).
3. The joints tested exhibited excellent leakage resistance.

The following determinations were made with respect to producing larger size 20.3 cm (8.0 in.), 30.5 cm (12.0 in.), and 43.2 cm (17.0 in.), O.D. joints:

1. The least expensive joint to manufacture in larger sizes (once tooling has been purchased) is the swaged construction.
2. Inertia welded, explosive welded, and swaged construction joints appear practical to manufacture in larger sizes. The coextruded joint is not a good candidate for larger sizes in 2219 aluminum alloy if it must be heat treated.
3. The construction method which is potentially lightest weight is inertia welding, due to its butt joint configuration.

RECOMMENDATIONS

1. Define corrosion protection devices for dissimilar metals joints used in applications which afford no inherent protection (as a vacuum jacket might provide), and establish long term corrosive environment demonstrations to evaluate those devices.
2. Perform structural load testing of each joint type, including vibration, shock, bending and torsion.
3. Complete the test program on the coextruded joints which were delivered after the test program described in this report was completed.
4. Reevaluate the material and heat treatment requirements in using dissimilar metals joints for specific applications within vehicles such as Shuttle and Tug.
5. Fabricate additional coextruded joints in the 6.4 cm (2.5 in.) size to a reduced heat treatment criterion, and subject them to a test program.
6. Perform additional development on the swaged construction 6.4 cm (2.5 in.) O.D. size to demonstrate leak elimination.
7. Fabricate and test inertia welded joints in 20.3 cm (8.0 in.) O.D. to demonstrate scaleability prior to committing to larger sizes.
8. Fabricate and test explosive welded joints in 20.3 cm (8.0 in.) O.D. to demonstrate scaleability prior to committing to larger sizes.

INTRODUCTION

The need to connect tubing systems constructed of dissimilar materials for complex propulsion systems exists if we are to realize the advantages of using an optimum material for a specific application. This may be illustrated by the situation of the flexible stainless steel bellows required between an aluminum propellant tank and feedline. The lightweight aluminum is an optimum choice for the tanks and feedline; however, it is not practical to specify aluminum to withstand the cyclic functions required of the bellows. In this case, stainless steel is the optimum bellows material. This combination of materials necessitates that a dissimilar metals joint be provided. This joint must be leak tight and structurally sound when subjected to extremes of mechanical and environmental conditions. Until recently, flanged mechanical joints were used to connect dissimilar metals such as these. These flanges, although adequate, are bulky, heavy and tend to leak.

With the present advances in solid-state welding, it is now possible to gain the advantages of optimum materials applications by directly bonding dissimilar metals. This practice is now operational in small tubing joints and shows promise of being feasible for large tubing joints such as those required for the Space Shuttle and Space Tug vehicles. These solid-state joints provide the benefits of being lightweight, leak free and are adaptable to joining a large variety of metals combinations.

It is, therefore, appropriate to pursue the development of the dissimilar metals tubular joint to the extent necessary to assure large diameter qualifiable hardware. The specific problem of transitions from aluminum to 300 series stainless steel is particularly necessary to solve, as these are primary materials currently used in aerospace applications, yet they are dissimilar in nearly all physical characteristics.

Weight Optimization

Bimetallic transitions become very desirable when weight is a major criterion as illustrated in Table 1. This table compares the weight of a typical bimetallic joint to the low-profile flange developed by Lockheed/NASA/MSFC. Considering the number of joints throughout a system such as that required for Space Tug, where weight is so critical, use of dissimilar metals joints to significantly reduce weight becomes imperative.

Joining Techniques

Dissimilar metals have been joined in a variety of ways (including soldering, brazing, and "welding") using a number of techniques to create a diffusion bond. The development of reliable welded or bonded joints promises to reduce the use of mechanical joints, since the welded bond, when properly controlled, is inherently superior in strength, leakage, and weight characteristics.

TABLE 1. - COMPARATIVE WEIGHTS OF SELECTED JOINTS

Nominal Diameter D cm (in.)	Length Assembled Flange or Bi-metal Joint L cm (in.)	Wall Thickness T cm (in.)	NASA Flange Weight Kg (lb)	Bi-metal Joint Thickness T Weight Kg (lb)	Bi-metal Joint Thickness 0.33 cm (0.13 in.)* Weight Kg (lb)
5.10 (2.00)	6.35 (2.50)	0.10 (0.040)	0.59 (1.30)	0.04 (0.09)	0.13 (0.30)
10.00 (4.00)	6.98 (2.75)	0.10 (0.040)	0.86 (1.90)	0.13 (0.29)	0.43 (0.94)
20.30 (8.00)	9.22 (3.63)	0.11 (0.044)	3.60 (7.90)	0.36 (0.79)	1.10 (2.40)
30.50 (12.00)	11.76 (4.63)	0.12 (0.050)	6.80 (15.00)	0.77 (1.70)	2.10 (4.70)
43.20 (17.00)	15.57 (6.13)	0.12 (0.050)	13.00 (27.00)	1.50 (3.30)	4.10 (9.10)

Note: The weight comparison is made using the same length bimetal joint that is required in the NASA low profile class A flange developed by Lockheed/NASA/MSFC. A butt-joint is assumed on the bimetal joints with the interface at the center of the joint length. The weight comparison assumes stainless steel is to be connected to aluminum. A Naflex cryogenic seal and A-286 steel bolts are assumed in the flange weight.

* Demonstrated thickness in 6.4 cm (2.50 in.) O.D. size.

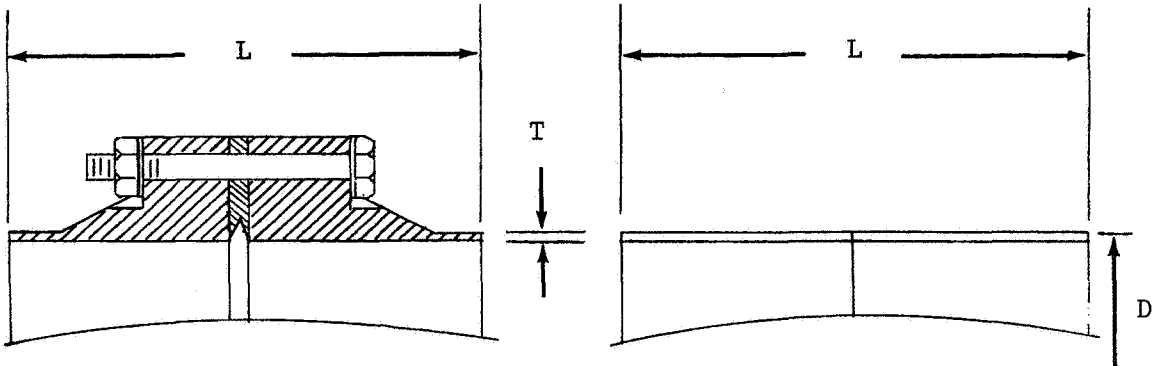

NASA Low Profile Flange

Bimetal Joint

Welding dissimilar metals by forming a diffusion bond between them appears to be the most desirable process; however, much of the effort in this field has been directed toward joining stainless steel to T-6 condition aluminum, usually 6061. All of the techniques described in this report, coextrusion, inertia welding, explosive welding, and swaged construction, have been successfully applied to these materials. When the aluminum to be bonded is 2219 in the T851 condition the application of each of these techniques requires reevaluation and refinement.

SPECIMEN DESIGN

The criteria for joint design were established to assure maximum yield of subsequent test data. First, the joint configuration must force evaluation of the bonded area with minimum influence from end fittings used for test purposes. Second, the design must be adaptable to the test fixturing including multiple specimen test setups. Third, the design must incorporate the parameters required by the selected vendor for his fabrication techniques. Fourth, each joint style must be designed so that a credible comparison may be made between styles during the test evaluation. Fifth, each joint must be designed to exhibit essentially parent metal strength in the bond area. Finally, the joint design must accommodate the requirement for approaching a leak-tight condition under high external vacuum conditions (1.0×10^{-9} torr) as well as under internal operating pressure conditions. The basic design chosen is shown in Figure 1, and was used for the inertia welded, explosive welded and coextrusion bonded joints. A cross-section of the bond plane shows the bond configuration peculiar to each process.

The design used for the swaged joints is shown in Figure 2, and varies somewhat from the others to allow use of existing tooling and to incorporate the swaged joining technique.

The manner in which each construction process was used to manufacture a joint meeting the design requirements is discussed in each fabrication section.

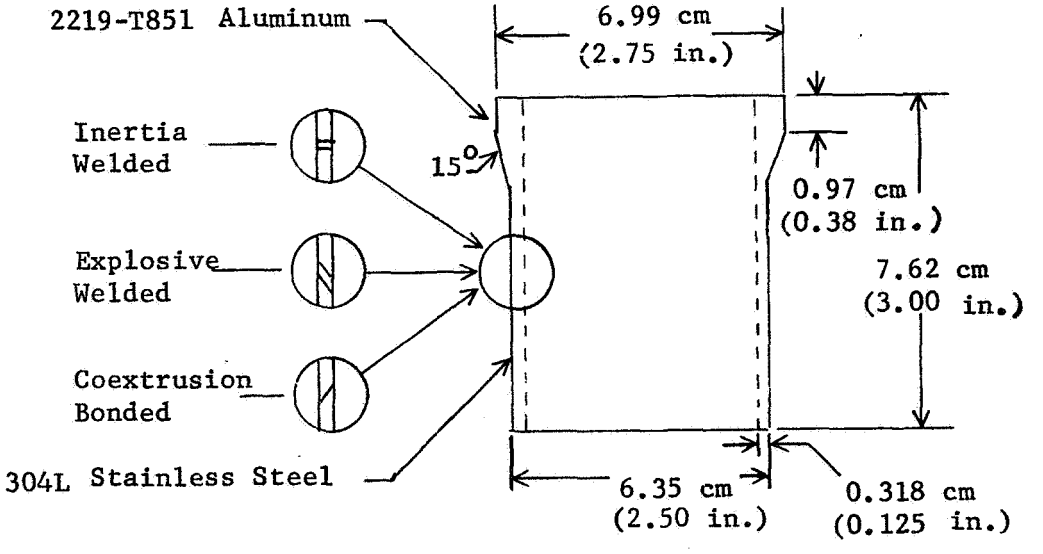

Figure 1.- Joint Configuration - Inertia Welded, Explosive Welded, Coextrusion Bonded

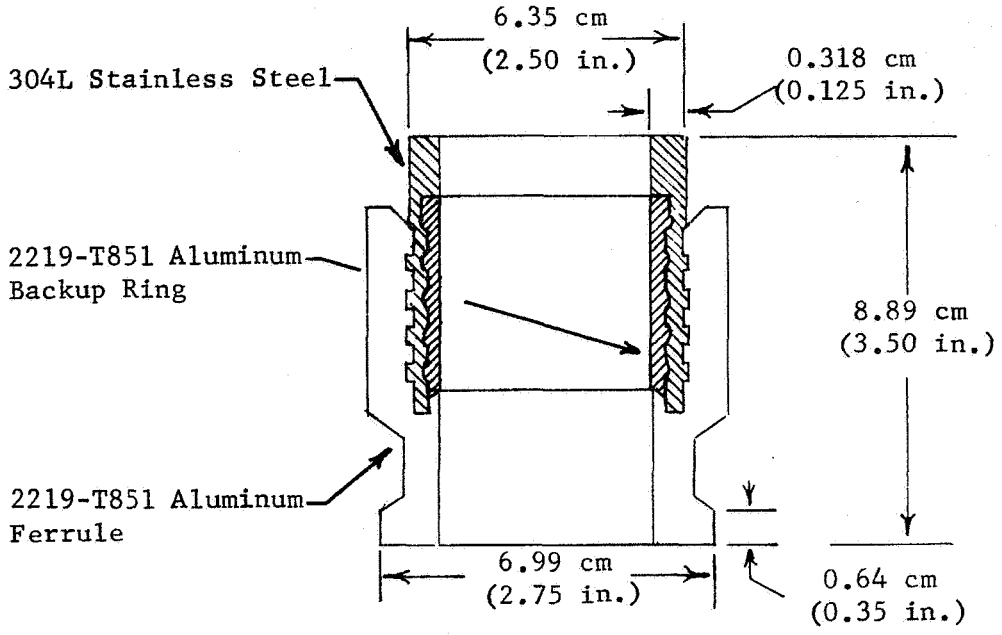

Figure 2.- Joint Configuration - Swaged Construction

COEXTRUSION BONDED JOINT FABRICATION

The process of coextrusion bonding has been used to provide bimetallic tubular connections for various aerospace applications. Recently, the use of stainless steel/titanium and stainless steel/aluminum joints on the Apollo Service Module, the Lunar Lander and Viking vehicles have met with significant success.

Coextrusion bonding involves the tandem extrusion of the candidate materials through a die to force relative motion between the two materials to the extent of breaking down the surface to expose nascent material. When this is done under controlled cleanliness and elevated temperature conditions, a diffusion bond is created between the two materials. An extrusion billet is assembled as shown schematically in Figure 3.

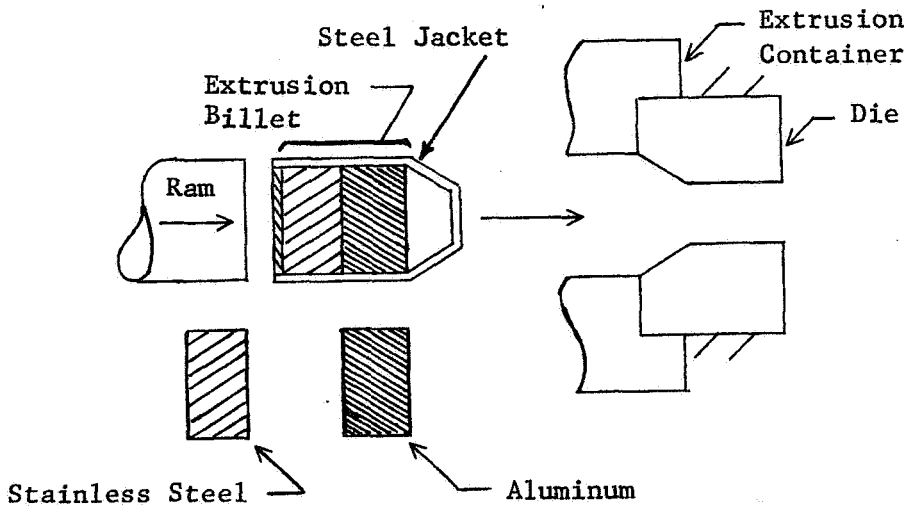

Figure 3.- Coextrusion Process

Footnote: Portions of this discussion are extracted from documentation produced by Nuclear Metals Corporation.

The materials to be bonded are cleaned, fitted together, and encased in a jacket, usually of steel, which has a port for evacuation of air to prevent oxidation or reduction of bonding surfaces when the billet is heated. After careful assembly the billet is evacuated and heated to a controlled temperature below the fusion point of the aluminum. The billet is extruded through the die and allowed to cool. The bonded materials are removed from the jacket and a preliminary machining operation performed to shape the joint near its final intended configuration. At this point, a solution heat treatment, quench and artificial ageing are required. In order to approach the T-851 condition, cold work of 1% to 3% is performed following the solutionizing and quenching operation, with artifical ageing following. The final machining operations are then performed.

Initially, five billets were assembled and subjected to the extrusion process. The temperature during extrusion was approximately 750K (900°F), and other extrusion parameters were varied to provide a range of results. The extruded billets were radiographed to establish the geometric center for subsequent machining, and also to establish if the proper flow of material had occurred during extrusion. This preliminary examination indicated that billets 4 and 5 were the best representatives of the proper conditions. In order to machine the aluminum portion more easily, it was elected to perform the heat treatment prior to machining the joint O.D.'s. The joints were solutionized in an air furnace at 810K (995°F) for one hour after oven temperature recovery, then quenched in a water bath. Hardness tests indicated that the aluminum components were at an approximate hardness of Bhn 75. This is somewhat less than the Bhn 95 hardness expected of "typical" 2219 in this condition, so the heat treatment was repeated, with some changes. This time in addition to the oven thermocouple, a thermocouple was securely attached to an aluminum portion of a joint, and the solutionizing was allowed to proceed for two hours. A water quench within slightly over three seconds after removal from the oven produced a hardness of approximately Bhn 83, which was a significant improvement. The billets were subjected to 1 to 3% permanent deformation using a rotating split collar which opened and closed rapidly to cold work the metal.

They were then artificially aged at 465K (375°F) for 18 hours at temperature. A mercury thermometer penetrating one of the billets was the temperature reference. Hardness readings of these billets indicated a hardness of 110 to 112 Bhn, which was more indicative of T-6 material rather than T-8. The billets were machined to a diameter 0.127 cm (0.050 in.) larger than the final requirement, and a dye penetrant test performed. All of the billets showed penetrant indications at the bond interface, with billets 4 and 5 showing the least. After machining billets 4 and 5 to the final O.D., the dye penetrant indications remained, so the billets were sectioned for metallurgical inspection. It was evident from this inspection that an excessively thick diffusion layer existed at the interface, and that this layer was broken and granular, as if shattered. The excessive diffusion was evidently promoted by cumulative time and temperature during the extrusion and two solutionizing processes. The shattering of the layer could have been a result of one of the solutionizing treatments, quenching, or cold work.

To determine at what point in the process the joint failed, two more billets were extruded at the apparent "best" conditions. One of these billets was cut apart, in the as-extruded condition. Metallurgical examination indicated a diffusion layer thickness of about 10 microns, which was felt to be optimum in light of previous extrusion bonding performed at this facility. The other billet was then subjected to solutionizing at 805K (985°F) for one hour followed by a water quench. When sectioned for examination, portions of this billet fell apart. Examination of the portion which remained intact again showed an excessive diffusion layer.

In order to accomplish the heat treatment without damaging the bond, it was felt that the time and temperature during solutionizing must be reduced by whatever means possible but within the parameters that still provide high joint strength. One of the ways of doing this is to reduce the sectional area of the part to be solutionized to minimize the time required for it to achieve proper temperature. This was done on all remaining program extrusions by performing rough machining inside and out prior to heat treatment. Another technique which assists the heating rate is use of a heated salt bath for solutionizing. The heat transfer from the bath is significantly better than that from the air furnace. To establish the minimum solutionizing time and temperature necessary to achieve the temper required, aluminum test rings were subjected to variations of the heat treatment process. First, solutionizing was accomplished at a lower temperature using both heating techniques, the air furnace and the heated salt bath. Three conditions were investigated.

1. 780K (940°F) for 40 minutes in air furnace
2. 780K (940°F) for 20 minutes in salt bath
3. 750K (900°F) for 40 minutes in air furnace

All of the aluminum rings were quenched in a water bath within five seconds of removal from the heating medium. They were then artificially aged at 465K (375°F) for 24 hours. The hardness measurements after ageing were:

1. 780K (940°F) in air - 89 Bhn
2. 780K (940°F) in salt - 107 Bhn
3. 750K (900°F) in air - 85 Bhn

This indicated that solutionizing in salt at reduced temperature and time (780K (940°F)) can achieve properties nearly as good as those achieved previously with extended air furnace conditioning at 805K (985°F).

Two more extrusions were made, solutionized at 780K (940°F) in salt, and water quenched. One of these was subjected to the cold working process, and both were artificially aged. Hardness readings indicated a hardness about 107 Bhn on both extrusions, with perhaps the cold worked unit showing more consistent and slightly higher hardness than the other. These extrusions were machined to the final configuration and inspected using dye penetrant. Unfortunately, penetrant indications were observed on the outside of the bond area. Both joints showed some penetrant indications from small spots up to 2.5 cm (1.0 in.) in length along the bond line. The joint which

had been cold worked appeared to have less penetrant indication than the joint which was not. Both joints were cut apart for inspection. The non-cold worked joint failed in the bond during sectioning. Superficial inspection of the bond area showed that the O.D. side of the bond should have apparently been better than the I.D. side, even though no penetrant indication was observed on the I.D. The cold worked joint was sectioned at an area of previous dye penetrant indication and at an area of no penetrant indication. The bond withstood all sectioning and trimming cuts. Micrographic examination of both areas was made. The area of dye penetrant indication showed no real evidence of a bond, only folded-over aluminum. The other area did show good bonding without excessive diffusion, but it also showed areas of separation within the aluminum structure near the bond line similar to what might be expected if a burst test failed a joint at the bond, leaving a thin layer of aluminum still bonded to the stainless.

These evaluations, while discouraging, led to renewed experimentation in the heat treatment cycle. One innovation which was tried was to quench a billet directly from the extrusion press. This eliminated the necessity to reheat the billet for solutionizing which would then keep the diffusion layer thickness optimum. The results were not encouraging. Another innovation tried was to encase the joint, particularly the aluminum, in a close fitting steel collar during solutionizing and quenching. The purpose of the collar was to provide hoop restraint on the aluminum during the solutionizing, preventing the aluminum from growing away from the stainless portion which is on the inside of the scarf angle. When the joint is quenched, hoop reduction of the aluminum is then absorbed by compressive loading at the bond which is more tolerable.

Some of the fifteen joints for the test program were produced using the steel collar. Others were successfully made by careful control over the heat treatment parameters, and by selectively eliminating completed joints which would not pass a one-atmosphere leakage test and a dye penetrant inspection.

INERTIA WELDED JOINT FABRICATION

Inertia welding (or friction welding) has been pursued for a number of years in the USSR, but until the introduction of a series of inertia welding machines by Caterpillar Company, widespread acceptance and interest had not occurred in this country.

The inertia welder resembles a lathe. One workpiece is held in a stationary holding device and the other workpiece is held in a spindle chuck, to which one or several stacked flywheels are attached. The chuck-held workpiece is spun to a predetermined speed, the driving power is disengaged, and the rotating part is thrust against the stationary part.

Deceleration of the rotating part converts stored kinetic energy into frictional heat to soften, without melting, the contacting faces of the parts. Then, immediately prior to rotation ceasing, the parts become bonded. The remaining energy and relative motion hot work the metal in the weld zone, creating a spiral grain flow. Impurities are expelled, and the grain structure is refined without creating voids.

Exceptionally consistent welds are obtainable because the factors that determine quality, such as flywheel mass, speed, and thrust force, are easily controlled. Furthermore, since the relatively small volume of metal that is heated in the weld zone is quenched by a heat sink of the cold adjacent metal, and since plastic metal is forged outwardly before melting can take place, each weld is a strong solid-state bond.

The joints fabricated by inertia welding were provided by Interface Welding of Carson, California. A Caterpillar Tractor Company, Model 100 Inertia Welder was used for the development and final production work. A history of the development effort is presented below through delivery of preliminary test specimens, followed by a description of the process used during production of the fifteen test joints.

Inertia Welding Development

Welding 2219 Aluminum to 304L Stainless Steel

In order to explore the variations in welding parameters and part geometry in welding 2219 aluminum to 304L stainless steel, parts were prepared with geometry as shown in Figure 4.

Footnote: Portions of this discussion are extracted from documentation produced by Production Technology, Inc., a Caterpillar subsidiary.

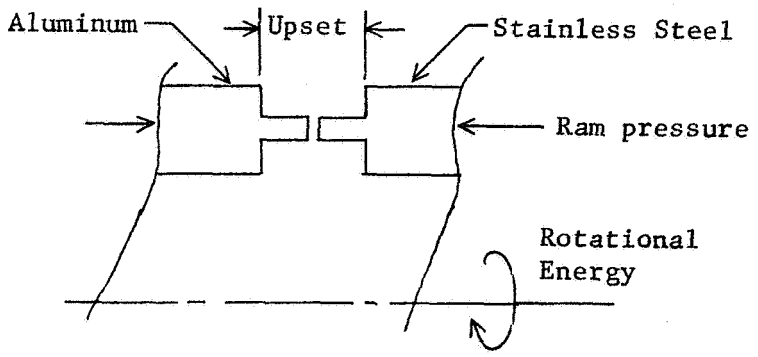

Figure 4.- Inertia Welded Parts Arrangement

Welds were attempted while varying many parameters. The rotating flywheel mass and RPM were varied to provide a wide energy range. The ram pressure was varied from low pressure up to approximately 14,000 N/cm^2 (20,000 psi) at the bonding surface. The contact area between the aluminum and stainless was varied from nearly the same to having the aluminum about twice as wide as the stainless. These conditions produced upsets from approximately 0.165 cm (0.065 in.) through 0.508 cm (0.200 in.). Welds were attempted using both 2219-T851 and T351 aluminum, and the mating face geometry and finish were varied.

An extreme number of experiments would be necessary to completely satisfy a matrix which varies each of these parameters independently. Instead, from a nominal starting configuration and welding parameters, successive parts were made while changing each variable in the direction which resulted in a better indication of bonding. At best, poor indications of bonding were produced; that is, parts would stay together during removal from the machine, but would readily fail when struck with a lead hammer. Some of the parts did not bond at all, and some failed on the machine while cooling. The best bonding indications, while poor, occurred in the low energy and low upset portion of the regime, which is very much unlike the conditions necessary for 6061-T6 to 304L bonding. Use of the T351 material resulted in no apparent advantage over T851.

Welding 2219 Aluminum to 6061 Aluminum

At this point, it was elected to introduce a 6061-T6 intermediate material layer. This material was chosen because the ability of inertia welding to successfully bond 6061-T6 to 304L had already been demonstrated, and the weld from 2219 to 6061, while new, was felt to be a good candidate for inertia welding. In order to develop this aluminum to aluminum bond, parts were prepared with geometry shown in Figure 5.

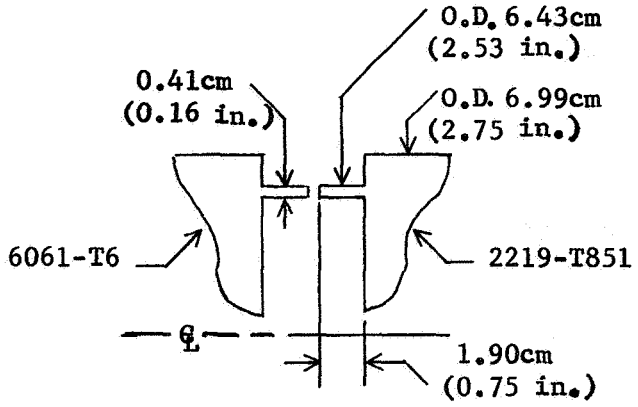

Figure 5.- Inertia Welding 2219 to 6061 Aluminum During Development

The materials appeared to weld readily at nominal machine settings for aluminum welding. Two tubular joints between 2219-T851 and 6061-T6 were made and subjected to tensile testing. Two sections were cut longitudinally from each joint, and one from each joint was subjected to an ageing process at 440K (340°F) for 10 hours. Tensile tests were performed and data is presented in Table 2.

TABLE 2.- TENSILE DATA, INERTIA WELDED 2219 to 6061 ALUMINUM

Weld Sample 2219-T851 6061-T6	1		2	
	As Welded	Aged	As Welded	Aged
Yield Strength N/cm^2 (psi)	25,200 (36,600)	28,300 (41,000)	23,400 (34,000)	28,600 (41,500)
Tensile Strength N/cm^2 (psi)	27,000 (39,200)	31,000 (44,900)	26,500 (38,500)	31,000 (45,000)
Elongation Percent	2.0	7.0	3.0	9.0

Figure 6 indicates the fracture area of one of each specimen type, showing the obvious difference in elongation as well as the relation of the bond line to the fracture.

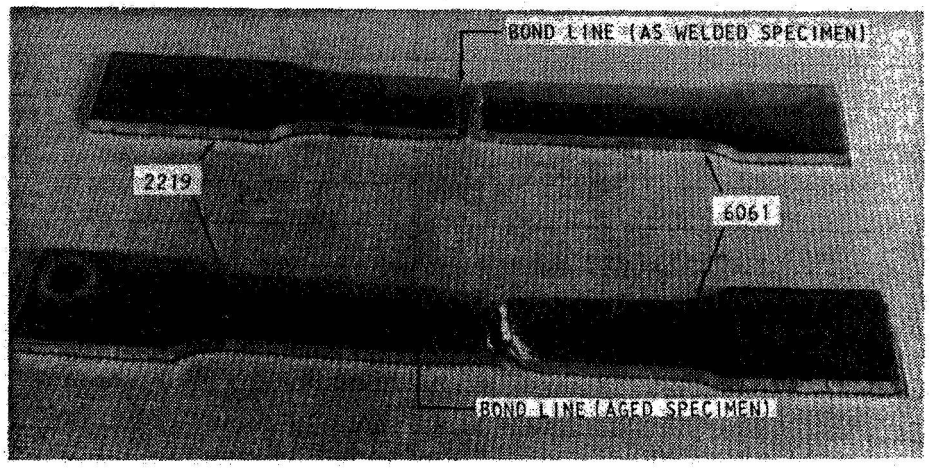

Figure 6. - Inertia Welded Tensile Specimens, 2219 to 6061

Vickers micro-hardness readings were also taken of the materials in the as-welded and aged condition, and indicated an improvement of approximately 15% in the vicinity of the bond line in the aged versus as-welded specimens.

Preliminary Joints

Using the parameters developed for welding 2219 to 6061, cylindrical parts as shown in Figure 7 were welded.

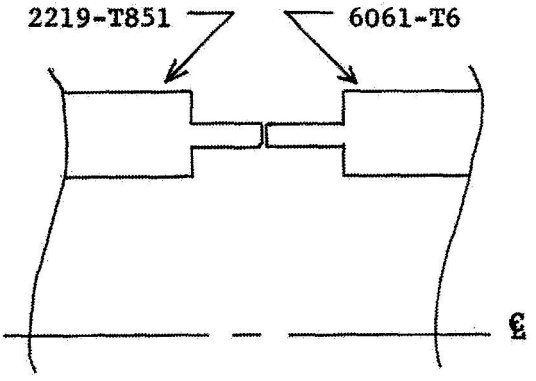

Figure 7.- Inertia Welding 2219 to 6061 Aluminum for Preliminary Joints

The 6061 portion of this joint was then machined as shown in Figure 8.

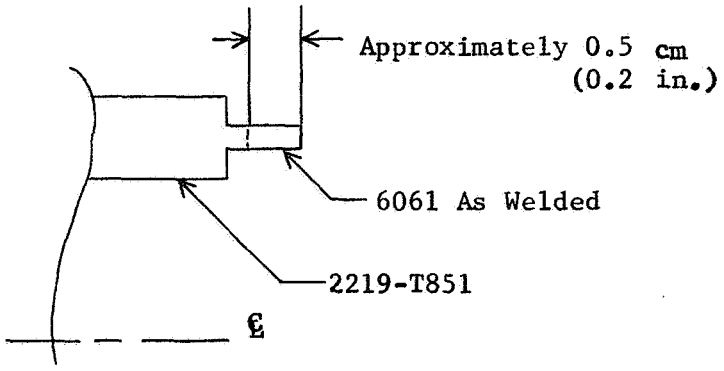

Figure 8.- Refacing of 6061 After Inertia Welding

This sandwich was then welded to the 304L stainless portion. The energy requirement for this weld was approximately 130% of that required to weld an aluminum piece of the same geometry to another aluminum piece. The amount of ram pressure (and therefore upset) was varied for the 6061/304L weld in producing six trial joints. The welding of these preliminary joints indicated some problems in concentricity of the components to be welded and resulted in only three of the six being machined to final configuration. Following machining, these joints were subjected to an ageing process at 440K (340°F) for 10 hours, in order to regain hardness in the aluminum transition area.

A caustic etch was applied to the interface on those joints where the interface was machined, in order to make the transition area between the two aluminum alloys apparent. Table 3 presents information on the preliminary joints.

TABLE 3.- PRELIMINARY INERTIA WELDED JOINTS 6061 DIMENSIONS

Preliminary Joint Number	Upset (Ref. Figure 4) cm	(in.)	6061 Axial Thickness After Welding cm (in.) Inside	Outside	Comments
1	0.208	(0.082)	N/A	0.368 (0.145)	O.D. Machined
2	0.566	(0.223)	0.096 (0.038)	0.030 (0.012)	Machined
3	0.551	(0.217)	0.064 (0.025)	0.038 (0.015)	Machined
4	0.343	(0.135)	N/A	0.191 (0.075)	O.D. Machined
5	0.358	(0.141)	0.279 (0.110)	0.216 (0.085)	Machined
6	0.460	(0.181)	N/A	N/A	As Welded

All of these joints were subjected to a one-atmosphere helium leakage test in the manner described in Appendix D. There was no indication of helium leakage in any of them, when a Consolidated Electrodynamics Corporation Leakage Detector having a sensitivity of 3.0×10^{-10} scc/sec or better was utilized for test. All of the joints which had been completely machined were examined with Uresco P-151 fluorescent dye penetrant. Some indications were seen on the inside surface in the 6061 area near the 304L. Since the 2219/6061 welded portion had been machined with the 6061 in approximately a relatively soft T-4 condition, this machined surface was rough and was the probable cause of the penetrant indication.

Two of the machined joints were subjected to Yield Determination and Burst Test in the manner described in Appendix D. The results that were obtained included a yield pressure of 1720 N/cm^2 (2500 psig) and burst pressure of 2600 N/cm^2 (3800 psig) for preliminary joint 2 and a yield pressure of 1580 N/cm^2 (2300 psig) and burst pressure of 4000 N/cm^2 (5800 psig) for preliminary joint 5. Both of these joints had closures welded at each end when the welding of the aluminum end closure was still in the development stage (see Welding Evaluation). Joint 2 failed in the aluminum end closure weld, so the burst data obtained is misleading. Attempts to reweld this joint succeeded only in annealing the aluminum in the end closure to the point of gross yield when pressure was applied. Evaluation of the two yield curves indicated no obvious advantage in the performance of either joint. Joint 2 did indicate a slightly higher yield pressure, however, and showed less compliance above the yield pressure which was felt desirable. Also, considering the effect on the stress field of the weaker 6061-T6 intermediate material between the 2219-T851 and 304L materials, it is believed the 6061 should be as thin as practical if its use must not degrade the bond strength. For this reason, it was elected to fabricate the remaining joints using the same upset parameters which produced preliminary joints 2 and 3.

Inertia Welding Production

Fifteen additional joints were fabricated by the sequence shown.

1. A cylindrical weld was made between 6061-T6 and 2219-T851 material.

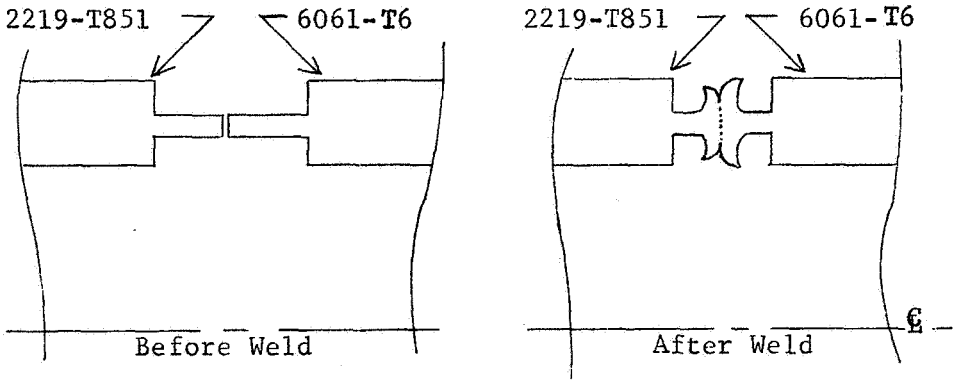

Figure 9.- Inertia Welding 2219 to 6061 Aluminum for Production

2. Excess weld flash and 6061 aluminum were machined as shown in Figure 8.
3. The final weld to the stainless steel was made as shown in Figure 10.

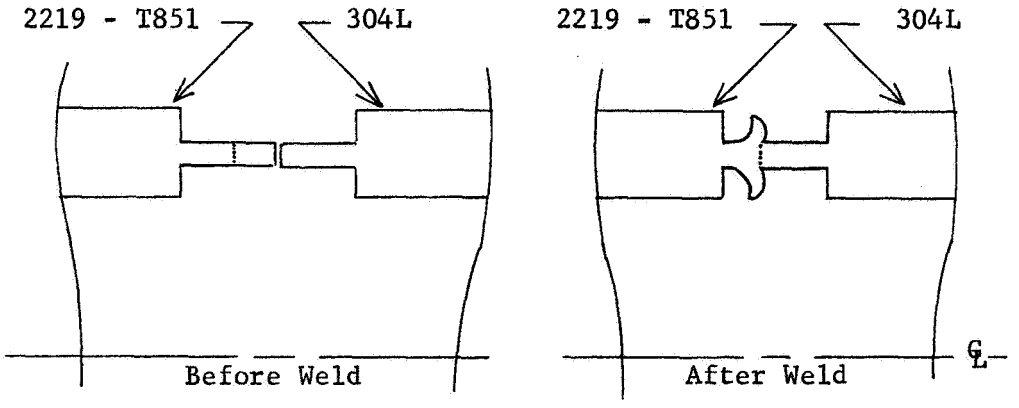

Figure 10.- Inertia Welding 304L Stainless to 2219/6061 Aluminum For Production Joints

4. Final machining was performed as shown in Figure 11.

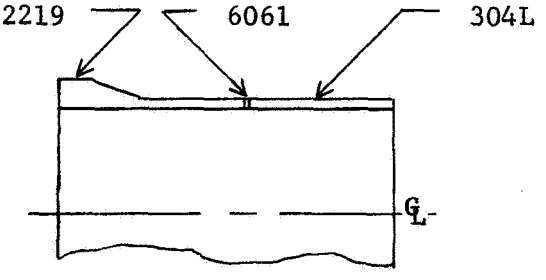

Figure 11.- Final Machining of Inertia Welded Joint

5. An ageing process was performed at 440K (340°F) for 10 hours.

EXPLOSIVE WELDING JOINT FABRICATION

Explosive Welding Development

Explosive welding is a means of joining metals by the explosive application of an impulsive load. The metals and explosives are arranged so that upon detonation, the contact point of the metals progresses across the area to be welded. This forces the generation of a high energy "surface jetting", which promotes mixing and diffusion of the metals. By using suitable controls, welds may be made between a variety of similar and dissimilar metals.

In order to facilitate bonding 2219-T851 to 304L, an intermediate material of sterling silver was chosen. Other intermediate materials are available, but the relative ease of bonding sterling silver to aluminum and stainless steel (coupled with a thermal coefficient which is between that of the aluminum and stainless which will reduce stresses during thermal extremes) indicated that silver was a logical choice. Experiments were conducted to determine the optimum parameters for bonding the silver to the aluminum. These experiments used flat plate configurations to simplify the setups. The silver thickness chosen was 0.025 cm (0.010 in.). While this is somewhat thinner than can easily be worked with, its use should result in a stronger joint with a minimum of degradation from the somewhat weaker silver.

A series of bonds were made on flat plate specimens to establish the parameters necessary to bond silver to 2219, and also to bond this combination to 304L. Satisfactory bonds were made and a photograph of a typical bonded section appears in Figure 12.

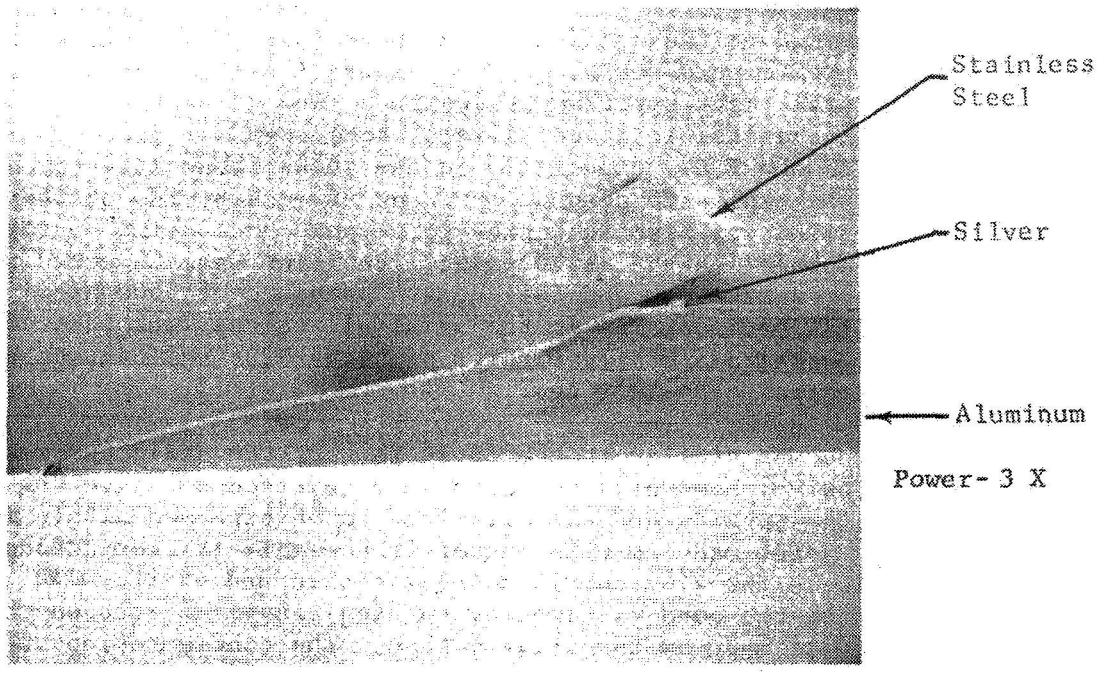

Figure 12. - Section of Explosive Welded 304L Stainless Steel to 2219-T851 Aluminum

Cylindrical bonds were then produced by each of three fabrication methods. The first technique consisted of initially bonding silver to an aluminum cone and then bonding stainless onto this sandwich. This technique is schematically illustrated in Figure 13.

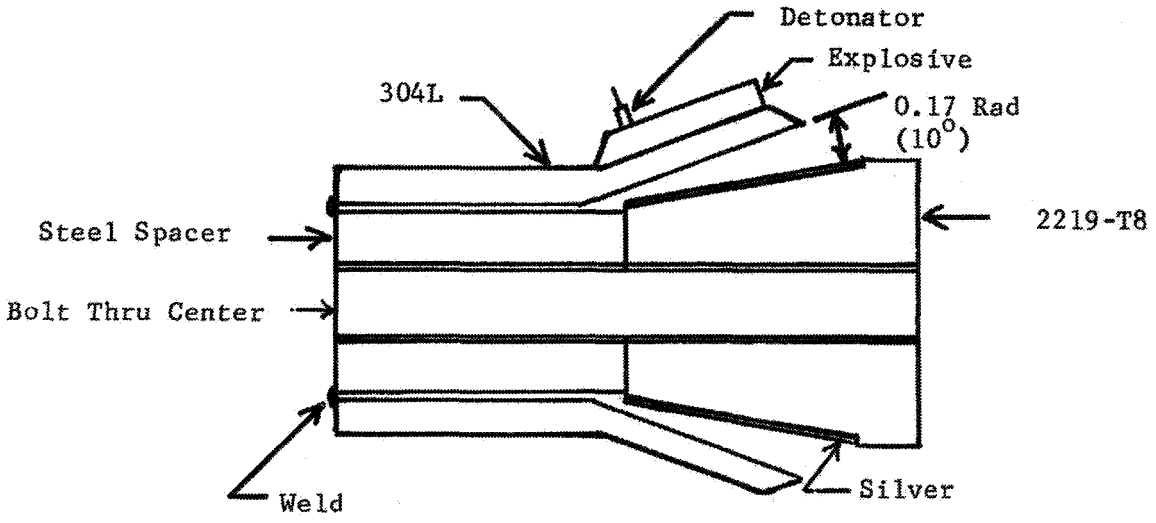

Figure 13.- Explosive Bond Joint Method #1 Setup

This joint was machined to the configuration shown in Figure 1 and then subjected to some preliminary tests. A dye penetrant test using penetrant visible in the natural light spectrum indicated a lack of bonding on most of the O.D. between the stainless and silver. Some areas of poor bonding were also evident on the I.D., especially in the shock front area (area of convergence of the explosive detonation front from each side of the cylinder). This joint was also subjected to a leak check using nitrogen gas and indicated bubble leakage at 30 psig. The joint was subjected to a hydrostatic burst pressure test and failed at a pressure of 5500 N/cm^2 (8000 psig). The failure occurred in the axial direction, with part of the bond between the stainless and silver failing at the O.D. and part of the parent aluminum material also failing.

The second technique was similar to the first in that the stainless was formed by the explosive; however, the parts were reversed to allow the aluminum to be on the outside and the stainless to be expanded within it. The advantage of a joint made in this manner is possibly its resistance to cryogenic shock, where the aluminum is quickly cooled and exerts high compressive forces on the bond as compared to high tensile forces on the bond if the joint were made by the first method. The configuration used for the second method is shown in Figure 14. The result was not good and illustrated that there were problems in assembling a joint in this manner.

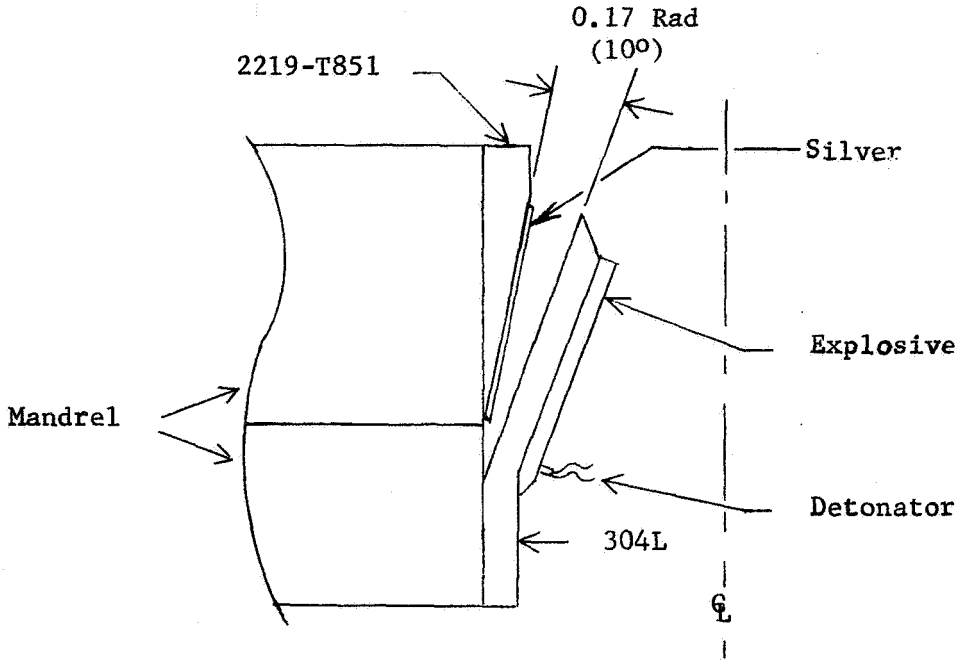

Figure 14.- Explosive Bond Joint Method #2 Stainless to Silver/Aluminum

In a joint of this small diameter, it is apparent that stainless steel will not withstand the deformation necessary when strained impulsively; and further, the explosive gaseous products cannot escape without causing erosion of the materials and probably becoming trapped in the bond area. The explosive charge used was probably too severe, and the amplifying effect of having the explosive confined was stronger than anticipated. The set-up of the explosive charges for both the silver and the stainless bonds was more difficult than anticipated and the use of the mandrel, while suitable, was not desirable if another technique could be developed.

The third technique used to assemble a joint was another attempt at keeping the aluminum on the outside of the stainless at the scarf angle interface. This technique required aluminum to be formed onto stainless as was the first method, which also required good aluminum ductility. It also required that the shock front area on the aluminum be attenuated to prevent the material from splitting and spalling. The basic configuration is shown in Figure 15.

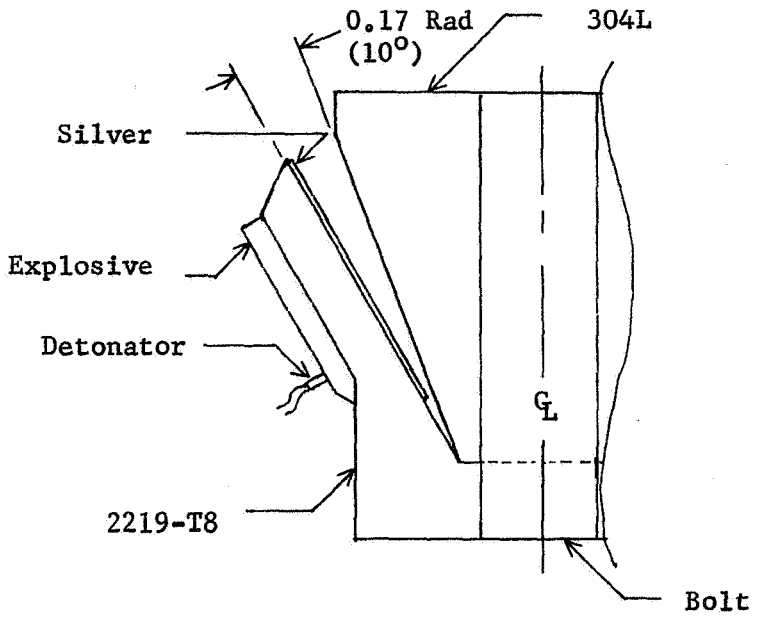

Figure 15.- Explosive Bond Joint Method #3 Silver/Aluminum to Stainless

The results of this final bond method, while far from perfect, indicate that with some further development this joint technique is probably useable. The joint leaked nitrogen gas excessively at 30 psig, so was sawed in half longitudinally for inspection. The most evident problem was the cracking of the aluminum. If the joint had been made using T351 aluminum with its significantly higher ductility, it would have had less tendency to crack, and could then have been artifically aged following bonding.

Explosive Welding Production

A sterling silver cone connected to an aluminum support ring was attached to the aluminum part of the joint and configured for bonding as shown in Figure 16. The powder support box was fabricated from three pieces of 0.013 cm (0.005 in.) mylar sheet and is shown as the upper three items in the center of Figure 17. The aluminum support ring is bolted down to the aluminum part of the joint and the powder and detonator are shown in place. This configuration allows the bonding of the silver to the aluminum portion of the joint.

See Figure 18 for the configuration used to bond the stainless portion of the joint to the Ag/Al portion. The stainless portion seats firmly on the aluminum and is bolted to it. In order to generate more energy on the initiation side of the joint, progressive layers of tape were applied on the surface of the explosive. These layers started by covering 3/4 of the circumference of the joint on the initiation side and became progressively shorter until the 11th (final) layer covered 1/4 of the circumference. The mass of the tape gave the effect of initiating more energy in the direction of the joint without actually increasing the explosive charge. The bond was created in a vacuum, since the quantity of explosives with the resultant hot gas products of very high acoustic velocity can contaminate the bond area before bonding occurs. The appearance of the joint after detonation is shown in Figure 19.

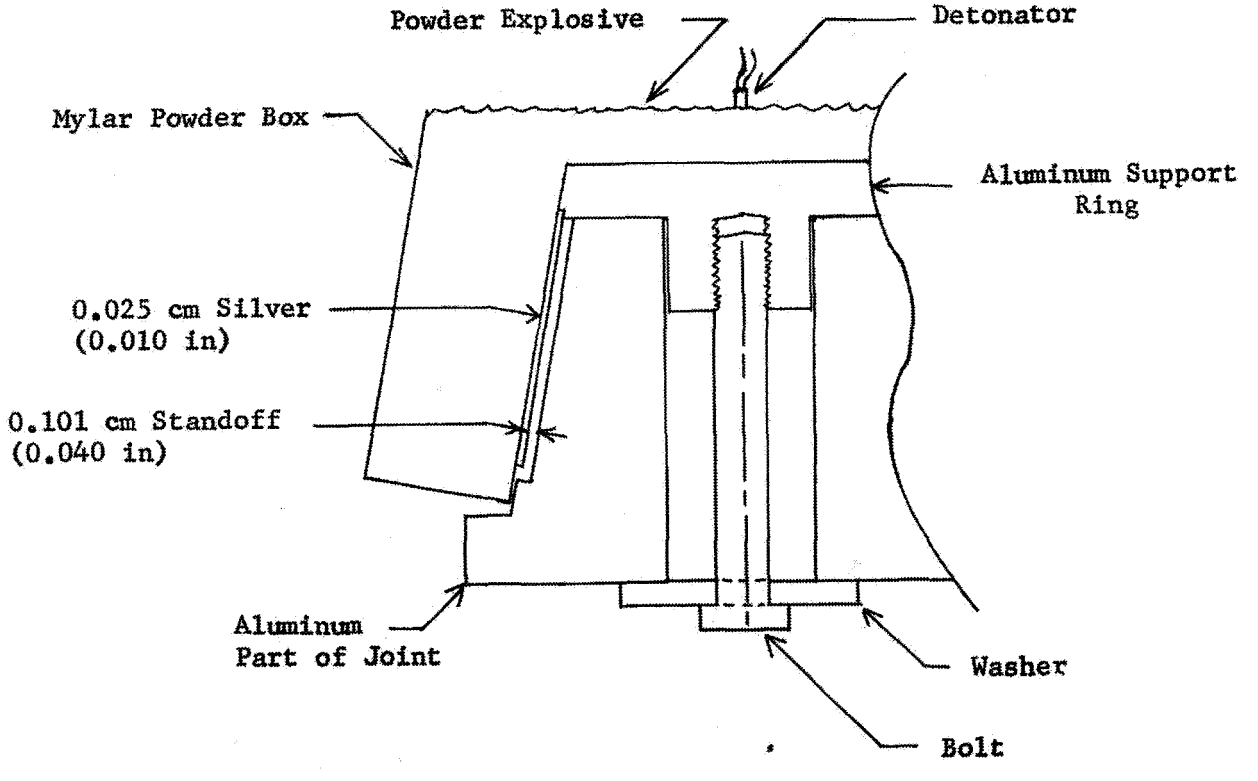

Figure 16.- Explosive Bond Joint Production Silver to Aluminum

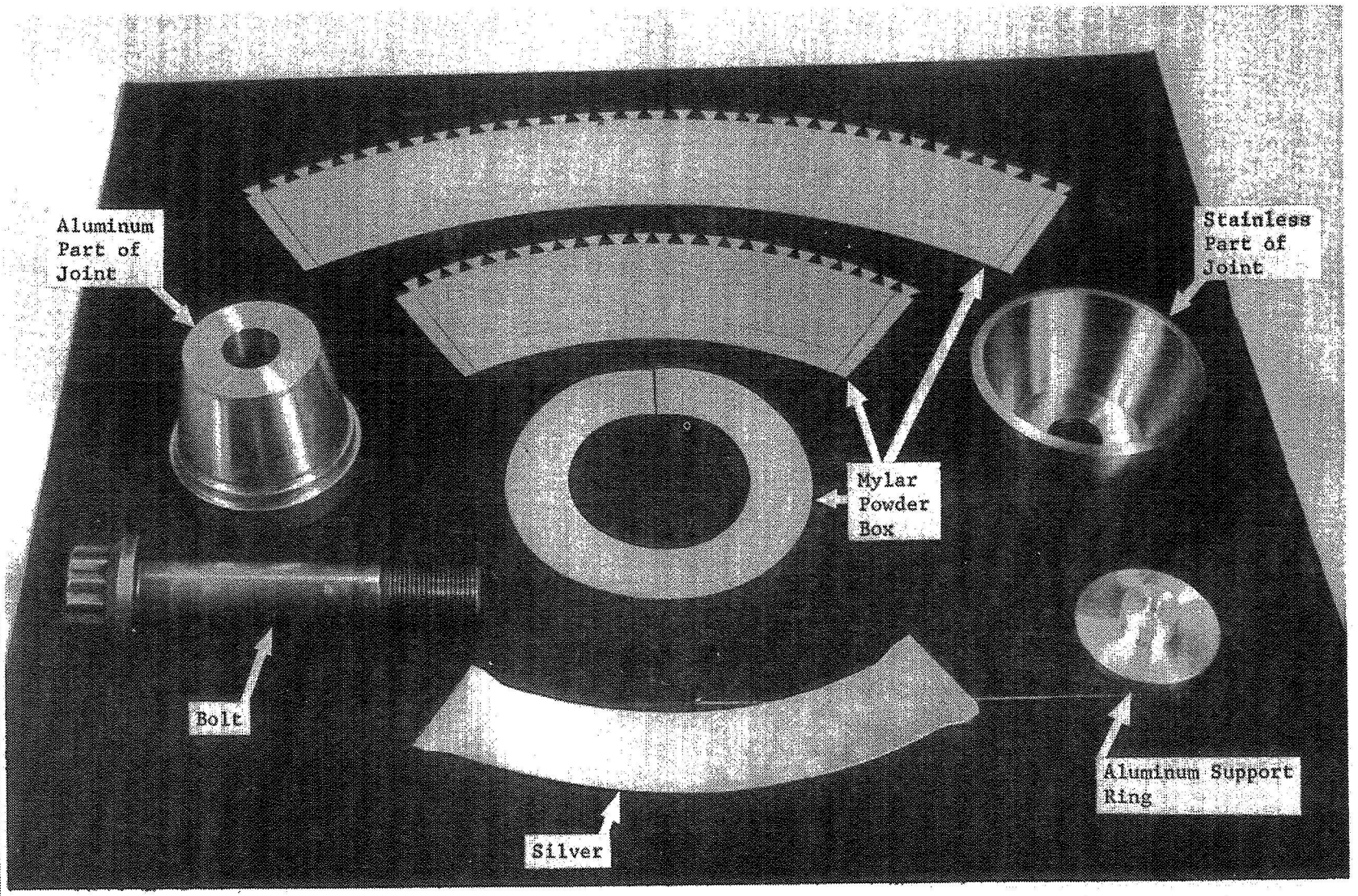

Figure 17. - Explosive Bonding Parts

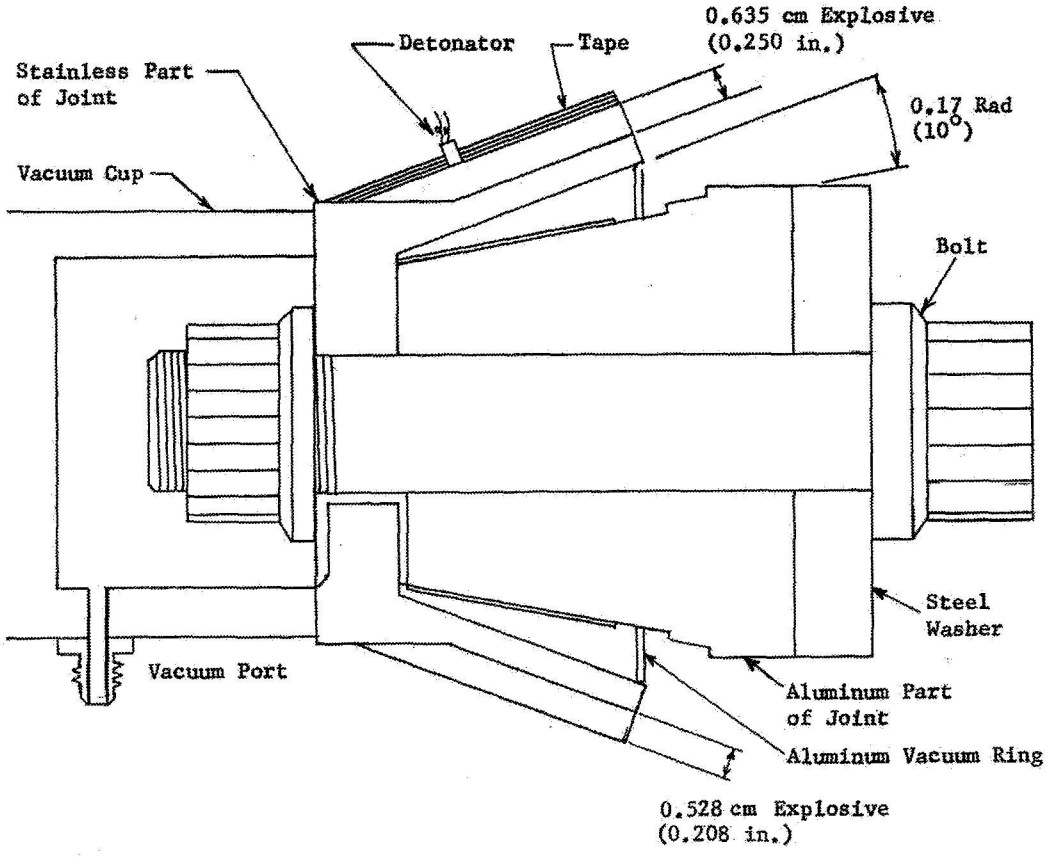

Figure 18. - Setup for Explosive Bond Joint Production Stainless to Silver/Aluminum

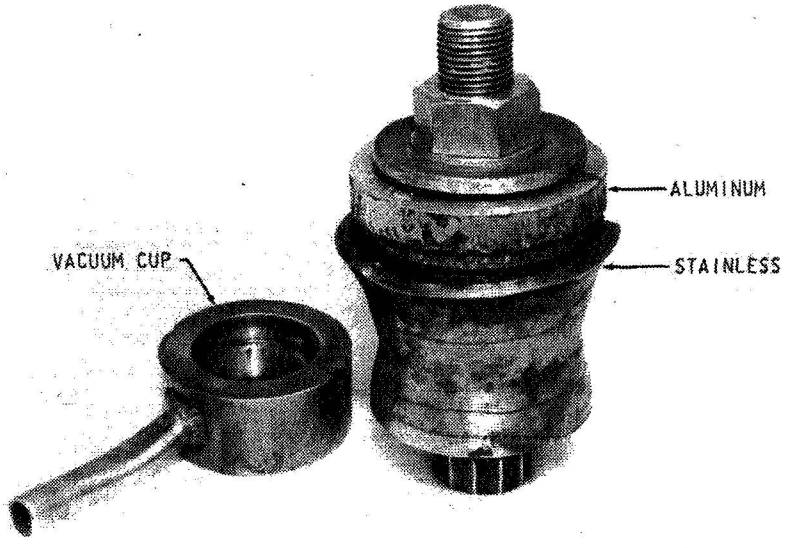

Figure 19. - Explosive Bonded Joint Following Detonation

SWAGED CONSTRUCTION JOINT FABRICATION

The swaged construction process produces a mechanical seal between the unlike materials by forcing one material to flow into serrations machined into the opposing piece. Aluminum ferrules composed of 6061-T6 aluminum or stainless steel are produced by Metal Bellows Corporation for use in aerospace and general industry. These production items are configured as shown in Figure 20 and are available in sizes from 1.91 cm (0.75 in.) through 17.8 cm (7.0 in.) diameter.

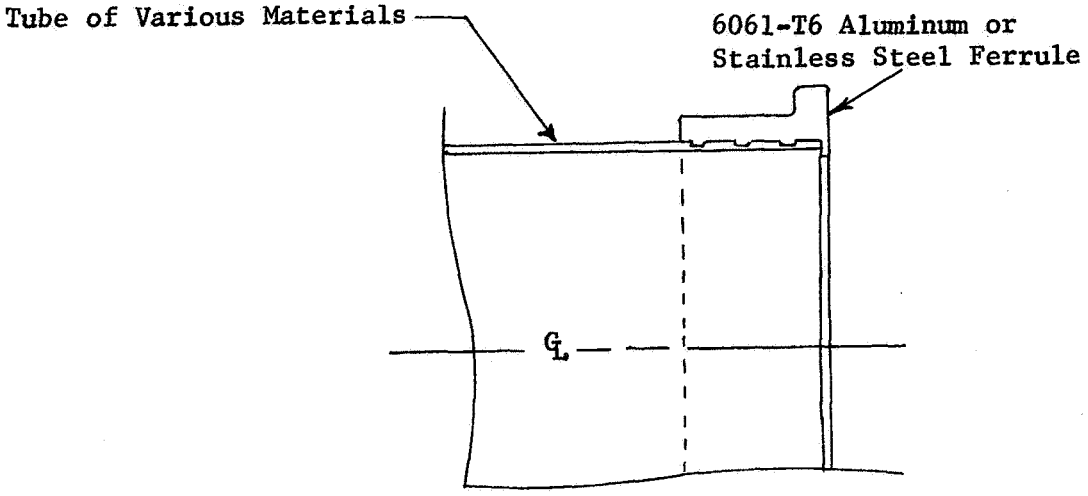

Figure 20. - Configuration of Commercial Swaged Joint

These ferrules are attached using installation tools which are portable and are, therefore, suitable for on site or field installation when moderate diameters are involved.

The basic tool required is an expanding rotational device, as shown in Figure 21.

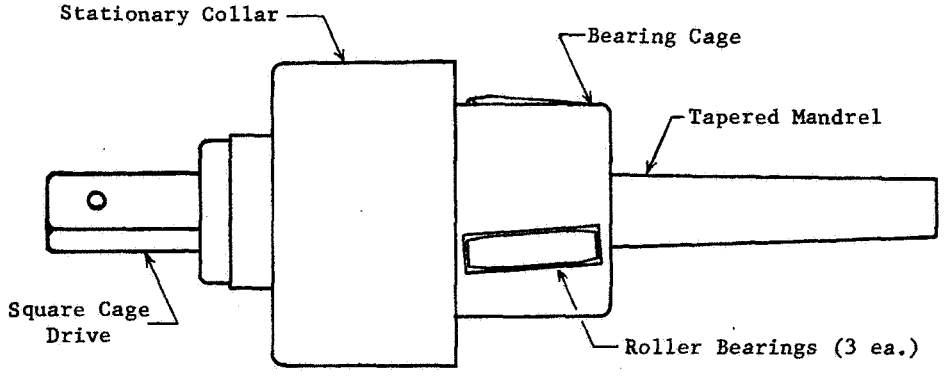

Figure 21. - Ferrule Installation Tool

With the use of a suitable holding jig for the ferrule and tube, this tool is inserted into the tube and ferrule until the stationary collar meets the ferrule, then the drive is rotated with a torque wrench. As the bearing cage rotates, the bearings force the mandrel to extend, which in turn forces the bearings to exert increasing force on the inside of the ferrule. Each ferrule is installed to a specified torque to assure consistent strength and sealing.

In order to provide a joint configuration similar to that in Figure 1, and to approach the problem of mating the very hard 2219-T851 alloy to the stainless steel, a modification was made to the standard ferrule design. The joint configuration is shown in Figure 2. An aluminum backup ring was added to help distribute plastic strain into the stainless portion of the joint, and to prevent the stainless portion from buckling due to its residual compressive stress resulting from the swaging operation.

All joints were not manufactured at one time. Initially two joints were fabricated and submitted to the test program. These joints had excessive leakage so were not felt suitable to use as test matrix joints numbers 1 and 2. Instead, they were designated test matrix joints numbers 14 and 15. Number 14 normally receives a burst test which was redundant with several other joints, and number 15 was normally used as an ultrasonic reference with EDM flaws, which was not required for this joint type. When these two joints were cut apart for inspection, it was found that the serrations in the aluminum had not penetrated the stainless material suitably. The design was modified to help promote shear of the opposing materials. The depth of the serrations in the aluminum outer shell was increased, and care was taken to assure sharp corners at these serrations. The stainless steel portion was reduced in thickness to approximately 0.127 cm (0.050 in.), to allow the metal to more easily flow into the aluminum serrations.

The remainder of the fifteen joints were made in this fashion after one atmosphere helium leak tests indicated acceptable leakage characteristics of most of the joints. The short time available prevented making additional modifications to the joints which could have helped assure their suitability.

TEST PROGRAM

The first test performed on each joint type was yield determination and burst. Yield determination was designed to establish the operating pressure level for subsequent proof and leakage tests on other joints. Burst was a pressurization to failure as a measure of joint ultimate strength. Two specimens of each type were subjected to this testing.

The thermal cycle test was performed on four specimens of each type. This test measured the joints' resistance to temperature excursions from 375K (+215°F) to 78K (-320°F). The test provided a thermal shock as well because the specimens were immersed into each respective liquid bath immediately after withdrawal from the other. The plan for test was to cycle two of each type for 100 cycles and to determine the thermal effect on bond leakage and residual burst strength. If significant degradation occurred, the remaining two joints of each type would be subjected to only 50 cycles and that effect noted. If little or no degradation occurred, the remaining two joints of each type would also be cycled 100 times and subjected to the post tests.

The pressure cycle test was intended to determine the fatigue strength of each bond type when subjected to pressure cycles of 50% theoretical ultimate pressure. Again, two joints of each type were planned to be cycled initially. The second two would be cycled at a pressure determined after the number of cycles to failure were established for the first two. By this method, an approximation of the shape of the joint fatigue curve could be made.

Test Description and Procedure

In order to describe the test program the joints were subjected to, the test procedure is included as Appendix D. Some changes have been made to make the procedure more easily understood in this context. The test matrices have been excerpted from the procedure and appear as Tables 4 and 5. They were designed to best utilize the limited number of specimens in characterizing the thermal cycle, pressure cycle, and corrosion resistance of each joint type, while allowing NDT evaluations periodically.

TABLE 4 TEST MATRIX FOR INERTIA WELDED, COEXTRUDED, AND EXPLOSIVE WELDED JOINTS

TEST \ SPECIMEN		1, 2	3, 4 5, 6	7, 8 9, 10	11, 12	13, 14	15**
NDT	Penetrant	X	X	X	X	X	X
	Leakage-One Atm	X	X	X	X	X	X
Weld End Closures SS		X	X	X	X	X	
Weld End Closures Al ***			X(6)			X(14)	
Yield Determination & Burst		X					
Proof			X	X	X	X	
Leakage-Operating Pressure			X	X	X	X	
NDT	Penetrant		X	X	X	X	
	Ultrasonic		X*				
Thermal Cycle			X				
Pressure Cycle				X			
Galvanic Corrosion					X		
Leakage-Operating Pressure			X		X		
Burst			X		X	X	
Metallographic		X	X	X	X	X	X
Interface Constituent Identification							X

*Specimen #3 only, or a specimen with helium leakage.
**To be EDM flawed as an ultrasonic reference.
***Mechanical end fittings to be used on non-welded joints

TABLE 5 TEST MATRIX FOR SWAGED JOINTS

Test \ Specimen	1,2	3,4 5,6	7,8 9,10	11,12	13,14	15
NDT Leakage-One Atm	X	X	X	X	X	X
Weld End Closures SS	X	X	X	X	X	
Weld End Closures Al*		X(6)			X(14)	
Yield Determination & Burst	X					
Proof		X	X	X	X	
Leakage-Operating Press.		X	X	X	X	
Thermal Cycle		X				
Pressure Cycle			X			
Galvanic Corrosion				X		
Leakage-Operating Press.		X		X		
Burst		X		X	X	

* Mechanical end fittings to be used on non-welded joints.

Welding Evaluation

When bimetallic joints are utilized in aerospace applications, three basic approaches may be used which require tradeoffs to be made in weight, cost, fabricability, etc. The first approach is to use a joint similar to the one developed under this program which requires welding at each end during installation. The second approach is to use a joint which incorporates a mechanical flange on one end and a welding boss on the other. The third approach is to fabricate the bimetallic joint directly on one of the items to be joined, and provide a flange at the other end of the joint. This approach requires no welding to install the joint. Since welding may be required, depending on which approach is used, the original test plan included welded closures on the ends of each joint.

The initial design of the joint and closures was as shown in Figure 22.

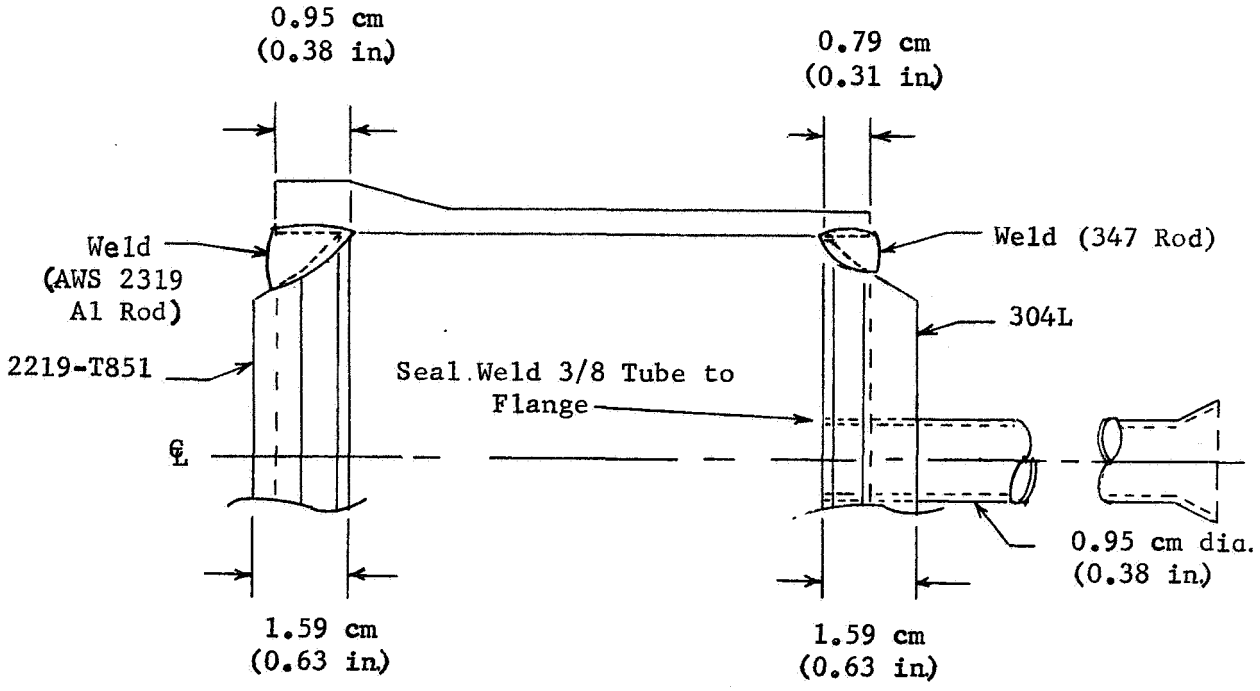

Figure 22.- Initial Concept for Welded End Fittings

While no difficulty was encountered when welding the stainless steel end of the joint, welding of the aluminum end resulted in fine cracks at the aluminum O.D. and with damaged bonds on some of the early joints tested.

When it become evident that welding of the aluminum ends could compromise some of the tests because of leakage and/or premature failure, the decision was made to fit mechanical fittings on most of the aluminum ends during test. Welding was limited to a few joints to get some indication if welding under controlled conditions degraded the joint bond.

The final configuration which was successfully used for welding is shown in Figure 23, and incorporated a chill ring to protect the bond.

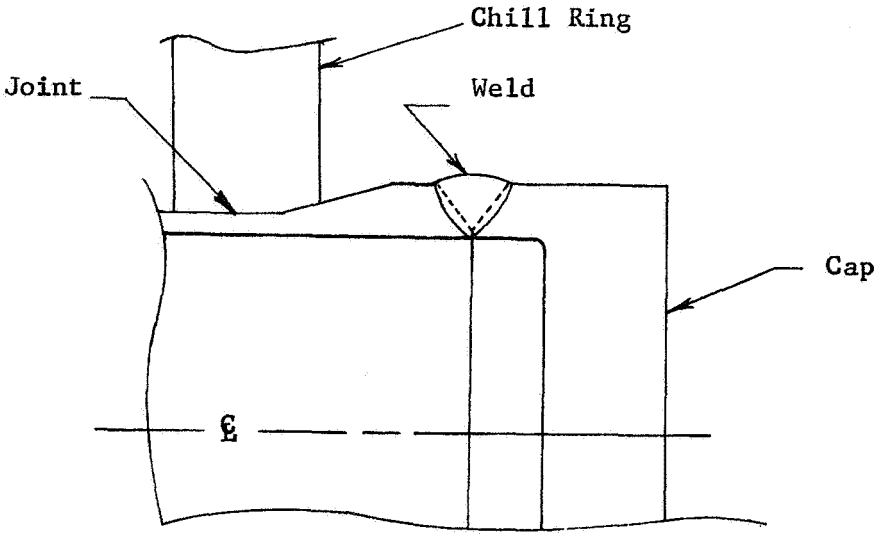

Figure 23.- Concept for Aluminum End Fitting Weld Using Tubular Cap

Receiving Inspection Results

After all joints were properly marked for program identification they were inspected, weighed and measured. The results are summarized in Table 6. Joint dimensions are illustrated in Figures 1 and 2. The weights differed due to variations in location of the bond area of each joint and variations in overall length. Each individual weight also included the thickened aluminum welding boss; therefore the weight results obtained were for a comparison between fabrication techniques rather than an indication of what the installed weight of a flight article might be.

Some general observations were made with regard to each joint type. Roughness was apparent on the inner surface in the area of the bond on the inertia welded specimens. This was due to final machining being performed prior to the final ageing operation since softer unaged aluminum is more difficult to machine to a good finish than aged aluminum. Also, since the thickness of the materials that were inertia welded was only slightly more than the final intended dimension, only a small amount of material could be removed for surface finishing. The presence of the 6061 aluminum intermediate layer was not easily visually detected. The area of shock front impingement was easily identifiable on all explosive welded joints, as an area of increased material deformation. The presence of the silver intermediate layer was also readily apparent. The coextruded specimens had the best surface finish of any of the joints that were examined. The swaged construction joints had the aluminum portion anodized.

A photograph of each joint type is included as Figure 24, 25, 26, and 27.

TABLE 6.- RECEIVING INSPECTION RESULTS

		Outside Diameter cm (in.)	Wall Thickness cm (in.)	Length cm (in.)	Weight Kg (lb)
INERTIA WELDED JOINTS	1	6.347 (2.499)	0.315 (0.124)	7.717 (3.038)	0.271 (0.597)
	2	6.358 (2.503)	0.318 (0.125)	7.628 (3.003)	0.277 (0.611)
	3	6.358 (2.503)	0.315 (0.124)	7.620 (3.000)	0.278 (0.613)
	4	6.365 (2.506)	0.315 (0.124)	7.676 (3.022)	0.278 (0.613)
	5	6.358 (2.503)	0.318 (0.125)	7.628 (3.003)	0.278 (0.613)
	6	6.358 (2.503)	0.318 (0.125)	7.635 (3.006)	0.279 (0.615)
	7	6.358 (2.503)	0.315 0.124)	7.892 (3.107)	0.278 (0.613)
	8	6.360 (2.504)	0.318 (0.125)	7.263 (3.001)	0.277 (0.611)
	9	6.360 (2.504)	0.315 (0.124)	7.635 (3.006)	0.278 (0.613)
	10	6.360 (2.504)	0.318 (0.125)	7.635 (3.006)	0.277 (0.611)
	11	6.360 (2.504)	0.318 (0.125)	7.620 (3.000)	0.277 0.611)
	12	6.358 (2.503)	0.315 (0.124)	7.579 (2.984)	0.276 (0.608)
	13	6.383 (2.513)	0.318 (0.125)	7.617 (2.999)	0.277 (0.611)
	14	6.363 (2.505)	0.318 (0.125)	7.569 (2.980)	0.276 (0.608)
	15	6.360 (2.504)	0.315 (0.124)	7.600 (2.992)	0.277 (0.611)

TABLE 6.- RECEIVING INSPECTION RESULTS (Cont'd)

		Outside Diameter cm (in.)	Wall Thickness cm (in.)	Length cm (in.)	Weight Kg (lb)
EXPLOSIVE WELDED JOINTS	1	6.345 (2.498)	0.335 (0.132)	7.676 (3.022)	0.283 (0.624)
	2	6.365 (2.506)	0.325 (0.128)	7.717 (3.038)	0.282 (0.622)
	3	6.380 (2.512)	0.320 (0.126)	7.671 (3.020)	0.275 (0.606)
	4	6.340 (2.496)	0.321 (0.123)	7.676 (3.022)	Not Weighed
	5	6.345 (2.498)	0.330 (0.130)	7.772 3.060)	Not Weighed
	6	6.325 (2.490)	0.292 (0.115)	7.849 (3.090)	0.262 (0.578)
	7	6.337 (2.495)	0.323 (0.127)	7.734 (3.045)	Not Weighed
	8	6.340 (2.496)	0.330 (0.130)	7.747 (3.050)	0.395 (0.871)
	9	6.330 (2.492)	0.335 (0.132)	7.625 (3.002)	Not Weighed
	10	6.330 (2.492)	0.356 (0.140)	7.760 (3.055)	Not Weighed
	11	6.330 (2.492)	0.351 (0.138)	7.808 (3.074)	Not Weighed
	12	6.337 (2.495)	0.356 (0.140)	7.826 (3.081)	Not Weighed
	13	6.358 (2.503)	0.292 (0.115)	7.752 (3.052)	0.384 (0.847)
	14	6.350 (2.500)	0.325 (0.128)	7.740 (3.047)	0.418 (0.922)
	15	6.327 (2.491)	0.320 0.126)	7.879 (3.102)	0.293 (0.646)

Note: Joints 8,13,and 14 were machined to leave the aluminum end sealed.

TABLE 6 RECEIVING INSPECTION RESULTS (Con't)

		Outside Diameter cm (in.)	Wall Thickness cm (in.)	Length cm (in.)	Weight kg (lb)
SWAGED CONSTRUCTION JOINTS	1	6.462 (2.544)	0.325 (0.128)	8.801 (3.465)	0.363 (0.800)
	2	6.360 (2.504)	0.328 (0.129)	8.590 (3.382)	0.365 (0.805)
	3	6.360 (2.504)	0.330 (0.130)	8.768 (3.452)	0.372 (0.820)
	4	6.365 (2.506)	0.328 (0.129)	8.821 (3.473)	0.376 (0.829)
	5	6.360 (2.504)	0.333 (0.131)	8.829 (3.476)	0.385 (0.849)
	6	6.352 (2.501)	0.330 (0.130)	8.824 (3.474)	0.328 (0.842)
	7	6.358 (2.503)	0.330 (0.130)	8.524 (3.356)	0.362 (0.798)
	8	6.439 (2.535)	0.328 (0.129)	8.598 (3.385)	0.367 (0.809)
	9	6.332 (2.493)	0.333 (0.131)	8.573 (3.375)	0.362 (0.798)
	10	6.345 (2.498)	0.325 (0.128)	8.542 (3.363)	0.361 (0.796)
	11	6.363 (2.505)	0.330 (0.130)	8.961 (3.528)	0.401 (0.884)
	12	6.350 (2.500)	0.330 (0.130)	8.999 (3.543)	0.397 (0.875)
	13	6.345 (2.498)	0.330 (0.130)	8.567 (3.373)	0.360 (0.794)
COEXTRUSION BONDED JOINTS	1	6.350 (2.500)	0.318 (0.125)	7.833 (3.084)	0.276 (0.608)
	2	6.350 (2.500)	0.315 (0.124)	7.874 (3.100)	0.274 (0.604)
	3-15	These joints not available in time for testing.			

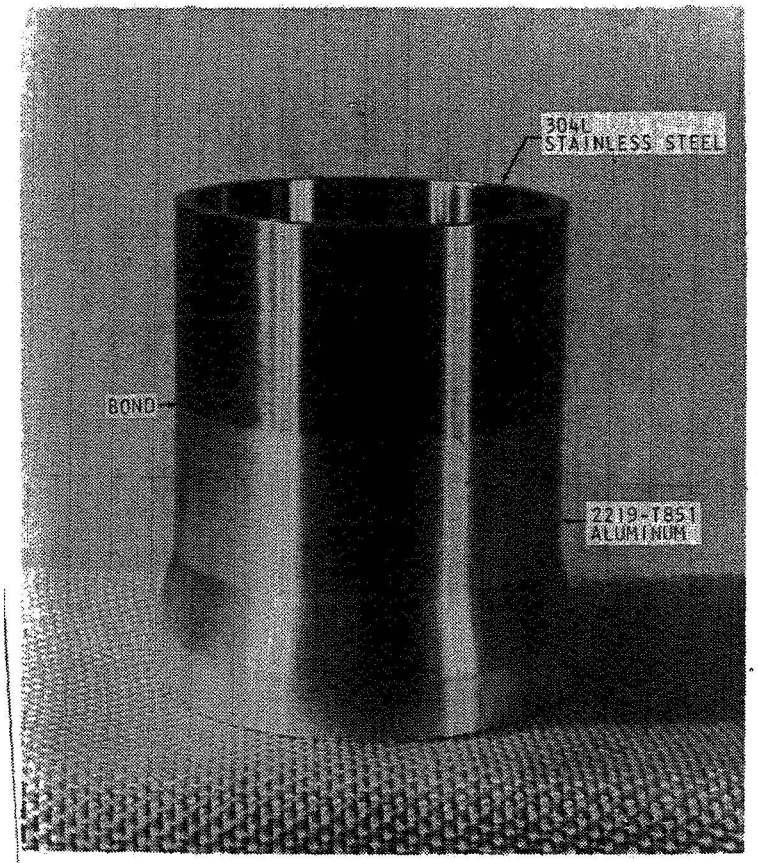

Figure 24. - Coextruded Joint

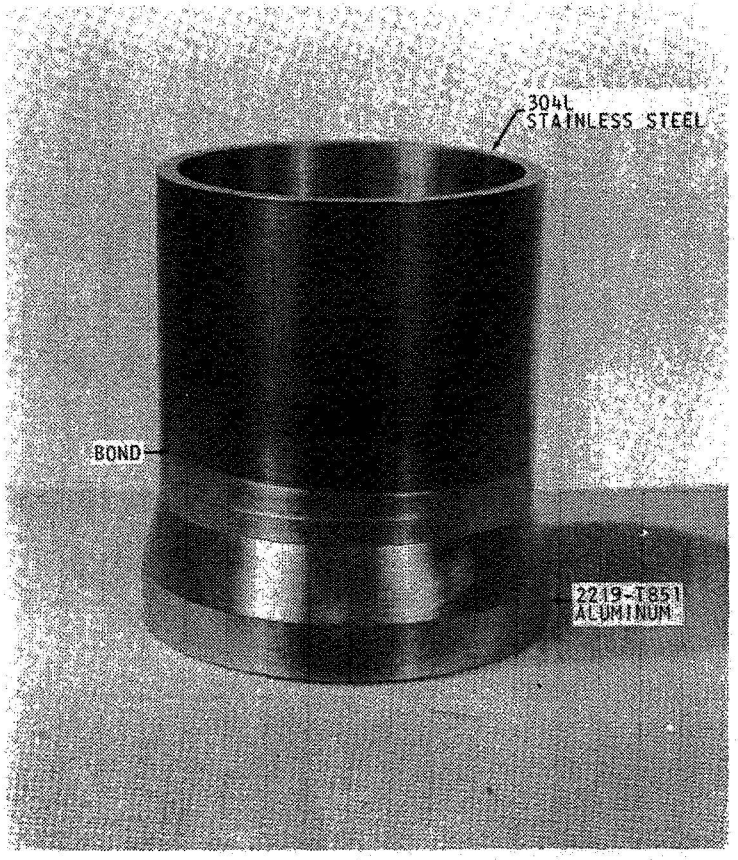

Figure 25. - Explosive Welded Joint

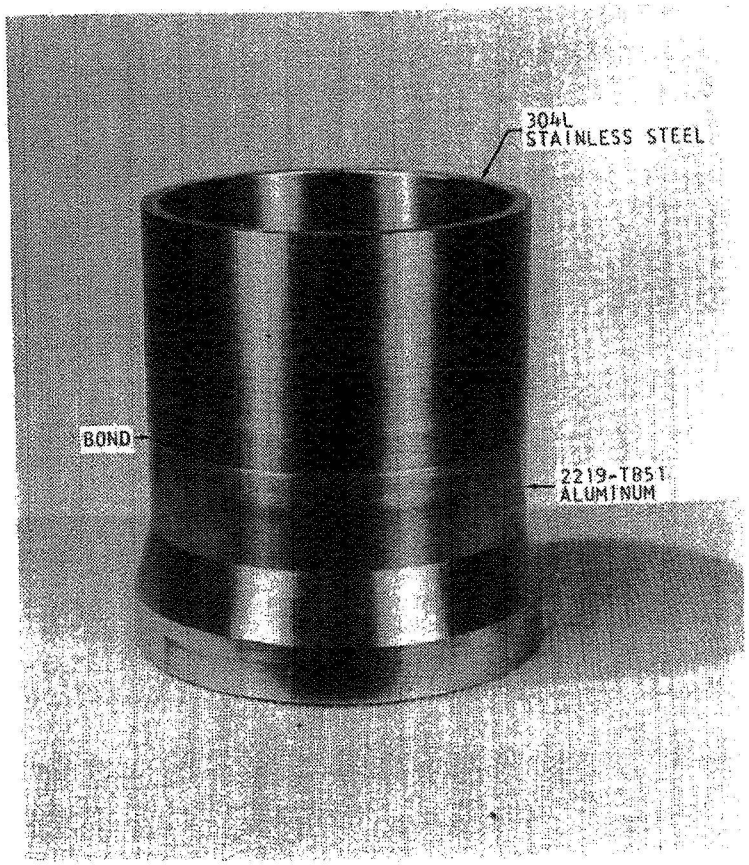

Figure 26. - Inertia Welded Joint

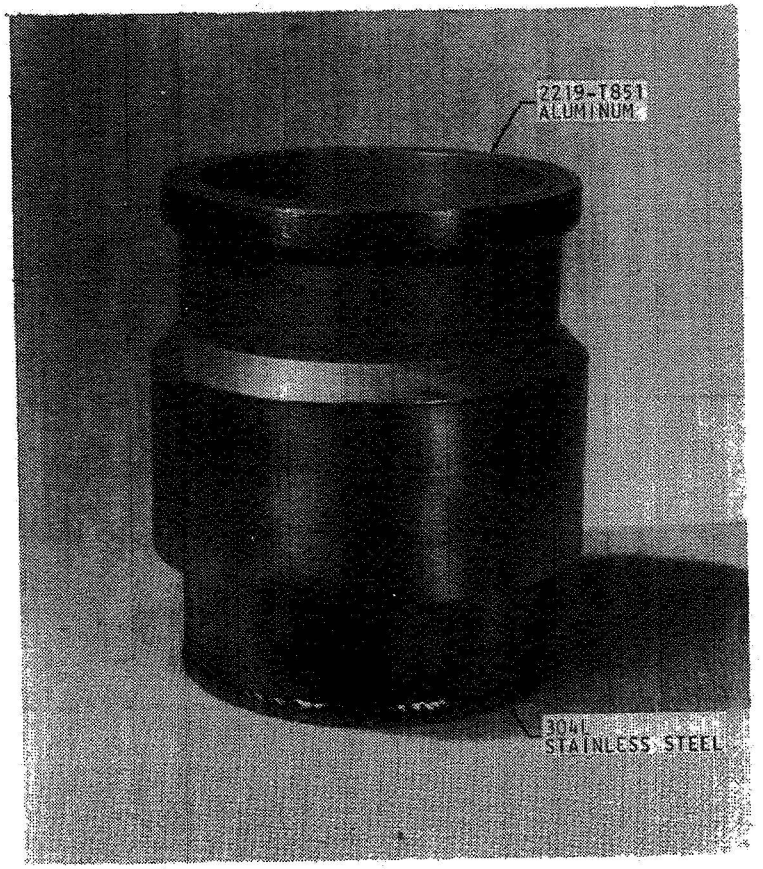

Figure 27. - Swaged Construction Joint

Yield Determination and Burst Test Results

This test was performed on two of each type of joint (only one coextruded joint) to establish the yield and ultimate pressure characteristics of the joint. This information was used to establish the proof and operating pressure level of each joint type for subsequent testing. The system used is shown schematically in Appendix D and the test vessel is shown in Figure 28. Each joint was pressurized by means of a positive displacement hydrostatic pump while being contained within an outer vessel. The outer vessel was designed to allow total water displacement thru a calibrated burette. The rising burette level was a direct visual indication of joint strain during pressurization and by selection of a suitable burette volume and transducer pressure range, a continuous recording of pressure vessel volumetric growth vs. joint inlet pressure was made. Inspection of the data disclosed the pressure level at which the pressure/volumetric growth deviated from the linear relationship which indicated that the yield point (at 0% strain offset) was reached in some part of the joint. These data are presented in Figure 29.

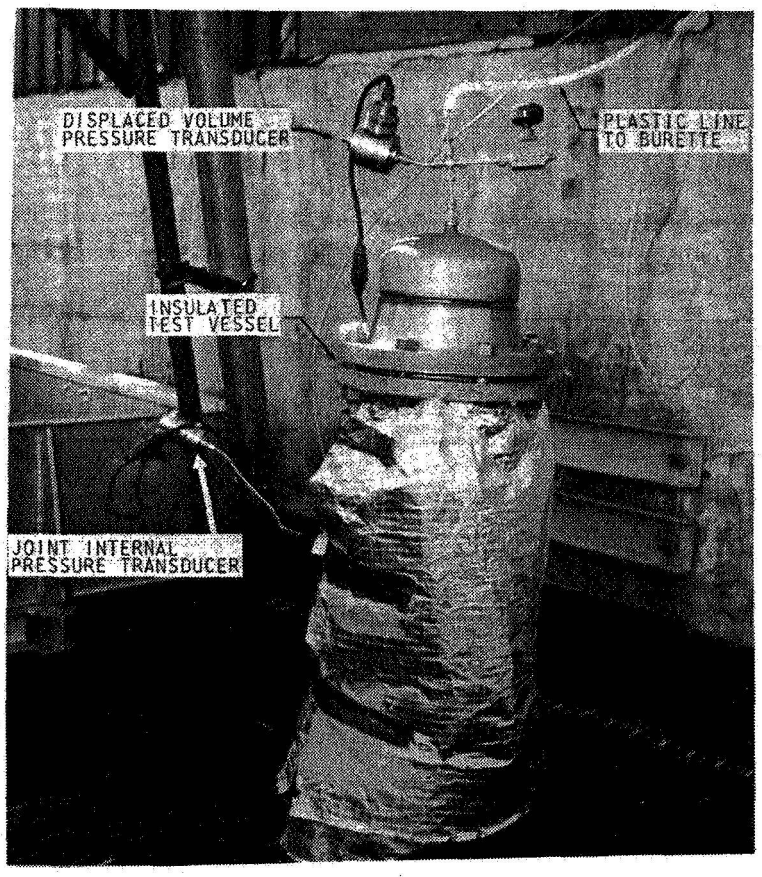

Figure 28. - Yield Determination and Burst Test Vessel

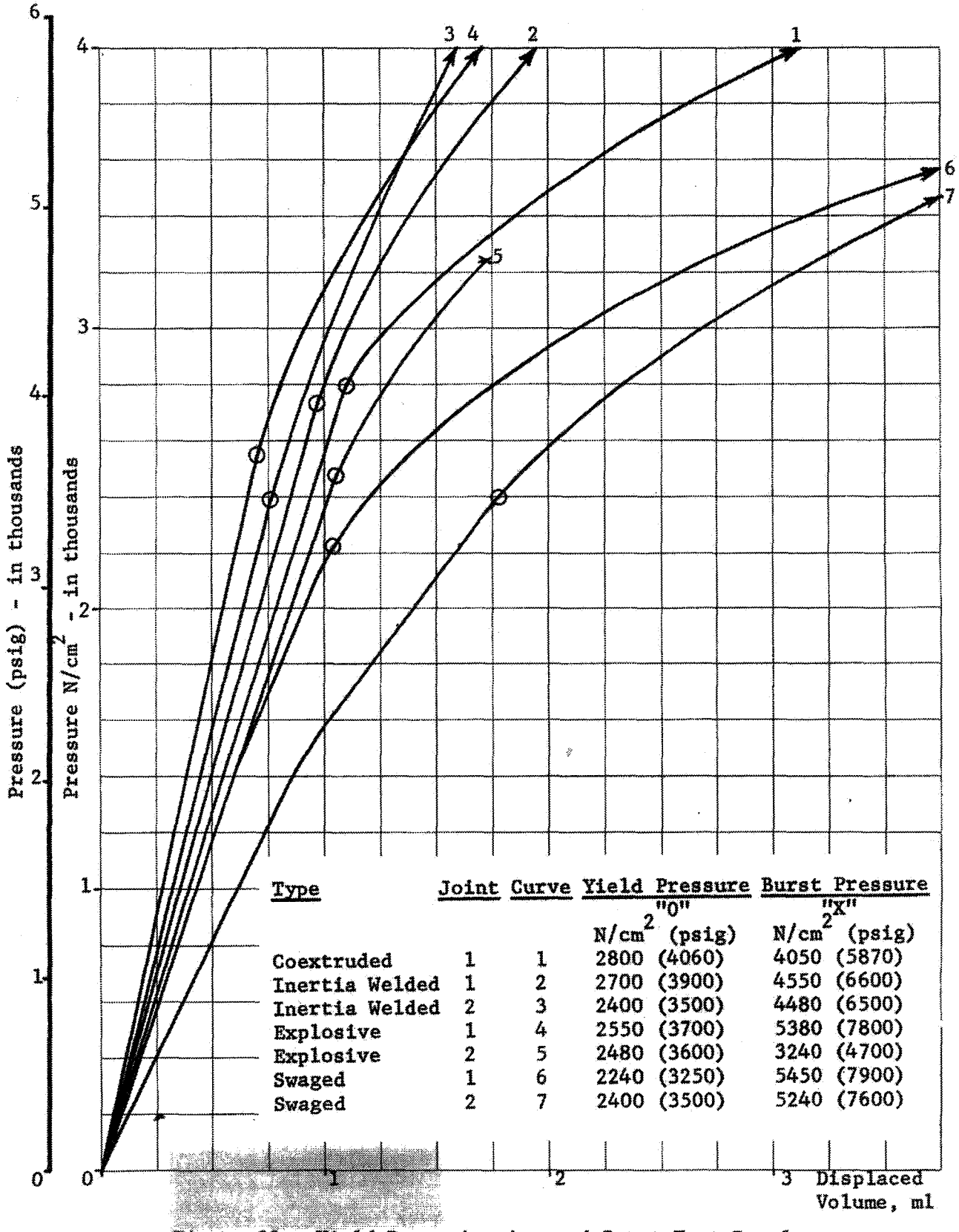

Type	Joint	Curve	Yield Pressure "0" N/cm² (psig)	Burst Pressure "X" N/cm² (psig)
Coextruded	1	1	2800 (4060)	4050 (5870)
Inertia Welded	1	2	2700 (3900)	4550 (6600)
Inertia Welded	2	3	2400 (3500)	4480 (6500)
Explosive	1	4	2550 (3700)	5380 (7800)
Explosive	2	5	2480 (3600)	3240 (4700)
Swaged	1	6	2240 (3250)	5450 (7900)
Swaged	2	7	2400 (3500)	5240 (7600)

Figure 29.- Yield Determination and Burst Test Results

Evaluation of the yield pressures obtained from each joint type indicated that the stainless steel in its annealed condition was probably the first portion of each joint to yield. This theoretically should happen in the hoop direction at a pressure of 2590 N/cm^2 (3750 psig) (reference Appendix B). The coextruded joint tested was made from cold worked stainless which allowed the yield pressure to become somewhat higher and perhaps allowed the yield to occur in the aluminum portion of the joint. The swaged construction joints both indicated a "minor" yield point at about 1450 N/cm^2 (2100 psig) where the compliance of the joint changed slightly; however, the pressure/strain relationship remained linear. This indication was not considered to be the yield of this joint type. In order to keep the testing of each joint type as comparable as possible (since no gross differences in yield pressure were observed), a proof pressure level of 2210 N/cm^2 (3200 psig) and a corresponding working pressure/leak check pressure of 1450 N/cm^2 (2100 psig) were established.

Proof Test Results

Each of the joints (except those subjected initially to the yield determination and burst tests and those used as ultrasonic inspection reference units) was subjected to a proof pressure test to a level of 2200 N/cm^2 (3200 psig) for a 5 minute period. Visual inspection following this test revealed no joint degradation.

Operating Pressure Leakage Test Results

All dissimilar metals joints were subjected to external leakage tests with the joints pressurized internally with gaseous helium to an operating pressure of 1450 N/cm^2 (2100 psig). Leakage measurements were accomplished using a Consolidated Electrodynamics Corporation Mass Spectrometer Leak Detector, Model 24-120. Figure 30 shows a typical operating pressure leakage test in progress. If gross leakage (leakage beyond the measurement capability of the MSLD) occurred, the metal joints were subjected to an external leakage test by using the water displacement method. The pressure during gross leakage tests was 1450 N/cm^2 (2100 psig), or less if the leak rate was too great to measure at operating pressure. Operating pressure leakage test results for each joint are tabulated in Table 7.

Examination of the test results for the explosive bonded joints indicates that seven out of thirteen joints that were tested were leakage free. The remaining joints had leakage rates from 15 cc/min to 400 cc/min at 10 N/cm^2 (15psig). Leakage test results after thermal cycling of the explosive bonded joints indicated that the joints that were leak free prior to the cycling remained leak free; while the one joint which exhibited leakage prior to cycling exhibited approximately twice that leakage rate following cycling. Results from galvanic corrosion showed that the corrosive environment did not influence the sealing integrity of the explosive bonds.

TABLE 7.- OPERATING PRESSURE LEAKAGE TEST RESULTS

	EXPLOSIVE WELDED	INERTIA WELDED	SWAGED CONSTRUCTION	COEXTRUDED
1			13 cc/min @ "E" 1.0 cc/min @ "E"	
2			1.5 cc/min @"E" 0 cc/min @ "E"	zero zero
3	Gross Leak @ "F"	zero zero	1.5 cc/min @"E" 0 cc/min "E"	
4	45 cc/min @ "E" 80 cc/min @ "E"	zero zero	25 cc/min @ "E" 0 cc/min "E"	
5	zero zero	zero zero	0.5 cc/min @ "E" 0 cc/min @ "E"	
6	Gross Leak @ "B"	zero zero	4 cc/min @ "E" 1.0 cc/min @ "E"	
7	zero	zero	65 cc/min @ "E"	
8	75 cc/min @ "A"	zero	55 cc/min @ "E"	
9	zero	zero	47 cc/min @ "E"	
10	zero	zero	7 cc/min @ "E"	
11	zero zero	zero 10 cc/min @ "F"	22 cc/min @ "E" [10 cc/min @ "E" zero]	
12	zero zero	zero 0 cc/min @ "G"	4 cc/min @ "E" zero	
13	400 cc/min @ "A"	zero	20 cc/min @ "E"	
14	zero	zero		
15	175 cc/min @ "B"			

NOTE: 1. "Zero" indicates less than 3×10^{-10} scc/sec at 1450 N/cm^2 (2100 psig) test pressure.

2. First entry is test prior to environment. Second entry is test after environment.

3. "A" indicates 10 N/cm^2 (15 psig) "E" indicates 345 N/cm^2 (500 psig)
"B" indicates 17 N/cm^2 (25 psig) "F" indicates 690 N/cm^2 (1000 psig)
"C" indicates 52 N/cm^2 (75 psig) "G" indicates 1034 N/cm^2 (1500 psig)
"D" indicates 276 N/cm^2 (400 psig) "H" indicates 1448 N/cm^2 (2100 psig)

Examination of the test results for the inertia welded joints indicates that the joints were essentially leak-free for all phases of testing. All of the thirteen joints tested exhibited zero leakage during initial test conditions. Leakage test results after thermal cycling of the inertia welded joints showed that the temperature cycles did nothing to affect the sealing integrity of the bonds. Leakage test results upon completion of the galvanic corrosion tests showed that the corrosive environment caused the bonds to degrade. Joint 11 exhibited a leak rate of 10 cc/min at 690 N/cm^2 (1000 psig) and joint 12 exhibited a leak rate of 0 cc/min at 1034 N/cm^2 (1500 psig) but both of the joints failed before a proof pressure of 2206 N/cm^2 (3200 psig) was achieved.

Examination of the test results for the swaged joints indicates that all thirteen joints exhibited high leakage during most phases of testing. Thermal cycle test results shown that the temperature cycling of the swaged joints had a beneficial effect upon the bonds. In all cases the leakage rates were improved, in one case quite drastically, from 22 cc/min to 0 cc/min at 500 psig. Exposure of the swaged joints to the corrosive environment during galvanic corrosion tests again produced beneficial results. In both cases the leakage rate of the joints was 0 cc/min at 1448 N/cm^2 (2100 psig) nitrogen after completion of the test.

Only one coextruded joint was available for leakage testing. The coextruded joint exhibited 0 cc/min leakage at 1450 N/cm^2 (2100 psig) helium before and after the thermal cycle test.

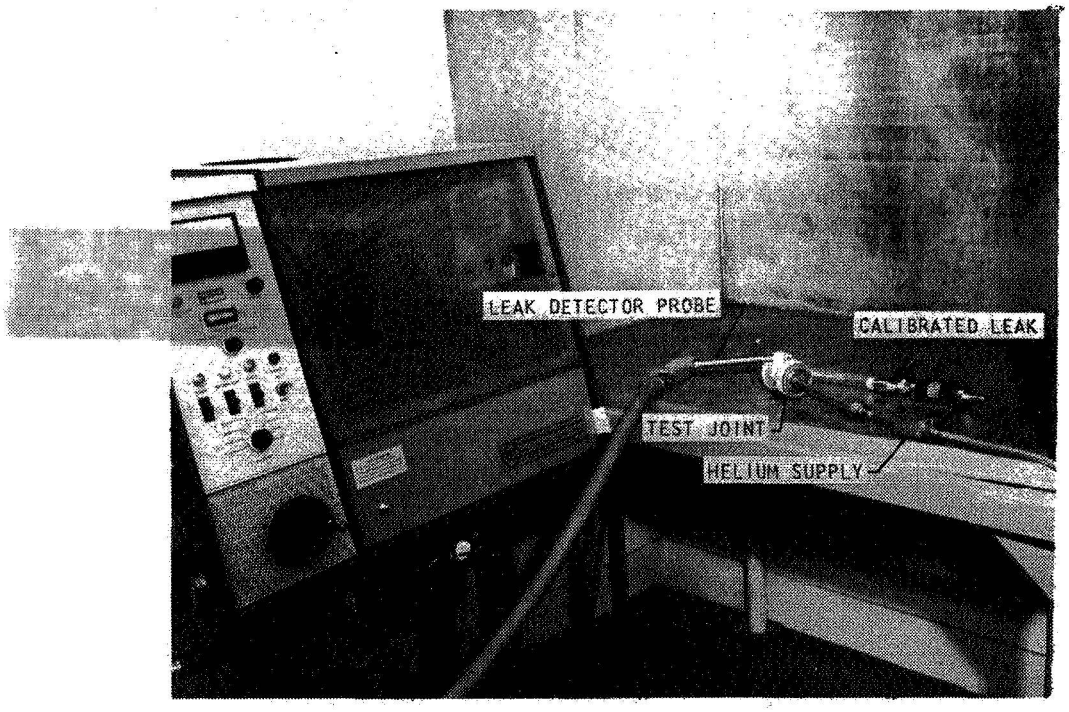

Figure 30.- Operating Pressure Leakage Test Setup

Thermal Cycle Test Results

The thermal cycle test was performed using the fixture shown in Appendix D. A photograph of the system appears in Figure 31. Joints listed in Table 8 were subjected to the thermal cycles. It became apparent during post test evaluations of the first of each joint type that little degradation to the bonds had occurred after 100 thermal cycles, so all subsequent joints were also subjected to 100 cycles.

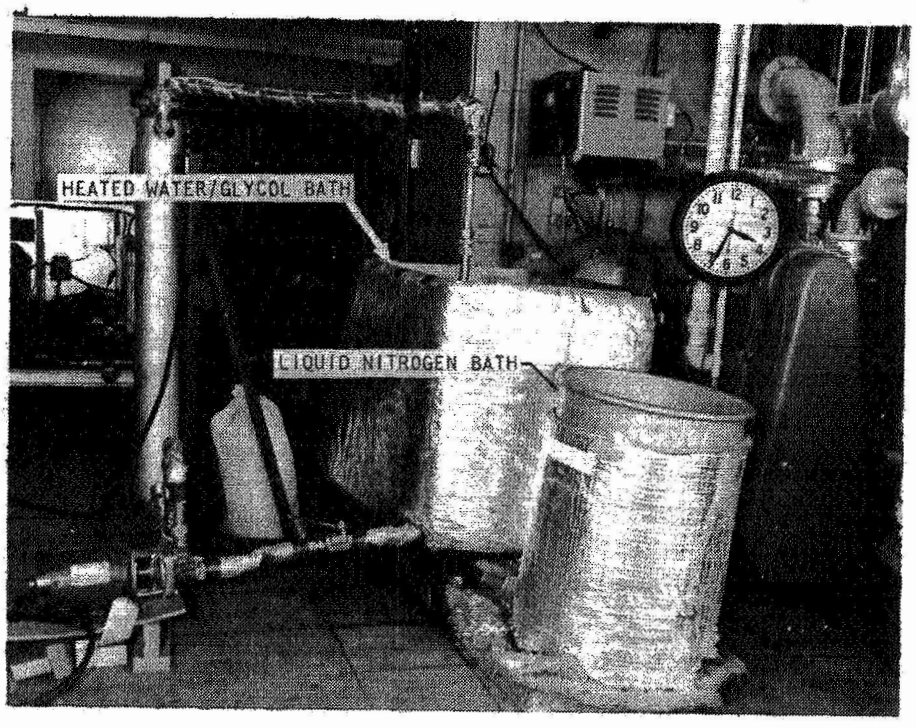

Figure 31.- Thermal Cycle Test Fixture

TABLE 8.- THERMAL CYCLE TEST

Joint Type	Joint Number	Number of Cycles
Inertia Welded	3,4,5,6	100
Explosive Welded	4,5,14	100
Swaged Construction	3,4,5,6	100
Coextruded	2	I00

Pressure Cycle Test Results

The pressure cycle test was planned to run from 10 to 50% of the theoretical burst strength of the joints. Based on an ultimate strength requirement for 2219-T851 extruded aluminum of 40,000 N/cm^2 (58,000 psi), the burst strength of the aluminum in the hoop failure mode is 4211 N/cm^2 6107 psig. This burst strength indicated that a cycling rate of 421 N/cm^2 (611 psig) to 2106 N/cm^2 (3054 psig) was necessary. This was altered slightly to establish cycling limits of 427 N/cm^2 (620 psig) to 2137 N/cm^2 (3100 psig). The upper limit was somewhat below the apparent yield pressure for each joint type (reference Figure 29) so the test was felt to be reasonable though severe, and was probably the most severe test to which the joints were subjected. The pressure cycle fixture was designed to stop automatically when joint pressure fell below specifications when cycling, thus indicating that a joint had developed a leak. The overall test fixture is shown in Figure 32. All of the joints subjected to the pressure cycling test were sealed at the aluminum end with the use of mechanical closures rather than welded closures. The stainless ends were sealed either by a welded plug, or by welding the joints together in tandem as shown in Figure 33. The joints were all pressure cycled until failure occurred. The number of cycles to failure observed on the first two joints of each type indicated a data scatter, so it was elected to test the remaining joints at the same pressure level rather than at a reduced level. The data appears in Table 9. The coextruded joints were not available in time to subject them to this test.

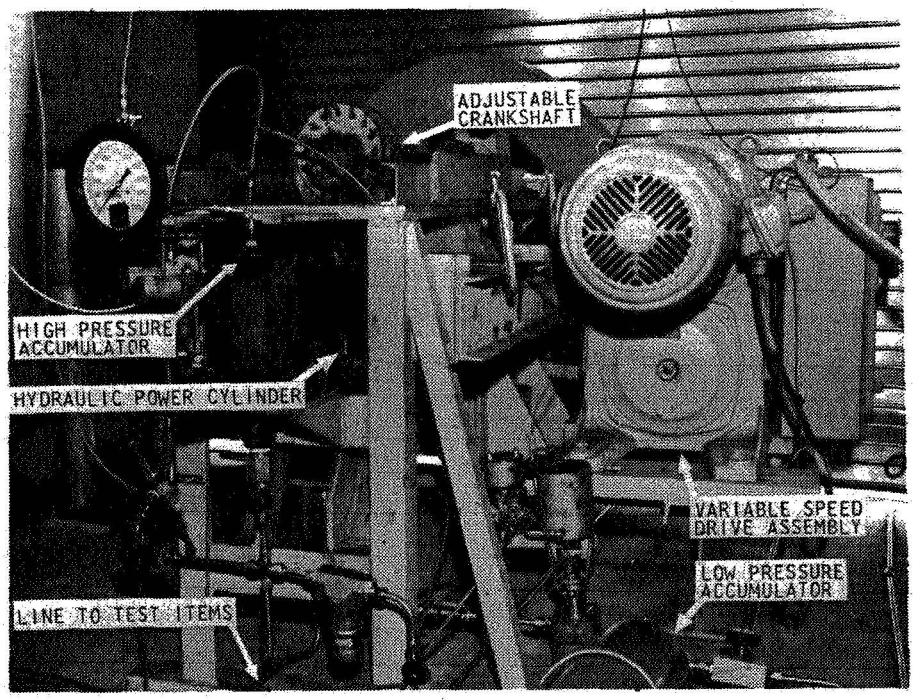

Figure 32.- Pressure Cycle Test Fixture

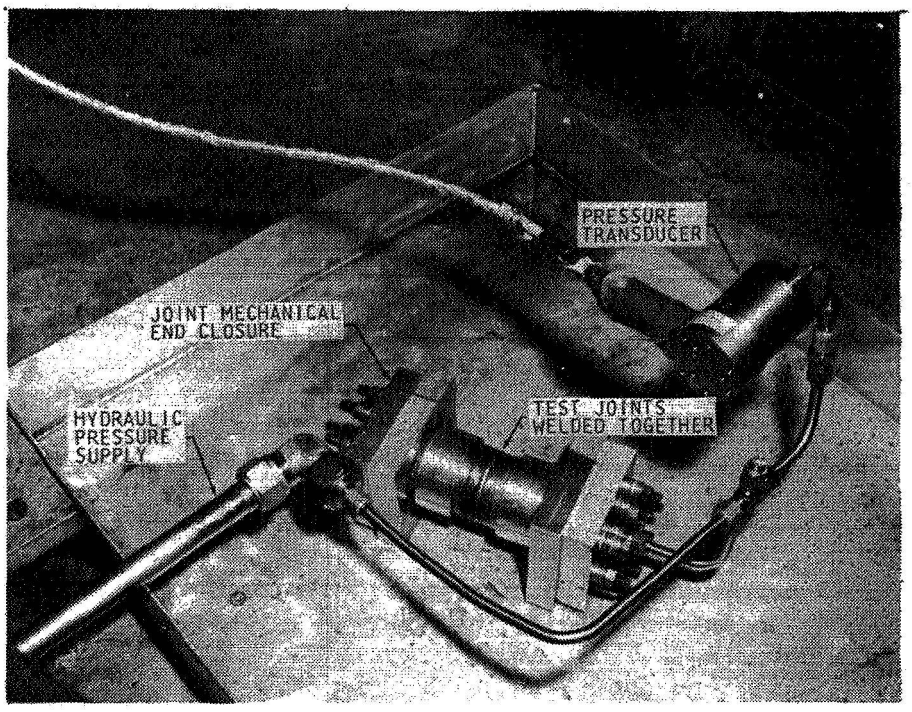

Figure 33.- Typical Joints Being Subjected to Pressure Cycle

TABLE 9. - PRESSURE CYCLE TEST RESULTS

TEST SPECIMEN NUMBER	CYCLES TO FAILURE FOR EACH JOINT TYPE		
	INERTIA WELDED	EXPLOSIVE WELDED	SWAGED CONSTRUCTION
7	151,154	27,079	24,276
8	118,017	Not Tested**	34,665
9	232,366	14,513	46,165*
10	189,107	29,747	40,697*

*Joint modified by machined relief of unnecessary notch.

**Joint not tested due to leakage.

The failure mode of the explosive welded joints was a slight separation at the SS/Ag bond line. The inertia welded joints, however, failed in the aluminum portion as illustrated in Figure 34. Swaged construction joints 9 and 10 failed in the aluminum portion as shown in Figure 35. Figure 36 shows one of the swaged construction joints which was sectioned after cyclic failure. This joint provided the best visual information for understanding of the swaged construction method since other joints that had been burst and then sectioned always had a portion of the bond destroyed. Visible are the aluminum and stainless steel portions, as well as the aluminum back-up ring. Serrations in the aluminum can be seen to have been penetrated by the stainless steel. The aluminum has also been axially penetrated particularly well by the end of the stainless steel portion.

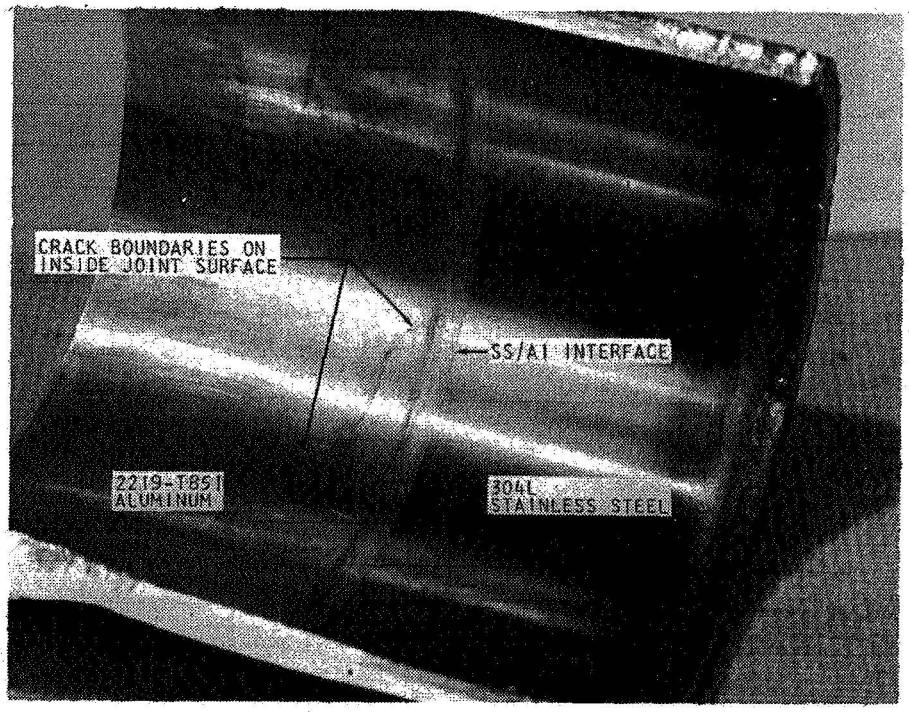

Figure 34.- Fatigue Failure of Inertia Welded Joint

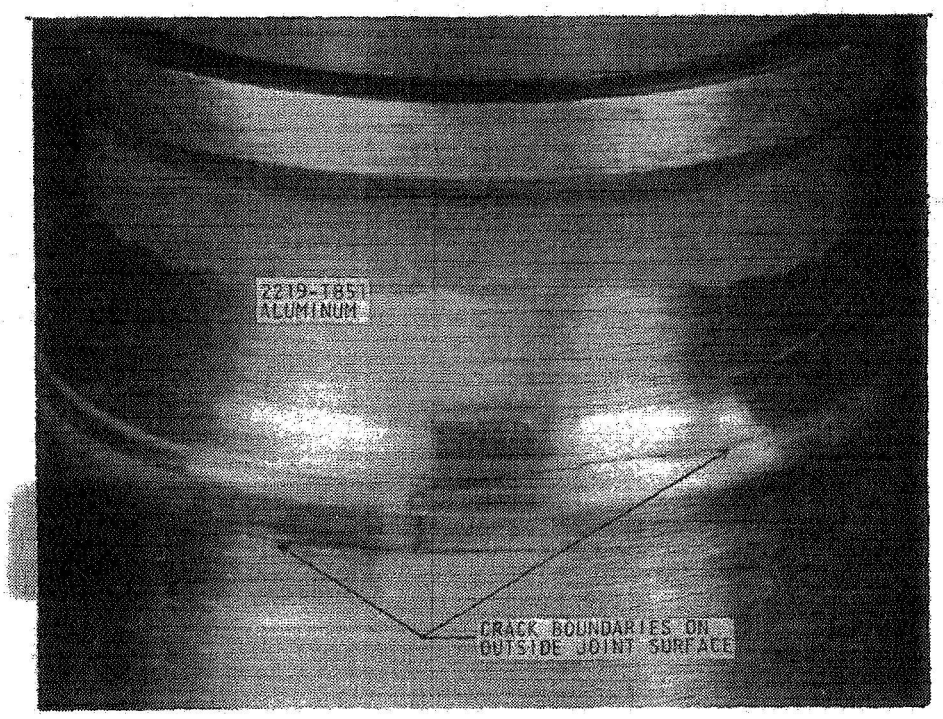

Figure 35.- Fatigue Failure of Swaged Joint

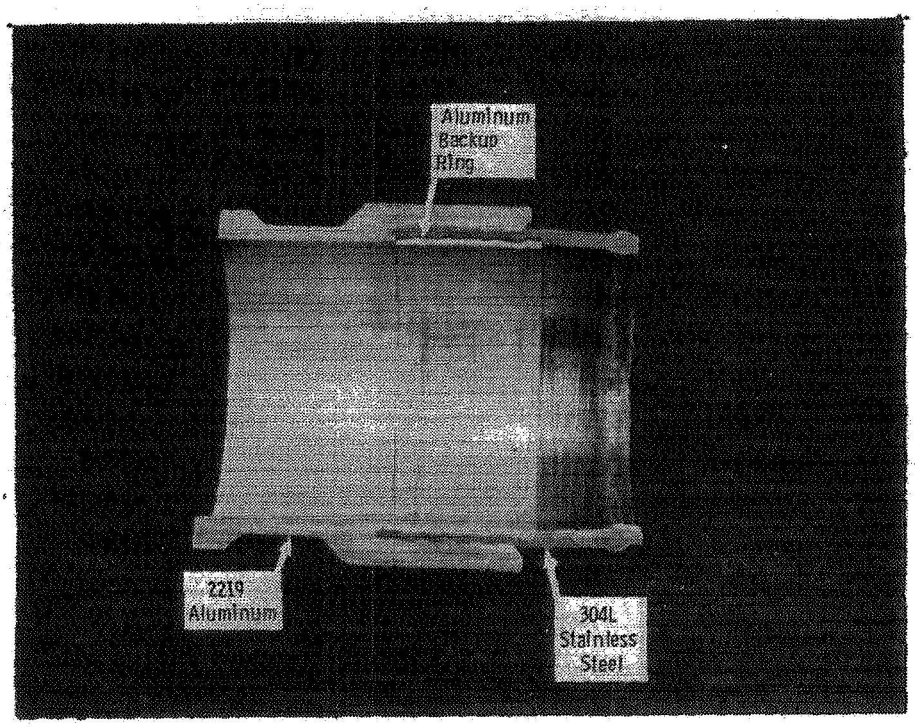

Figure 36.- Section of Swaged Construction Joint

Galvanic Corrosion Test Results

This test was performed to establish the relative resistance of each joint type to galvanic corrosion when submerged in a 5% by weight $NaCl/H_2O$ solution. The bonds were not protected from the electrolyte during this test in order to determine the effect of residual stress or metallurgical alteration on the corrosion process. In order to monitor any gross corrosive deterioration of the joints during the four week submersion period, electrical leads were connected to the joints to allow resistance measurements through the bond area. Since the electrical connection on the joints could also corrode and cause misleading resistance measurements, the connections were protected with RTV silicone sealer. Two connections were made at each end of each joint so that a tare resistance could be established in order to assure connection integrity before evaluation of the bond. This method of protecting the connections worked quite well, as no apparent resistance change was observed in the tare readings and subsequent dissassembly of the joints after the corrosion testing showed that the RTV provided a good seal from the salt water solution. The joints were all subjected to leakage and burst tests after removal from the bath, and these data are presented in those respective test sections. Figure 37 is a photograph of the fixture used for the corrosion test showing joints prior to submersion, the test tank, and the 4735-1 Leeds and Northrup Guarded Wheatstone Bridge and the 2430-0 Leeds and Northrup Galvanometer used for the resistance measurements.

The resistance through the bond area for each of the joints subjected to the electrolytic solution was measured at 4 to 6 day intervals to determine if corrosion of the metals had a deleterious effect upon the bond. The resistance measurements were monitored to an accuracy of six places and were found to change very little throughout the 4 week test period. Any small variations in resistance measurements were determined to have been caused by slight temperature differences of the solution between resistance measurement periods. Inspection after removal from the bath indicated the explosive bonded joints and swaged joints appeared to have been affected very little by galvanic corrosion. The inertia welded joints showed the most galvanic corrosion reaction to the salt water electrolyte. The corrosion occurred primarily in the 6061 portion of the bond. Figures 38 and 39 show typical galvanic corrosive attacks on the inertia welded bond.

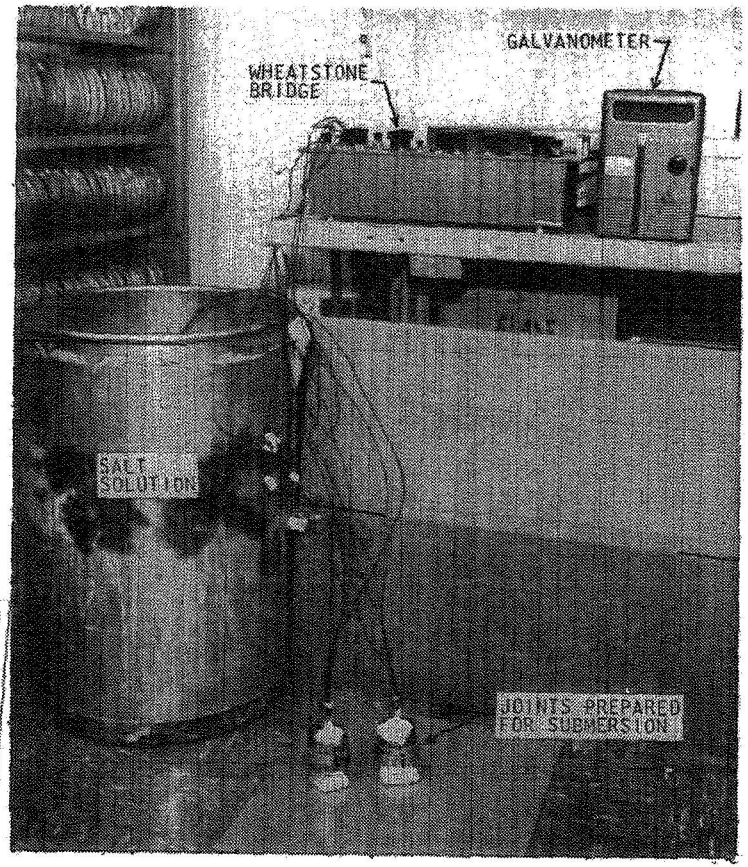

Figure 37.- Corrosion Test Fixture

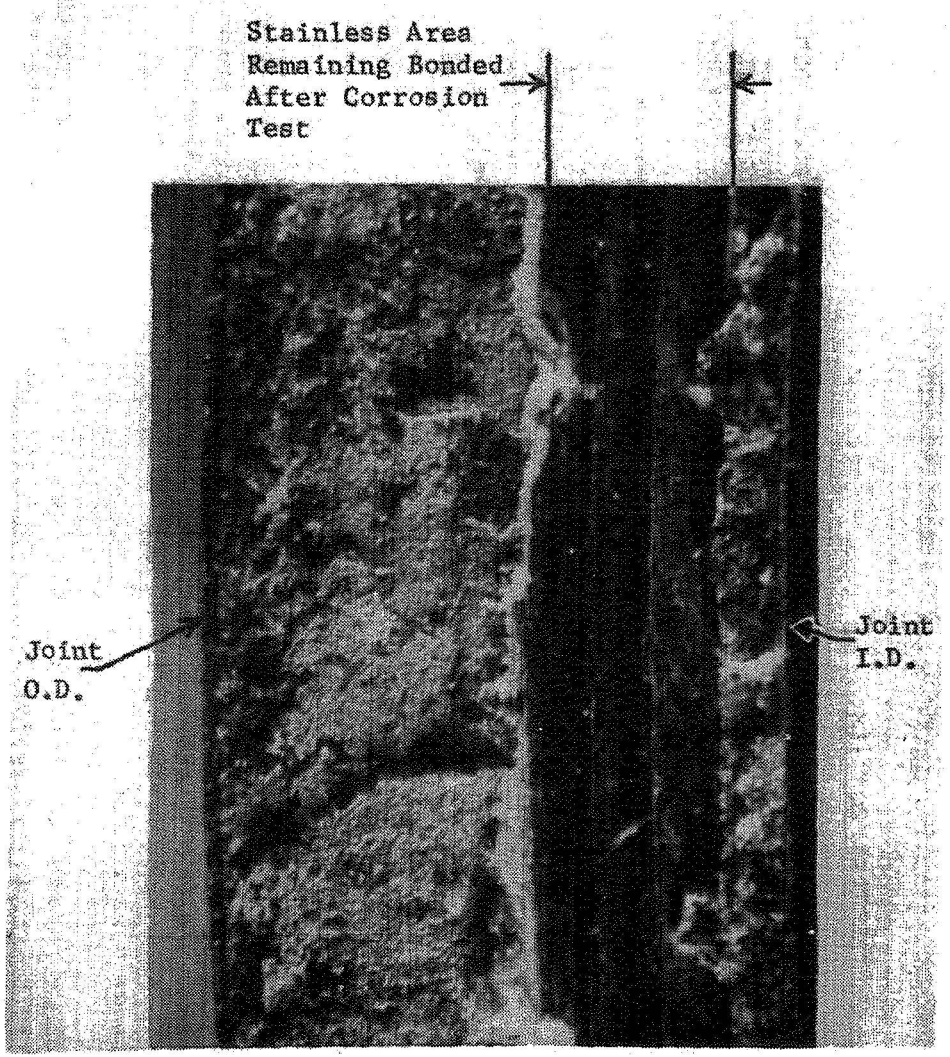

Figure 38.- Inertia Welded Joint After Corrosion and Burst Test-View of Stainless Surface at Interface

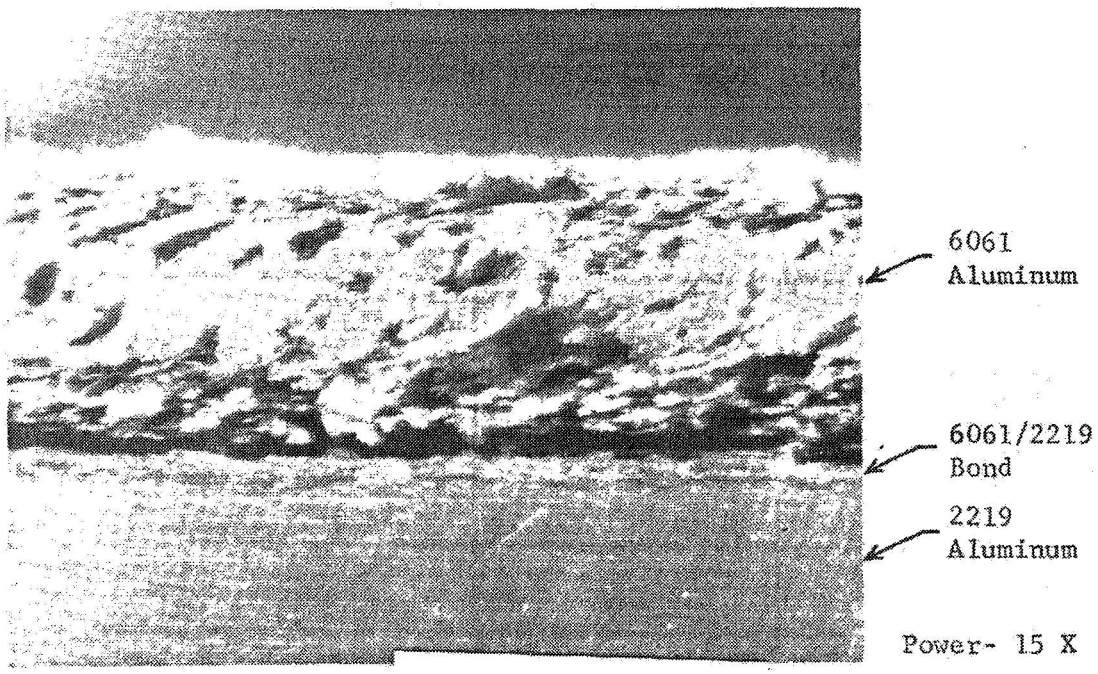

Figure 39.- Inertia Welded Joint After Corrosion and Burst Test-View of Aluminum Joint Half O.D. at 2219/6061 Interface

Burst Test Results

As a determination of a joint's structural strength, many of them were subjected to internal pressurization until burst occurred. This test was performed on some joints prior to any other test, some after a proof pressure and leakage test, and some following environmental testing to determine residual strength. The results are presented in Table 10. A comparison of the observed burst pressures with equivalent axial and hoop stresses can be obtained by referring to Appendix B. Most of the joints of each type failed in the same structural manner when hydroburst. Typical burst modes are shown in the following figures:

Figure 40 shows an explosive welded joint after burst and Figure 41 shows the typical appearance of the joint when it was then separated into two pieces. The failure occurred partially in the bond between the silver and stainless and partially in axial shear in the aluminum. One of the explosive welded joints failed in the hoop mode as shown in Figure 42.

Figure 43 shows an inertia welded joint after burst. There was no apparent "necking" of the aluminum and very little residual aluminum remained on the stainless portion. This apparent "brittle" behavior of the bond at the 304L/6061 interface was evident on all inertia welded joints subjected to burst, and none of the joints showed separation of the 6061/2219 aluminum interface. Even though the bond appeared to fail in a "brittle" manner, the strength level and consistency of these joints was excellent.

TABLE 10.- BURST TEST RESULTS

Test Joint No.	BURST PRESSURE N/Cm^2 (PSI)			
	INERTIA WELDED	EXPLOSIVE WELDED	SWAGED CONSTRUCTION	COEXTRUDED
1	4550 (6600)	5310 (7700)	5450 (7900)	4070 (5900)
2	4480 (6500)	3240 (4700) Weld Damage	5240 (7600)	4070 (5900) (After Thermal Cycle)
3	5650 (8200)	N/A (Leak)	5520 (8000)	3 thru 15 not tested
4	5240 (7600)	5450 (7900)	5650 (8200)	
5	5890 (8550)	5550 (8050)	6070 (8800)	
6	4760 (6900)	N/A (Leaks)	5650 (8200)	
7	N/A (Cycle Tested)	N/A (Cycle Tested)	N/A (Cycle Tested)	
8	N/A (Cycle Tested)	N/A (Leaks)	N/A (Cycle Tested)	
9	N/A (Cycle Tested)	N/A (Cycle Tested)	N/A (Cycle Tested)	
10	N/A (Cycle Tested)	N/A (Cycle Tested)	N/A (Cycle Tested)	
11	1520 (2200) (Corrosion Fail.)	3100 (4500)	4100 (5950)	
12	1030 (1500) (Corrosion Fail.)	6340 (9200)	5170 (7500)	
13	5790 (8400)	830 (1200) (Leak)	5580 (8100)	
14	5650 (8200)	5520 (8000)	N/A (Leak)	
15	N/A	N/A (Leak)	N/A (Leak)	

NOTE: Theoretical burst pressure in the hoop mode is 4206 N/cm^2 (6,100 psig) based on 40,000 N/cm^2 (58,000 psig) ultimate stress for 2219-T8511 aluminum.

Figure 44 shows a typical hydroburst failure of a swaged construction joint. The stainless end slipped axially from the aluminum to a degree sufficient to allow leakage. One joint failed in a manner different from that shown in Figure 44; the stainless portion failed in axial shear where its sectional area had been thinned for the swaging process, and is shown in Figure 45.

Figure 46 shows a hydroburst failure of a coextruded joint. This was also a "brittle" type failure and had essentially no necking of the aluminum portion of the joint. The bond failed similarly to the inertia welded joint in that only a small amount of aluminum remained attached to the O.D. of the stainless cone following burst.

It should be pointed out that if these joints were sufficiently long in the aluminum portions to allow hoop stress failure in the aluminum, the failure pressure would have been 4206 N/cm^2 (6100 psig) assuming a 40,000 N/cm^2 (58,000 psi) ultimate stress for 2219-T8511 aluminum. Since most of the failure pressures were well above this, it can be concluded that the joints were generally stronger than the parent material of the weaker component.

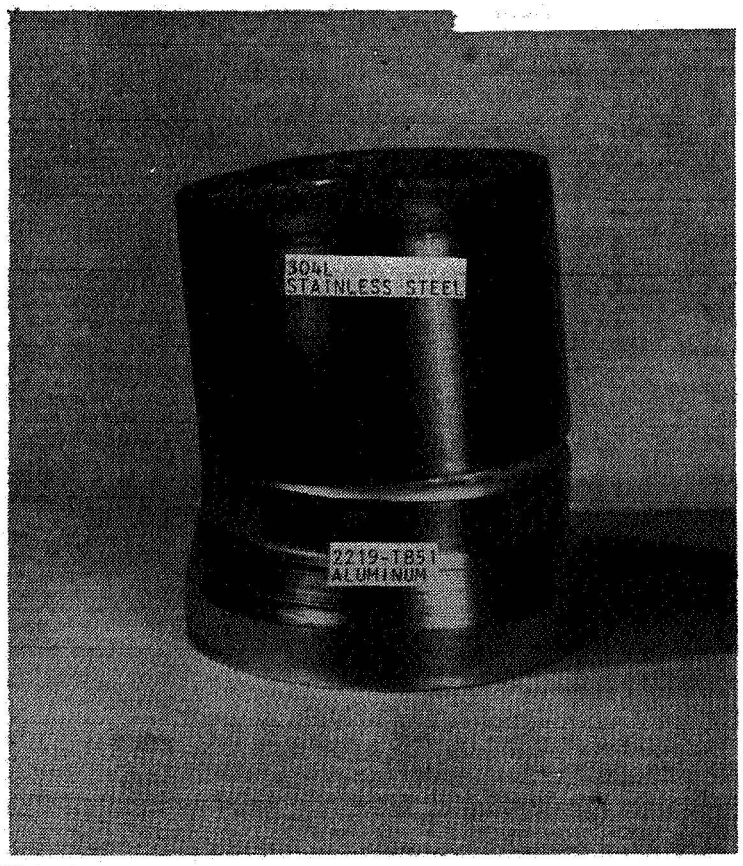

Figure 40.- Explosive Welded Joint Burst Failure

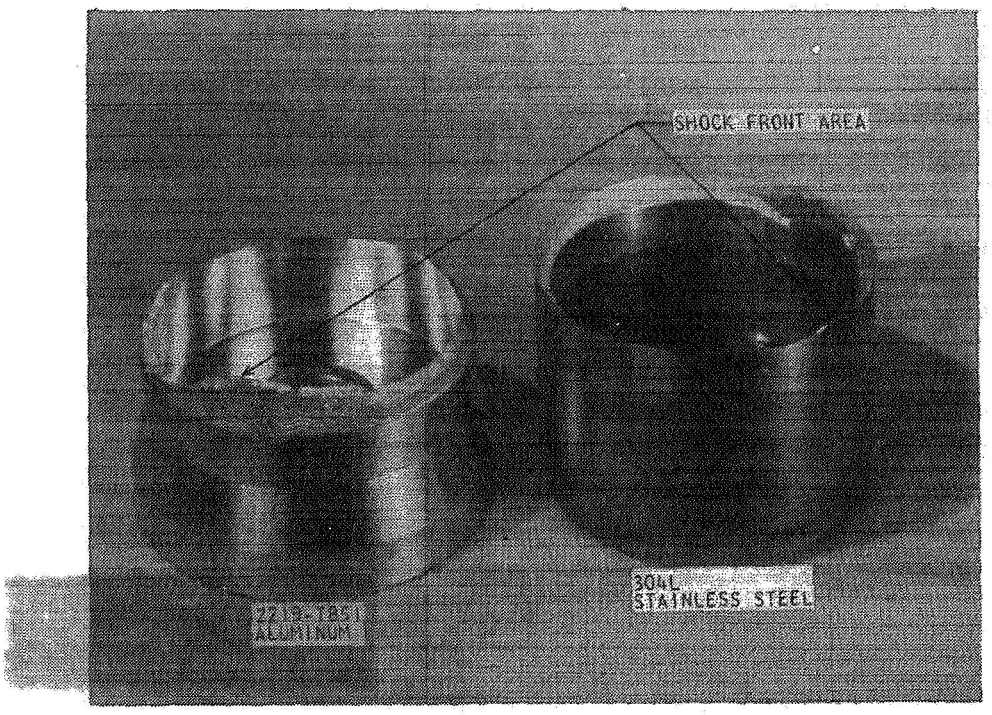

Figure 41.- Explosive Welded Joint Burst Failure After Separation

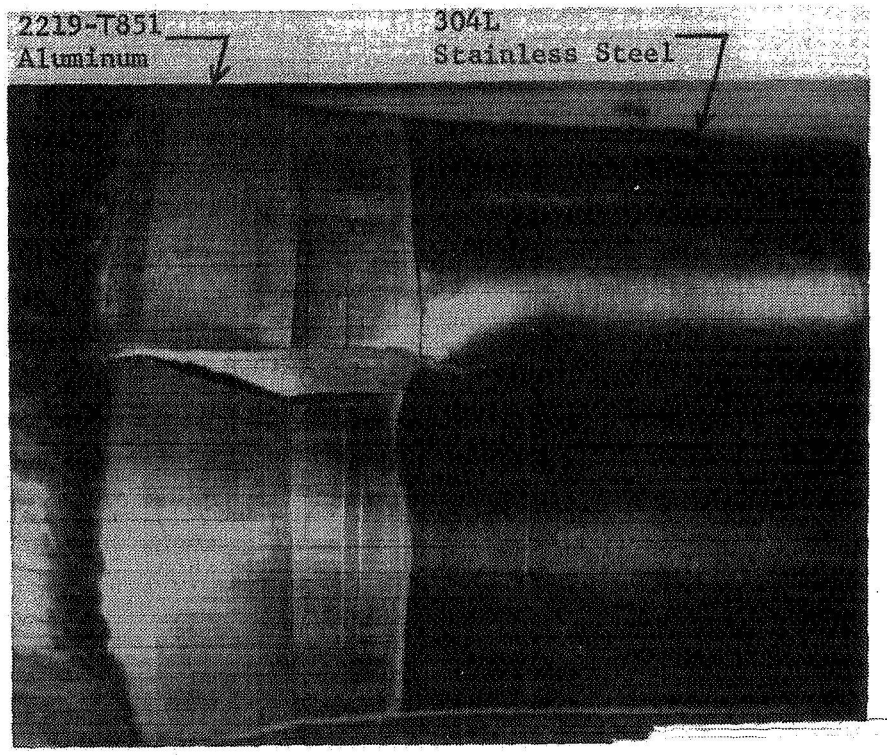

Figure 42.- Hoop Mode Failure of Explosive Welded Joint

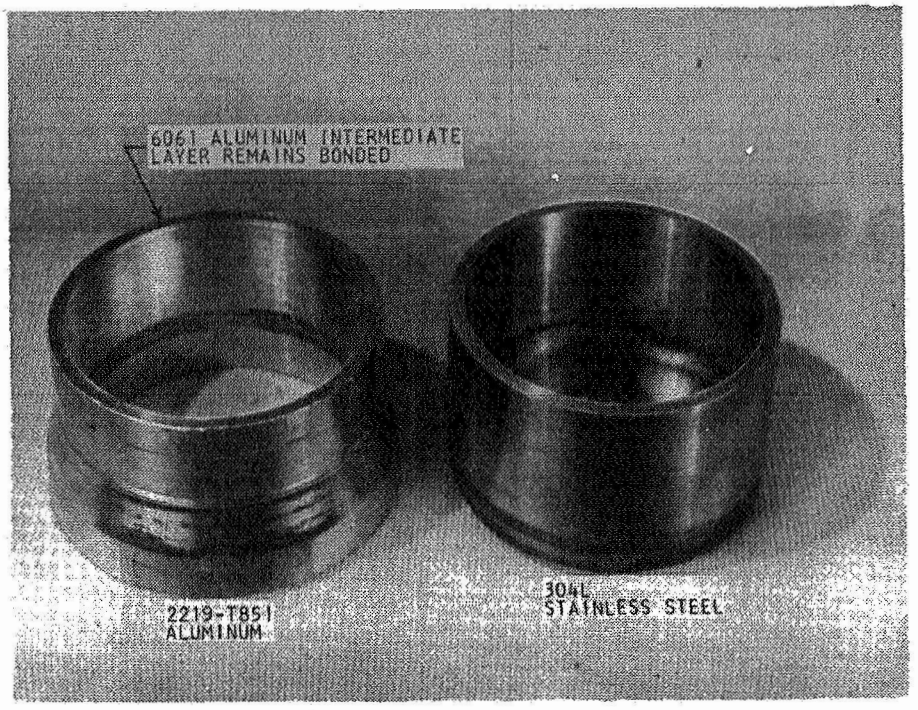

Figure 43. - Inertia Welded Joint Burst Failure

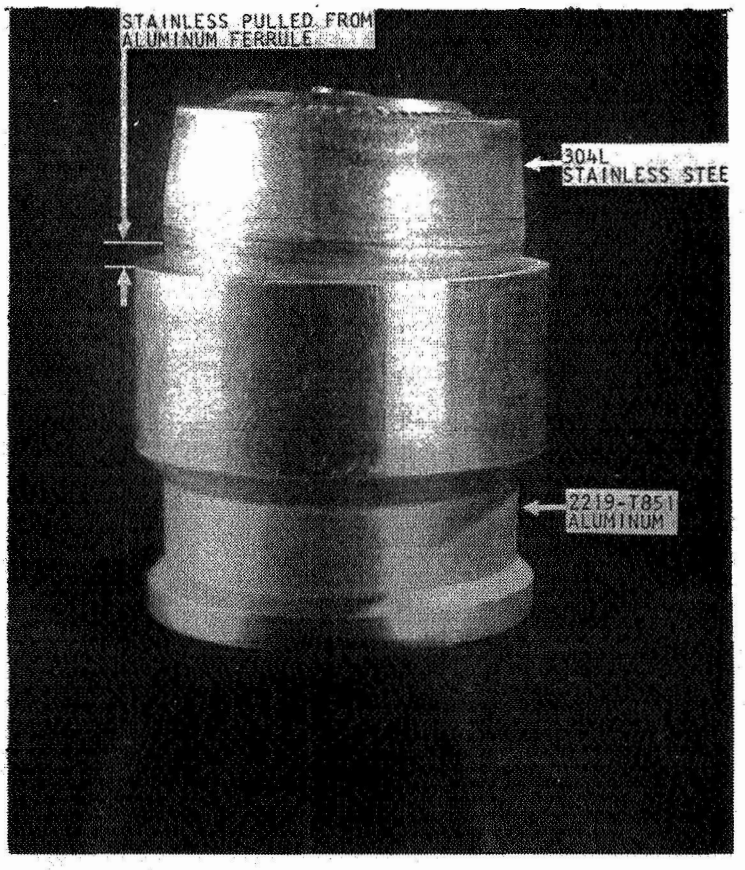

Figure 44. - Swaged Construction Joint Burst Failure

Figure 45. - Singular Occurrence of Axial Shear Failure of Swaged Construction Joint

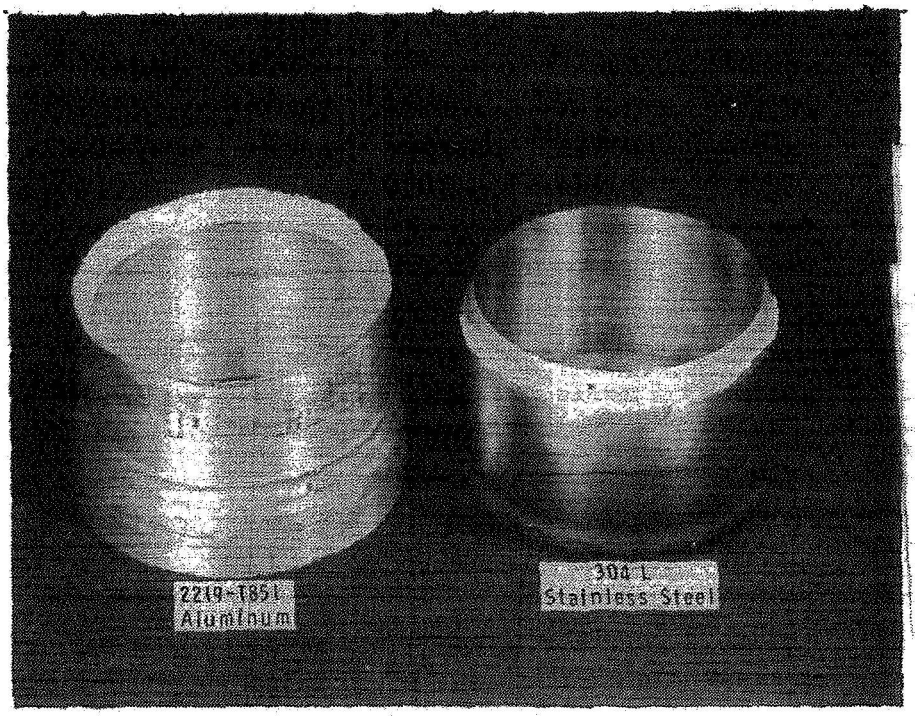

Figure 46. - Coextruded Joint Burst Failure

Non-Destructive Test Results

All dissimilar metals joints were subjected to various types of non-destructive tests to determine if any flaws could be found in the bonds. The types of non-destructive tests that were chosen to be performed on the joints were as follows: Dye penetrant, one atmosphere helium leakage, and ultrasonic. X-ray analyses were also considered but a decision was made not to include them as part of the non-destructive test format. The determination was made that an x-ray analysis of a dissimilar metal bond could not really determine if two different metals were actually bonded to one another or if the two metals were only pressed together. It was also determined that only major flaws would be revealed by an X-ray scan and small voids, inclusions, or cracks could remain undetected.

Dye Penetrant Test Results

Dye penetrant inspection was performed on each joint (except swaged construction) in the following manner: (1) the inner and outer bonds were thoroughly cleaned of any oils or contaminants, (2) a fluorescent penetrating solution was sparingly wiped over the inner and outer bonds and allowed to remain for a 5 minute time period, (3) all excess penetrating solution was removed from the bond surfaces by wiping with a cloth moistened with penetrant remover, (4) developer was sprayed over the inner and outer bond surfaces, and (5) the bond surfaces were carefully examined for fluorescence by examining the areas under ultraviolet light.

All data obtained during dye penetrant testing is shown in Table 11. Swaged joints were not subjected to dye penetrant inspection because the construction and geometry of these joints are not well suited to penetrant inspection.

One Atmosphere Helium Leakage Test Results

All dissimilar metals joints were subjected to a one atmosphere helium leakage test per the method described in Appendix D. A photograph of the test appears as Figure 47. All leakage rates for the dissimilar metals joints are shown in Table 12.

TABLE 11. - DYE PENETRANT TEST RESULTS

	EXPLOSIVE WELDED	INERTIA WELDED	COEXTRUDED
1	O.D. Spotty I.D. None ———	O.D. None I.D. None O.D. None I.D. None	O.D. None I.D. None ———
2	O.D. Spotty I.D. None ———	O.D. None I.D. None O.D. None I.D. None	O.D. None I.D. None ———
3	O.D. Spotty I.D. None ———	O.D. None I.D. Spotty O.D. None I.D. Spotty	
4	O.D. Heavy I.D. S.F. O.D. Heavy ———	O.D. None I.D. Spotty O.D. None I.D. Spotty	
5	O.D. Heavy I.D. None O.D. Heavy ———	O.D. None I.D. Spotty O.D. None I.D. Spotty	
6	O.D. S.F. I.D. S.F. ———	O.D. None I.D. Spotty O.D. None ———	
7	O.D. Heavy I.D. SF O.D. Heavy I.D. SF	O.D. None I.D. Spotty O.D. Spotty I.D. Spotty	
8	O.D. Heavy I.D. SF ———	O.D. None I.D. Heavy O.D. Spotty I.D. Heavy	
9	O.D. Heavy I.D. S.F. O.D. Heavy I.D. S.F.	O.D. None I.D. Spotty O.D. None I.D. Spotty	
10	O.D. Spotty I.D. None O.D. Spotty I.D. None	O.D. None I.D. Spotty O.D. None I.D. Spotty	
11	O.D. Heavy I.D. None O.D. Heavy I.D. None	O.D. None I.D. Heavy O.D. None I.D. Heavy	
12	O.D. Spotty I.D. None O.D. Spotty I.D. None	O.D. None I.D. Heavy O.D. None I.D. Heavy	
13	O.D. Heavy I.D. Heavy ———	O.D. None I.D. Heavy O.D. None ———	
14	O.D. Spotty I.D. S.F. ———	O.D. None I.D. Heavy ———	
15	O.D. Heavy I.D. S.F. ———	O.D. None I.D. Heavy ———	

NOTE:
1. First entry represents test prior to proof-second follows proof.
2. S.F. indicates a penetrant observation was made at the shock front area only.
3. All inertia welded indications were at Al/Al bond, except 11, 13, 14 & 15, which were at Al/SS and Al/Al bonds.
4. Uresco P-151 fluorescent penetrant used.

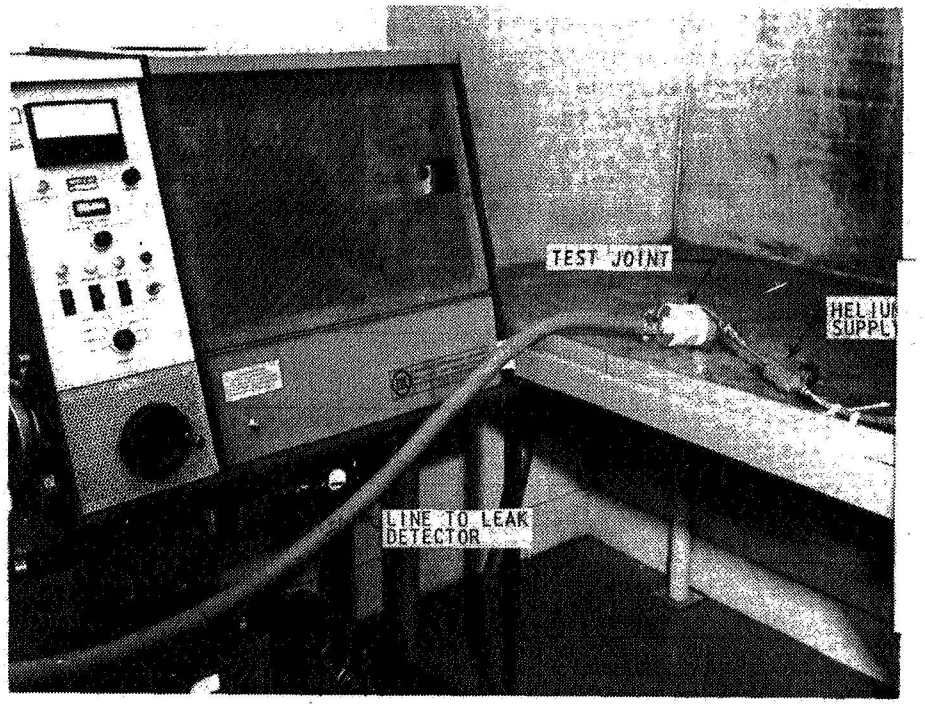

Figure 47. - One Atmosphere Helium Leakage Test

TABLE 12. - ONE ATMOSPHERE HELIUM LEAKAGE TEST RESULTS

	EXPLOSIVE WELDED	INERTIA WELDED	SWAGED CONSTRUCTION	COEXTRUDED
1	Zero	Zero	Off-Scale	Zero
2	Zero	Zero	Off-Scale	Zero
3	Zero	Zero	Zero	
4	Off-Scale	Zero	Zero	
5	Zero	Zero	Zero	
6	Off-Scale	Zero	Zero	
7	Zero	Zero	Zero	
8	Off-Scale	Zero	Zero	
9	Zero	Zero	Zero	
10	Zero	Zero	Zero	
11	Zero	Zero	Off-Scale	
12	Zero	Zero	Zero	
13	Off-Scale	Zero	Zero	
14	Zero	Zero	Off-Scale	
15	Off-Scale	Zero	Off-Scale	

NOTES: 1. "Zero" indicates leakage less than 3×10^{-10} scc/sec

2. "Off-Scale" indicates leakage greater than 3×10^{-5} scc/sec

Ultrasonic Inspection Test Results

Ultrasonic inspection of selected joints was performed to determine the applicability of this flaw inspection method for finding anomalies in the different bonds. An ultrasonic transducer and test joint were submerged in a water bath. The bond was then examined ultrasonicly by a shear wave inspection technique. Figure 48 is a schematic of the test arrangement used. The turntable speed was adjustable up to about 20 RPM, and was run near its upper limit for this test. The transducer was capable of moving constantly upward as the turntable rotated, and was adjusted to provide a C-scan across the joint at approximately 0.051 cm (0.020 in.) intervals. The electronics used were an Automation Industries UM-715 Reflectoscope in conjunction with a 10N Pulsar/Receiver and Transigate E550. A 0.635 cm (0.250 in.) diameter transducer with a flat end was operated at a frequency of 10 MHZ.

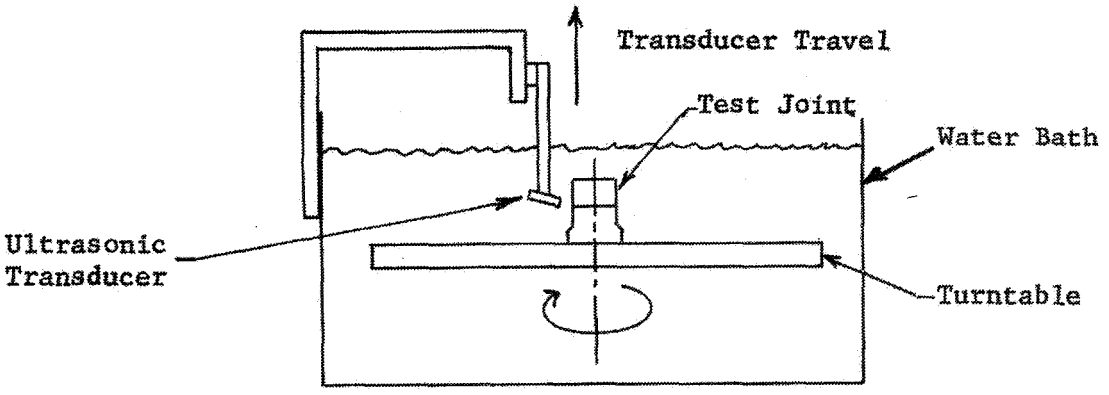

Figure 48. - Ultrasonic Test Setup

In order to provide a reference for a known flaw condition, EDM (electro-discharge machined) flaws were made in one of the inertia welded and one of the explosive welded joints. A decision was made to exclude swaged construction joints from the ultrasonic evaluation because of the difficulty in preparing meaningful flaws in a reference joint, and also because the ultrasonic determination of dissimilar metal contact would be difficult to properly relate to a leakage criterion. The EDM flaw orientation and geometry is shown in Figure 49.

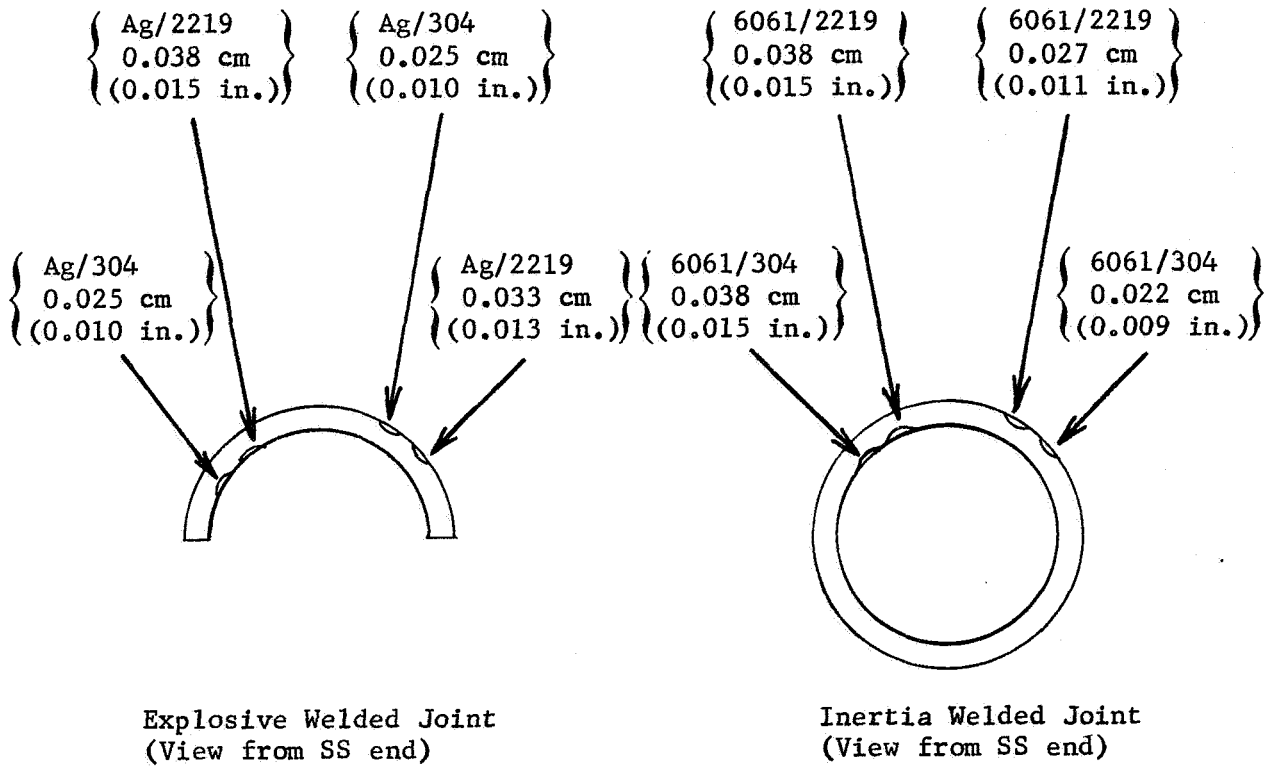

Figure 49. - EDM Flaw Depth - Ultrasonic Reference Joints

Inertia welded joint numbers 9 and 10 were inspected. These were examined prior to pressure cycle testing and also midway thru the cycling procedure to try to identify any flaw growth. The reference joint was placed in the inspection fixture and parameters were varied to allow identification of the EDM flaws. The transducer was placed at an angle of 0.28 rad (16°) relative to a plane normal to the joint axis. This angle had been developed previously during inspection of flat plate specimens as the angle providing the best compromise between sensitivity and capability of inspection to the surfaces of a specimen. Since the possibility existed that significant flaws existed in the bond area at or near the inner or outer surface, the inspection of only the internal volume of the bond would have been improper.

An initial inspection of the inertia welded reference joint was made to establish the proper sensitivity for the scan; that is, the level of reflected wave considered significant. The readout chart was triggered to print or not print based on the level of this sensitivity. Figure 50 is the inspection pattern obtained from the inertia welded reference joint. This pattern represents a "picture" of the joint looking from the outside surface at all the flaws present on or in that wall. The width of the pattern represents the length along

the joint which was scanned, at a full scale relationship; while the length of the pattern represents the distance around the joint circumference at the ratio of 2.3 units of pattern length for every unit of circumferential distance. The data in Figure 50 represents a vertical scan over a distance much greater than the bond width and a pattern length corresponding to slightly more than half of the joint circumference. The light patches in the pattern represent echoes caused by discontinuities in the acoustic field. In this case the spots due to the intentional flaws are identified while the other spots visible are due to internal surface irregularities from previous machining operations on the joint. When the sensitivity was adjusted to a slightly lower level the machining irregularities were no longer visible; but neither were the intentional flaws on the outside surface, so the sensitivity shown in Figure 50 was felt to be optimum. A pattern of the bonds for inertia welded joints 9 and 10 was generated prior to subjecting them to pressure cycle testing. Figures 51 and 52 show the inspection patterns from joints 9 and 10 that were produced at the same sensitivity as the pattern in Figure 50. The obvious increase in indication was traced to the poor surface finish on the joints. Reduction of the sensitivity and reinspection of the reference joint resulted in the pattern shown in Figure 53. This pattern shows only the inside surface flaws. At this same reduced sensitivity, patterns for joints 9 and 10 were obtained and are shown in Figures 54 and 55. Joint 9 pattern shows no echoes in the bond area while joint 10 pattern still shows three major flaw indications. Patterns 54 and 55 are considered to be tare readings for joints 9 and 10 before they were subjected to pressure cycle tests. The joints were then pressure cycled and after 66,000 cycles were again ultrasonicly inspected to determine if flaw growth could be observed. The reference joint was then examined at the same reduced sensitivity as the patterns shown in Figure 53. This pattern is shown in Figure 56. Post-pressure cycle patterns of joints 9 and 10 appear as Figures 57 and 58. A comparison of Figure 58 with Figure 55 indicates that very little if any change occurred due to the pressure cycling. The only pattern variations observed are felt to be due to possible minor changes between inspection fixture preparations and changes in the surface finish of the joints due to handling. Some scans were also made at the previous higher sensitivity patterns. The fact that joint 9 pattern appears to be much cleaner in all inspections compares well with pressure cycle data that shows joint 9 survived 232,366 cycles as compared to only 189,107 for joint 10. Joint 9 was the only inertia welded joint to fail partially at the bond line during pressure cycle testing. Inspection of the failed area revealed that no flaws existed in the bond prior to failure.

Explosive welded joint 5 was evaluated in a similar manner, but the ultrasonic inspections were performed before and after thermal cycle testing. The explosive welded reference joint into which EDM flaws were machined was a half-joint. The flaws were arranged on the joint surfaces as shown in Figure 49. When this half-joint was ultrasonicly inspected, it was fitted into the side of a tube which had been machined to accept it. Figure 54 shows a pattern resulting from a scan of the reference joint at low sensitivity. The only EDM flaw which the inspection identified is the one on the O.D. between the stainless and silver. At this low sensitivity other areas showed echoes, and at increased sensitivity (Figure 60) this became

more pronounced. If the I.D. flaws had been present on the pattern, they would be located about 1.3 cm (0.5 in.) above the other indications due to the scarf configuration. The white area on the patterns represents the angular portion of the welding boss, on the aluminum half of the joint. The other indications shown on the same pattern level with the O.D. flaws may have been due to poor bonding at the feather edge of the stainless portion of the joint.

Ultrasonic inspection patterns of explosive bonded joint 5 that were taken at two sensitivity settings prior to the thermal cycle testing are shown in Figures 61 and 62. The flaw indications shown in Figure 61 are in the area of the silver/silver explosive bond. Figure 62 shows this area as well as the shock fron area. Joint 5 was subjected to thermal cycle testing, where 100 cycles were completed without leakage occurring. Ultrasonic inspection was repeated and the results are shown in Figure 63. The silver/silver bond and shock front areas are still visible as before, and except for a slight increase in the effective sensitivity (compared with Figure 62) the results are the same. When this joint was eventually burst, the initial failure point was near the silver joint area; so the indications of a possible disbond area in that vicinity were probably valid.

The primary problem that hampered the ultrasonic evaluation was the surface finish characteristics of the joints used for reference and test items. When it is important to identify flaws at or near a surface by ultrasonic inspection, the surface finish must be much better than that required to meet other joint useage criteria. A finish of 32 RMS is recommended for any further ultrasonic evaluation of dissimilar metal joints where a high resolution is desired. The intentional flaws were made small when compared to the wall thickness in an attempt to get some evaluation of the sensitivity that could be expected of the technique. Even though all of the intentional flaws did not appear on the scans, the sensitivity obtained (even with poor finishes) is very adequate to make ultrasonic inspection a valuable tool in NDT or dissimilar metals joints.

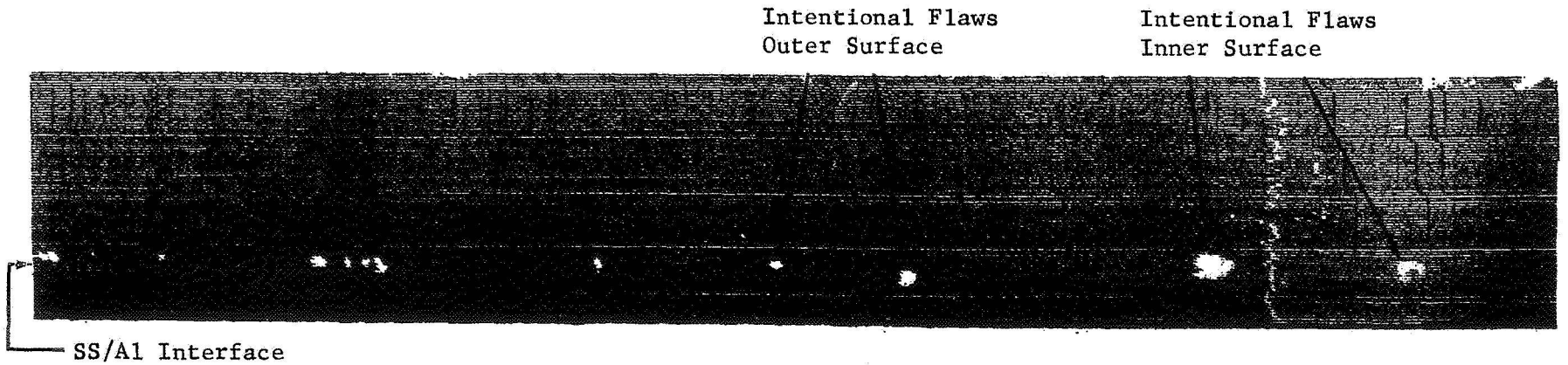

Figure 50. - Ultrasonic Inspection Readout of Inertia Welded Reference Joint

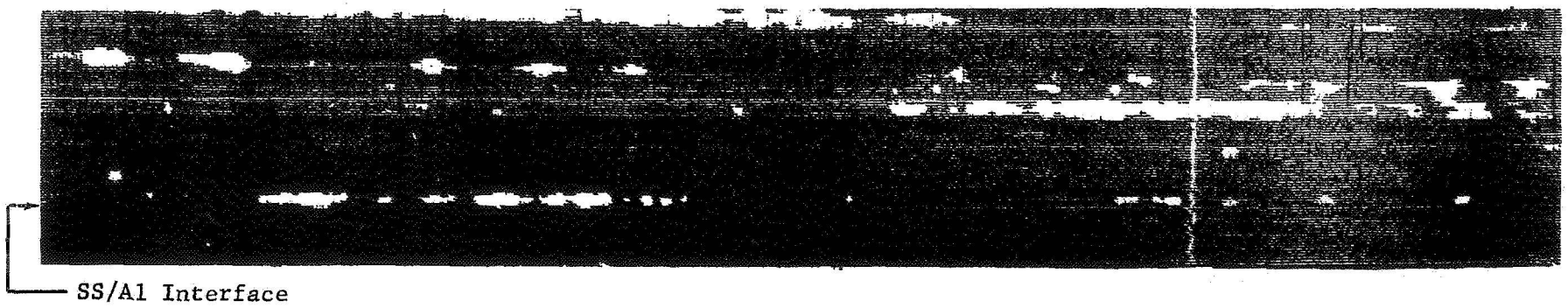

Notes: Scale ↕ 1" = 1" (Length)
↔ 2.3" = 1" (Circumference)

Orientation ↑ Stainless Steel
↓ Aluminum

Figure 51. - Ultrasonic Inspection Readout of Inertia Welded Joint-9

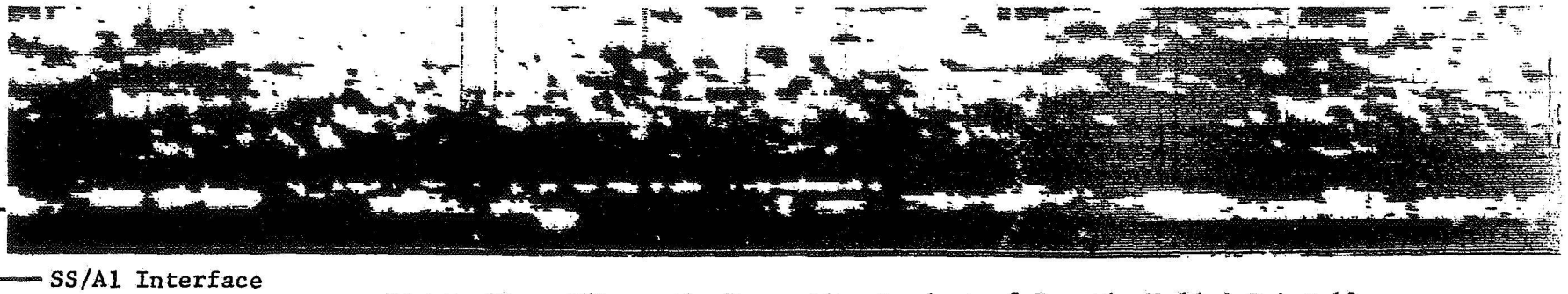

Figure 52. - Ultrasonic Inspection Readout of Inertia Welded Joint-10

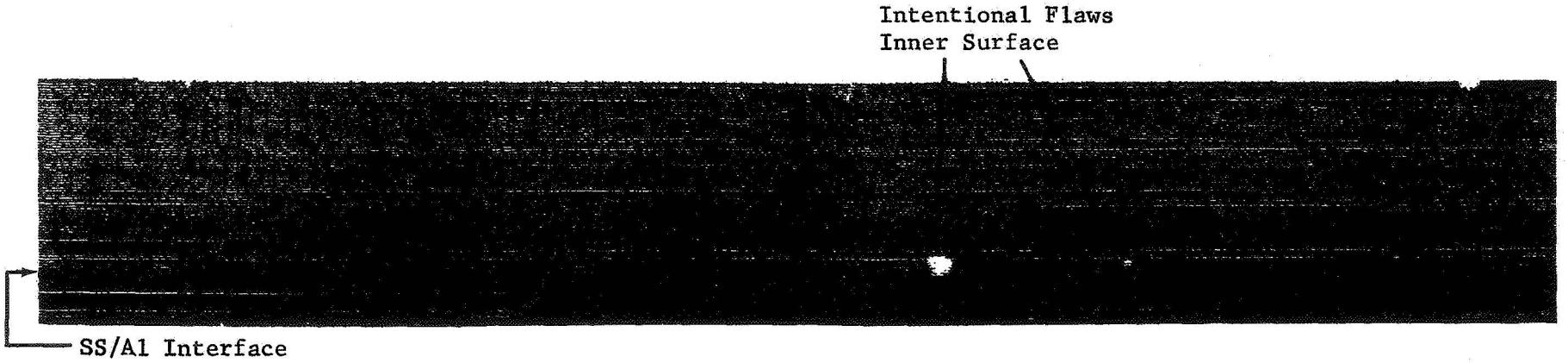

Notes: Scale

1" = 1" (Length)

2.3" = 1" (Circumference)

Orientation:

Stainless Steel

Aluminum

Figure 53. - Ultrasonic Inspection Readout of Inertia Welded Reference Joint (At Reduced Sensitivity)

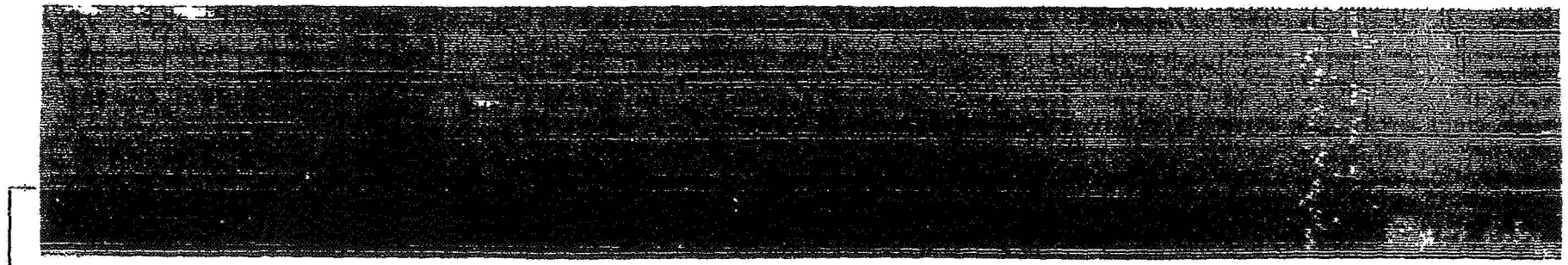

Figure 54. - Ultrasonic Inspection Readout of Inertia Welded Joint-9, (At Reduced Sensitivity)

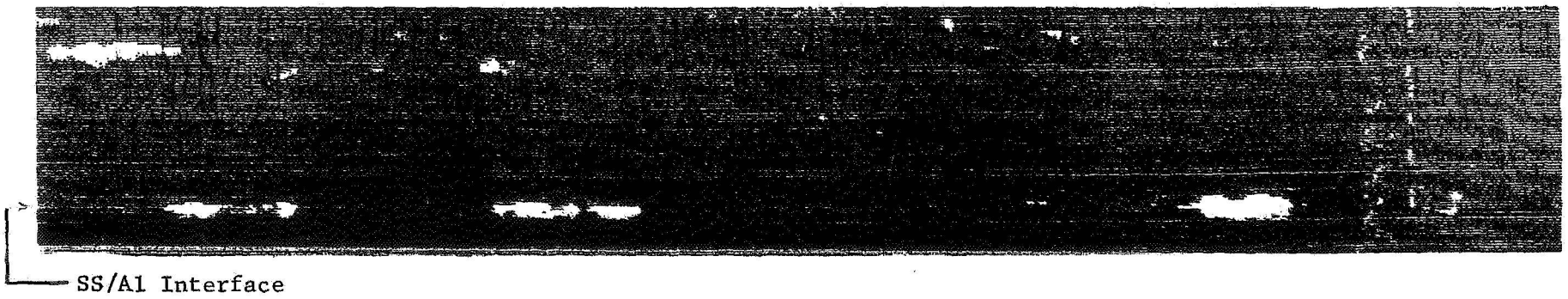

Notes: Scale ↕ 1" = 1" (Length)

↔ 2.3" = 1" (Circumference)

Orientation: ↕ Stainless Steel

Aluminum

Figure 55. - Ultrasonic Inspection Readout of Inertia Welded Joint-10, (At Reduced Sensitivity)

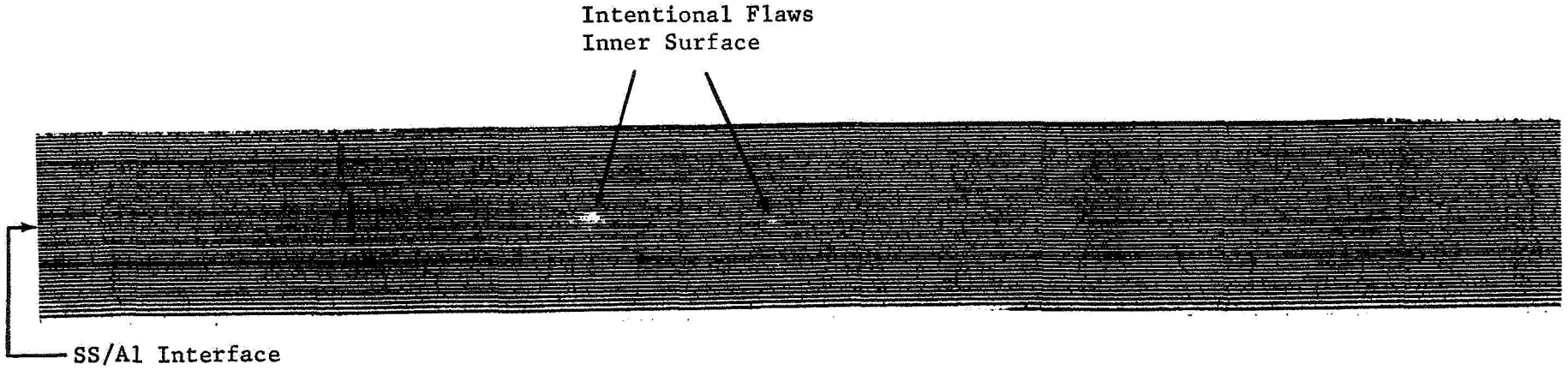

Figure 56. - Ultrasonic Inspection Readout of Inertia Welded Reference Joint (Adjusted Post-Pressure Cycle)

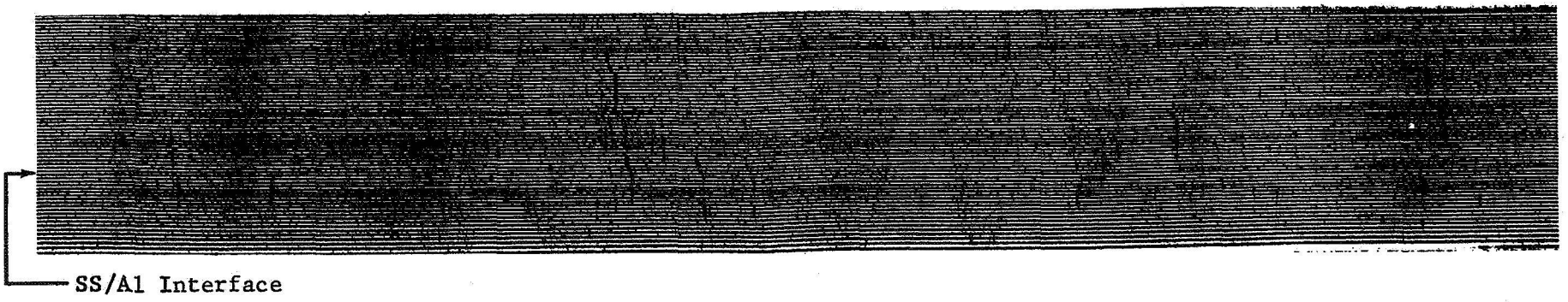

NOTES: Scale ↕ 1" = 1" (Length)

↔ 2.3" = 1" (Circumference)

Orientation: ↕ Stainless Steel

↕ Aluminum

Figure 57. - Ultrasonic Inspection Readout of Inertia Welded Joint-9, (Post-Pressure Cycle)

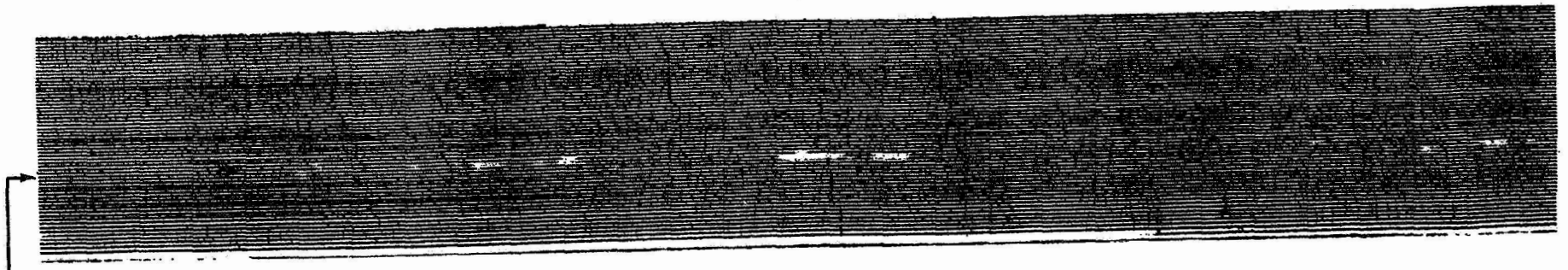

Figure 58. - Ultrasonic Inspection Readout of Inertia Welded Joint-10, (Post-Pressure Cycle)

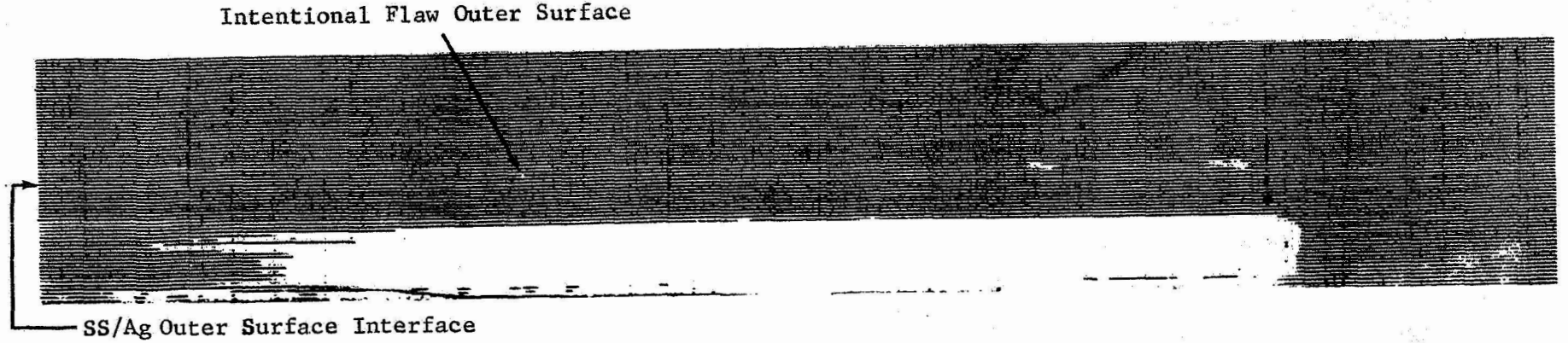

Notes: Scale ↕ 1" - 1" (Length)

↔ 2.3" = 1" (Circumference)

Orientation: ↕ Stainless Steel

Aluminum

Figure 59. - Ultrasonic Inspection Readout of Explosive Welded Reference Joint (Low Sensitivity)

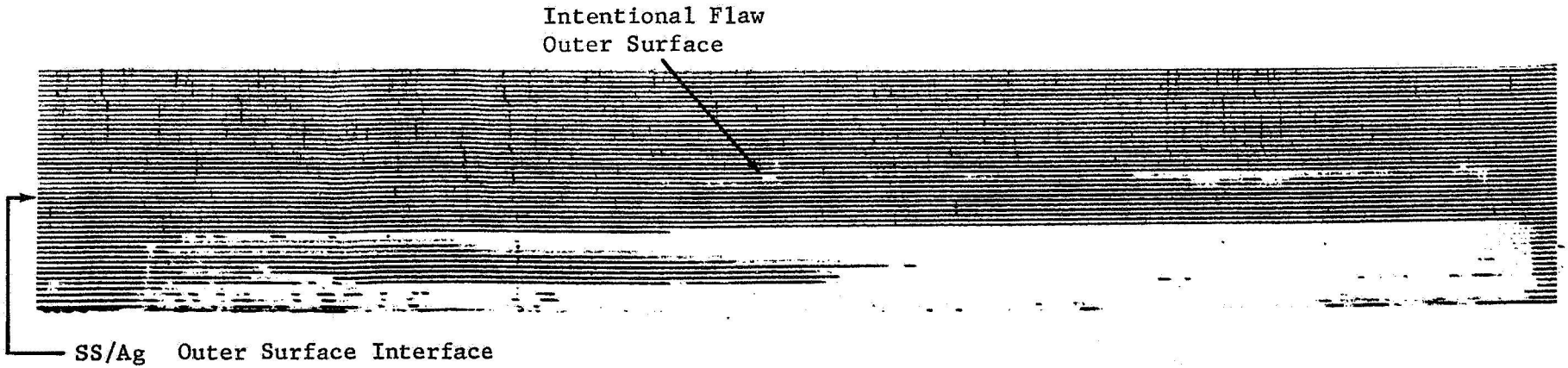

Figure 60. - Ultrasonic Inspection Readout of Explosive Welded Reference Joint (High Sensitivity)

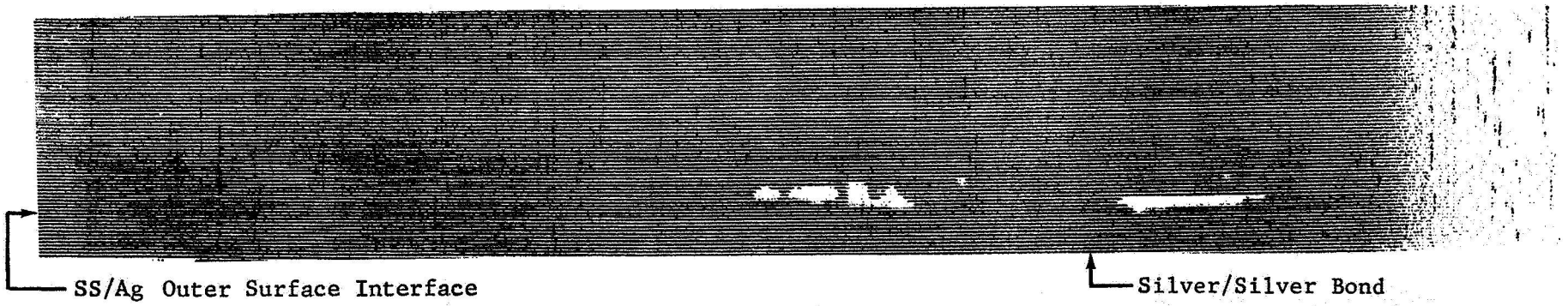

Notes: Scale ↕ 1" = 1" (Length)
↔ 2.3" = 1" (Circumference)

Orientation: ↑ Stainless Steel
↓ Aluminum

Figure 61. - Ultrasonic Inspection Readout of Explosive Welded Joint-5, Pre-Thermal Cycle (Low Sensitivity)

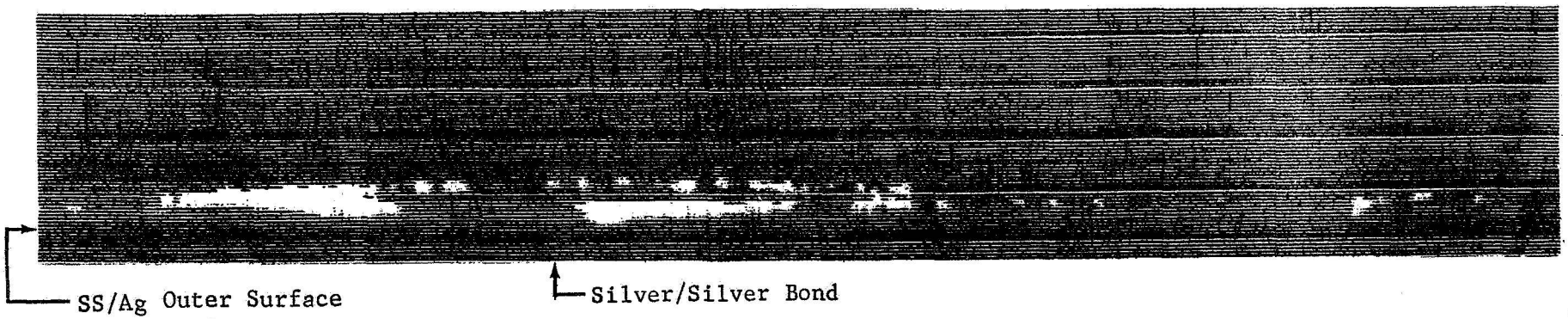

Figure 62. - Ultrasonic Inspection Readout of Explosive Welded Joint-5, Pre-Thermal Cycle (High Sensitivity)

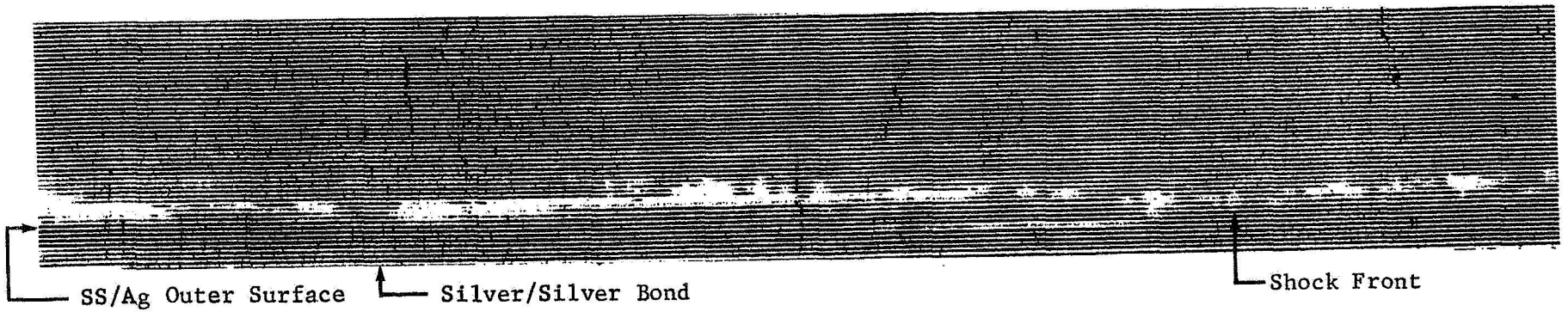

Notes: Scale

1" = 1" (Length)

2.3" = 1" (Circumference)

Orientation:

Stainless Steel

Aluminum

Figure 63. - Ultrasonic Inspection Readout of Explosive Welded Joint-5, (Post-Thermal Cycle)

METALLURGICAL EVALUATION

Metallographic Inspection Results

Samples were cut from the bond areas of the dissimilar metals and prepared for metallographic and microscopic inspection. The specimens were mounted, ground, polished and final polished to provide the smooth surfaces necessary for microscopic examination. The different metals were etched to show individual metallurgical characteristics such as grain size, grain boundaries, alloying, contaminant particles, flow patterns and other physical characteristics. The etching reagents used during the examinations were as follows: Ferric chloride and hydrochloric acid for 304L stainless steel, Keller's etch for the 6061 and 2219 aluminums, and Potassium cyanide-ammonium persulphate for the silver. During the examinations polarized light of different intensities was used to contrast different characteristics and structures that were observed in the metals. The samples were examined and photographed at various magnifications on a Bausch and Lomb Research II Metallograph and a Zeiss Universal microscope.

Inertia Welding Bond Analyses

The inertia welded bond is in essence a metallurgical bond due to friction welding. Friction welding is a variation of pressure welding in that the welded connection is formed without melting the metal. The connection is formed by joint plastic deformation of the metals due to the heat resulting from frictional forces. This plastic deformation plays a special role in the friction welding process - on the one hand contributing to the destruction and elimination of surface oxide films and contamination and on the other hand aiding in temperature stabilization at the bond area.

Microscopic analyses of the friction welded connections (304L stainless steel/6061 aluminum and 6061 aluminum/2219 aluminum) revealed that the bond lines did not contain any voids, flaws, oxide, foreign inclusions or microscopic defects. In addition to this a specific texture and small grain size that are typical for a friction welded joint and the adjacent zones were prevalent. These were apparently the result of mechanical smearing of grains during the course of crushing the surface layers of the metal due to friction and plastic deformation. Figures 64 and 65 show the typical friction bond lines between the 304L stainless steel/6061 aluminum and 6061 aluminum/2219 aluminum.

The cleanliness of the friction bonds between the 304L stainless steel/6061 aluminum and 6061 aluminum/2219 aluminum must be particularly emphasized. Microscopic examination of the two bond lines under higher magnification (greater than 400X) revealed no voids, secondary phases, oxides or inclusions existing between the different metals. No anomalies occurred between the faying surfaces of the different metals. Examination of the friction bond between the 6061/2219 aluminums appeared to show that the two metals were diffused along the bond line. Examination data obtained

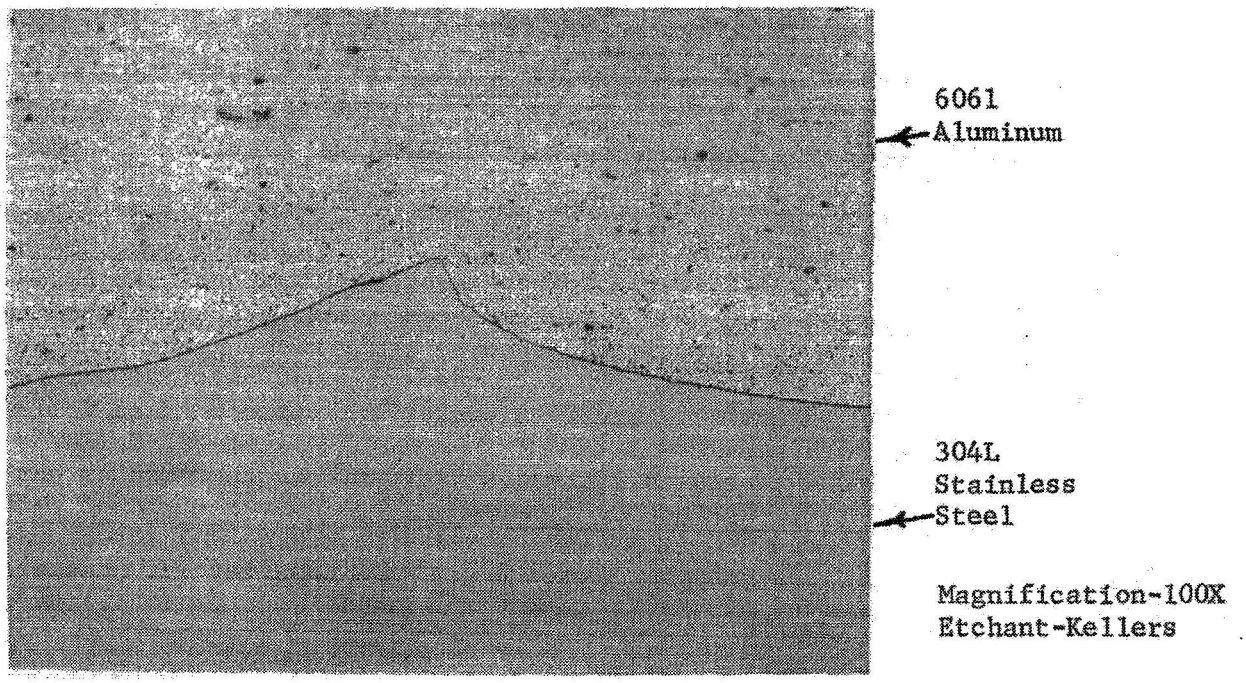

Figure 64.- Micrograph of Typical 304L Stainless Steel/
6061 Aluminum Inertia Weld

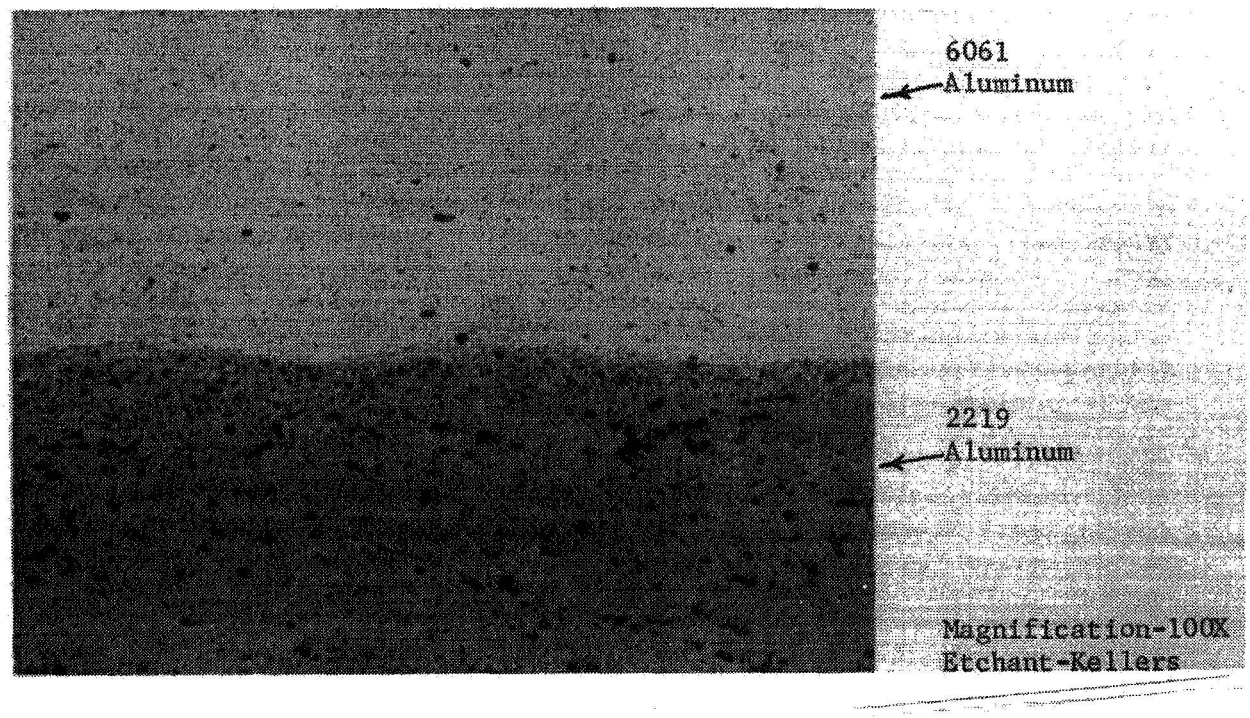

Figure 65.- Micrograph of Typical 6061 Aluminum/2219
Aluminum Inertia Weld

with the use of the ARL Electron Microprobe X-Ray Analyzer - Scanning Electron Microscope supported this observation. Examination data obtained from the electron microprobe also indicated that a diffusion bond existed between the 304L stainless steel and the 6061 aluminum.

Explosive Bond Analyses

Explosive bonding is an operation in which metal surfaces with suitable geometry and orientation are brought together with a high relative velocity and pressure such that plastic interaction occurs between the metal surfaces. In this process, when one part is collapsed against the other, heavy plastic interaction between the metals (termed surface jetting) occurs which produces a high strength weld. Figure 66 shows a typical explosive bond produced between 304L stainless steel and 2219 aluminum, using a silver intermediate material.

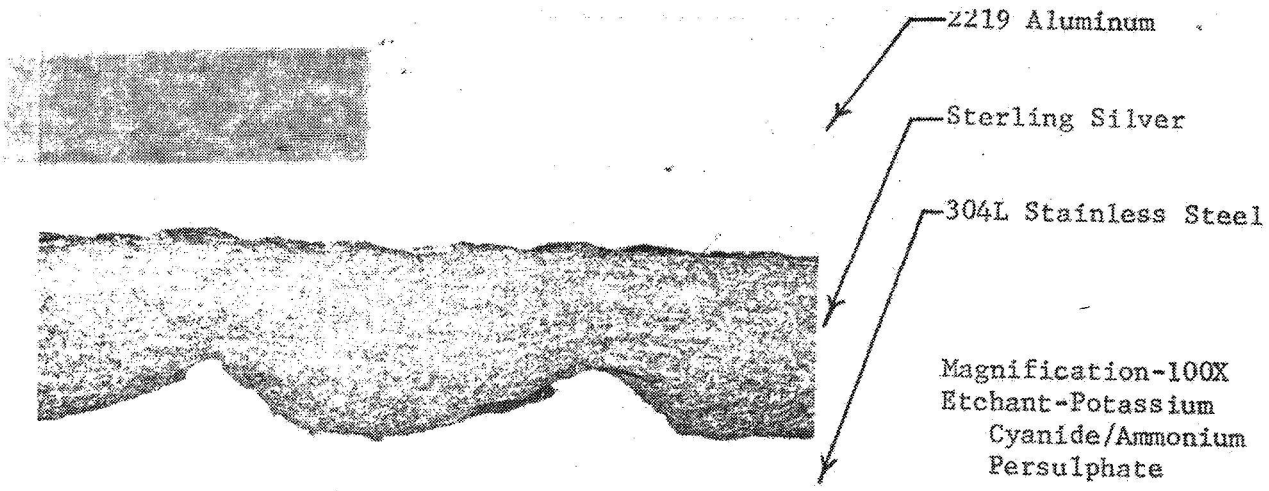

Figure 66.- Micrograph of Typical Explosive Bond Between 304L Stainless Steel and 2219 Aluminum, Using Silver Intermediate Material.

As the detonation wave propagates along the explosive charge, the stainless steel sequentially collapses against the silver producing the distinctive wave pattern that is typical of explosive bonds. The surface jetting effect scrubs the surfaces of the metals of any contamination, oxide layer or scale as the detonation wave propagates in order to produce a strong metallurgical bond between the two metals.

Figure 67 shows a single wave produced when 304L stainless steel was explosively bonded to sterling silver.

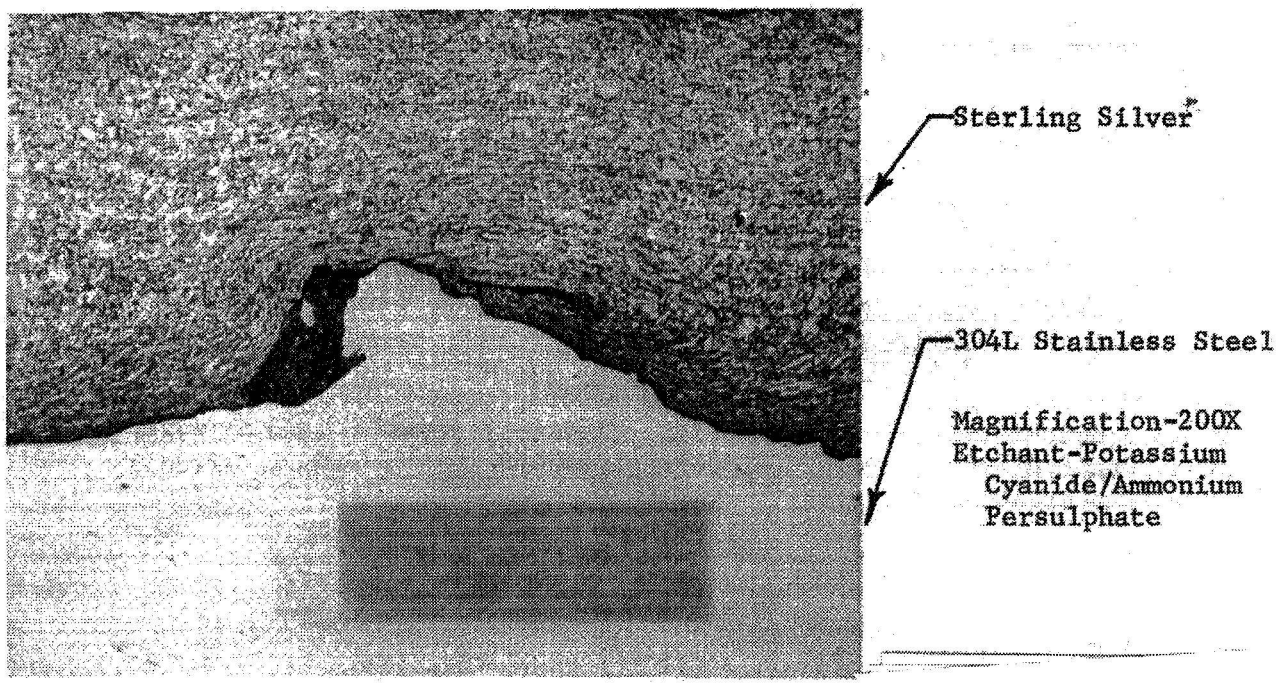

Figure 67.- Micrograph of Typical Single Wave Pattern of Stainless Steel Explosively Bonded to Silver

A mass of material that was scrubbed from the metal surfaces was deposited under the curl of the wave and at the upper reaches of the wave trough thus leaving the rest of the surface cleansed for bonding. Microscopic examination revealed that this mass consisted of a mechanical mixture of small pieces of stainless steel, silver, metal oxides and contaminants.

Microscopic examination of the 304L/Ag bond indicated that the grain structure of the silver underwent a tremendous amount of plastic deformation. The grain size was small and elongated and flowed along the stainless steel waves. Small voids were observed in the vicinity of the wave curl. Deformation of the stainless steel grain structure also occurred along the bond line. The grains were small and appeared to be mechanically twinned due to the explosive loading. The stainless steel also appeared to diffuse into the silver at each wave tip. Data obtained from the electron microprobe supported this apparent observation of diffusion.

Figure 68 shows a typical wave produced when sterling silver was explosively bonded to 2219 aluminum.

The silver wave shows a tumbled effect, indicating that the surfaces of the two metals were not brought together in an optimum manner either because the amount of explosive used or the contact angle was incorrect, or a combination of the two. However, even though the tumbled wave was not optimum, it must be noted that no leakage or mechanical failure ever occurred at the Ag/Al bond. Again, scrubbing action occurred which trapped the mass of mechanical mixture under the curl of the wave.

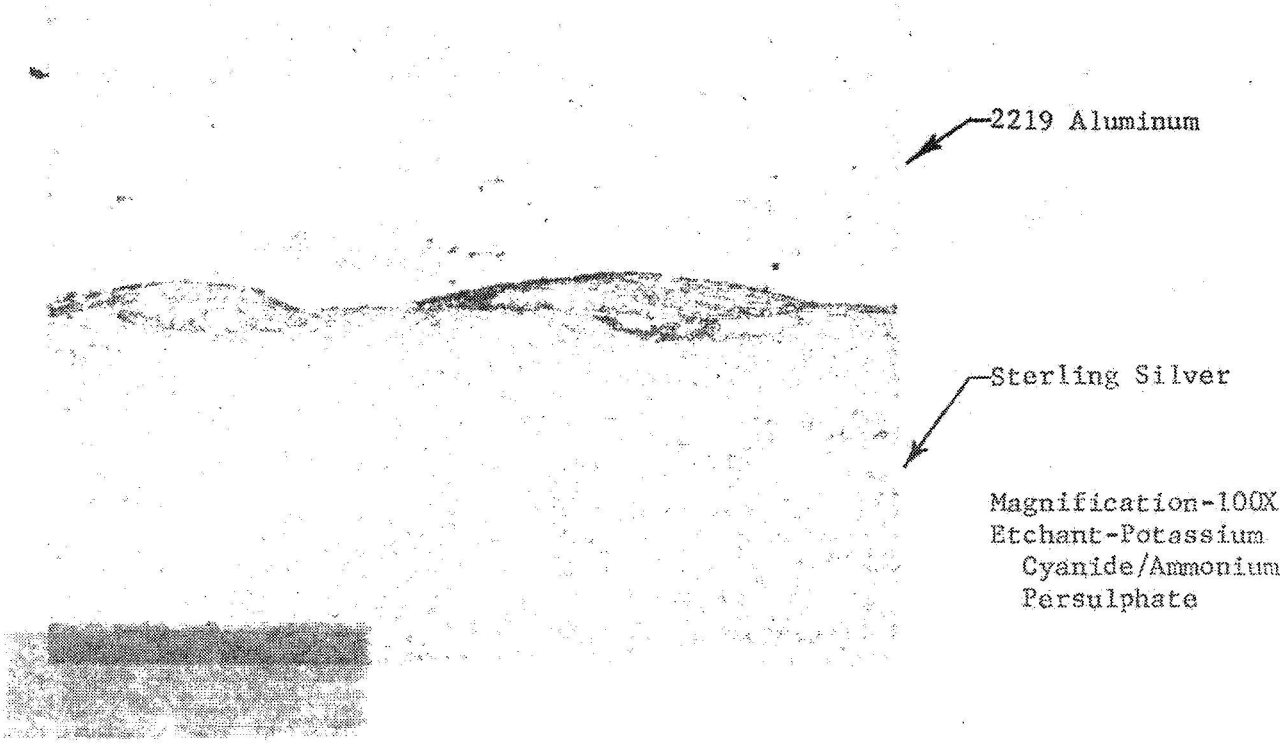

Figure 68.- Micrograph of Typical Wave Pattern of Silver Explosively Bonded To Aluminum

Microscopic examination of the Ag/Al bond line also showed the tremendous plastic deformation incurred by the silver. The grain structure of silver was again small and elongated along the bond line. Small voids were observed at the tips of the silver waves. A complex aluminum alloy or mixture was observed around the silver waves and became entrapped in the collapsed and tumbled silver waves. Figure 69 shows this alloy or mixture and the voids in the silver waves.

Deformation of the aluminum grain structure occurred along the bond line. The grains were small and appeared to be smeared because of the tremendous pressures occurring along the bond line. Microscopic examination of the Al/Ag bond showed that the aluminum appeared to diffuse into the silver, but only at the tips of the silver waves. Again the electron microprobe data in the next section supports this apparent observation.

The presence of the small voids in the waves, especially in the Ag/Al bond, may be a characteristic attributable to the materials being bonded when the proper conditions are provided, rather than due to any error in power or in configuration when the bond was made. Apparently the voids did not interconnect between waves in the bond, or none of the joints could have been free of helium leakage. This represents a significant advantage for an explosive welded joint having a scarf angle configuration at the interface, where the waves of the bond are concentric with the joint. A joint made with a butt weld configuration which is machined from a thick sandwiched plate may have a high probability of leaking thru these voids.

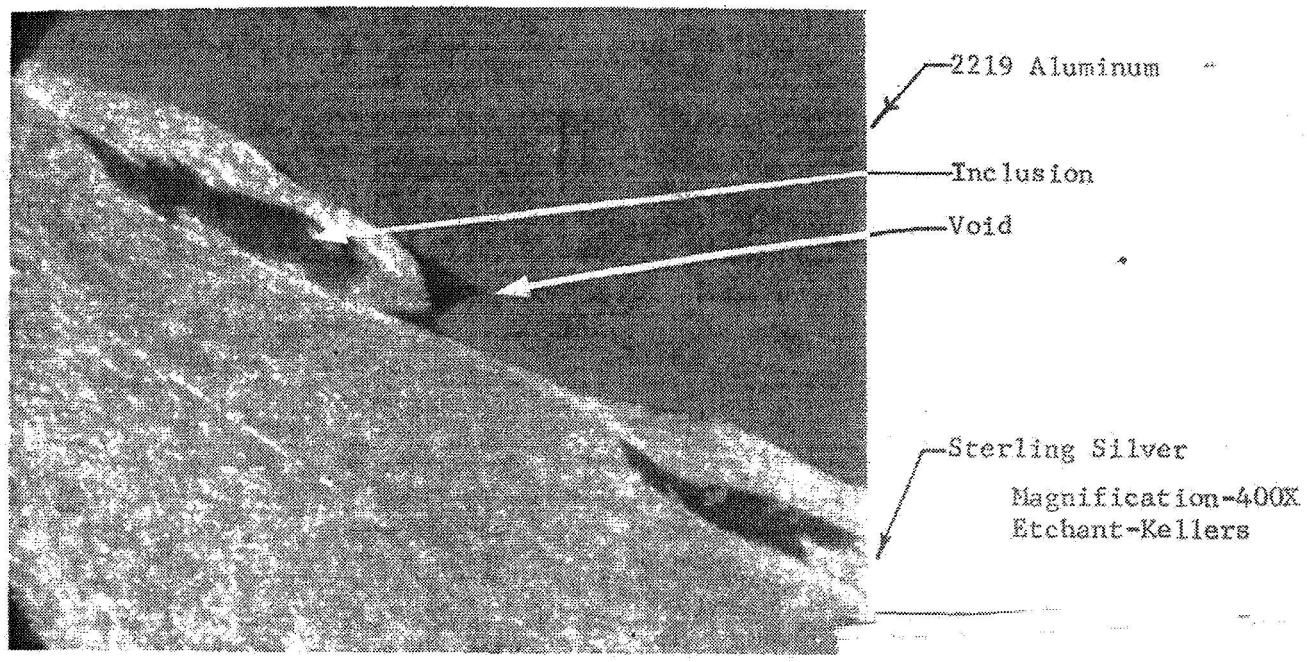

Figure 69.- Micrograph of Silver/Aluminum Explosive Bond Showing Voids and Inclusions.

Bond Diffusion Evaluation

In order to determine the microstructure characteristics of the bonds, scanning electron microscopy was utilized. By scanning across the boundaries between the various materials, the intermediate structure can be identified and analyzed. This technique was used for the inertia welded and explosive welded bonds at each side of the intermediate materials. This technique was not applied to the swaged construction joints, as they consist of pure mechanical bonds which rely on induced residual stresses within the materials to maintain intimate contact.

In performing the evaluation described here, a Model EMX-SM Scanning Electron Microscope by Atlantic Research Laboratories was utilized. Micro-specimens were prepared equivalent to those shown in Figures 64, 65 and 66. The specimens were placed within the ARL, and subjected to a high vacuum. Electron scans were made across the bonded areas with one or two spectrometers set to identify specific atoms. Many scans were made at each of the four interfaces. This is particularly necessary in the explosive bonds, because the wave activity often appears as a mixture of metals when observed by other means other than the ARL. When evaluating all interfaces, the amount of diffusion at each bond was the characteristic of prime interest.

When analyzing the inertia welded bond between the 2219 and 6061 aluminums, two methods of scanning were utilized. One method used two spectrometers that were both set to identify Cu atoms and the other method had one spectrometer set to identify Cu and the other set to identify Mg. The choice of magnesium was made because of its relatively high content in 6061 (1.0%) versus its low content (0.02%) in 2219. The choice of copper was made because

of its relatively high content (6.3%) in 2219 versus its low content (0.25%) in 6061. Several scans of each type were made with similar results. Figure 70 is a typical ARL recording of the Cu/Cu scan. When the speed of the electron beam scan, the recorder sensitivity and paper speed are accounted for, the apparent diffusion area was about 4.5 microns thick. Figure 71 is a typical recording showing a Cu/Mg scan. The scan indicated a magnesium diffusion layer about 6.0 microns thick and a copper diffusion layer about 6.6 microns thick.

When analyzing the inertia welded bond between the 6061 aluminum and 304L stainless steel, scans were made with spectrometer identifications of Fe and Fe/Al. Typical recorder traces of these are shown in Figures 72 and 73. Figure 72 shows the Fe scan and indicates about 5.6 microns of diffusion. Figure 73 shows the Fe/Al scan and indicates about 5.0 microns of Fe diffusion and about 6.0 microns of Al diffusion.

When the explosive welded bond between the 2219 aluminum and the sterling silver was analyzed, scans were made with one spectrometer set to identify aluminum. The results of typical scans made by this method are shown in Figure 74. The amount of diffusion observed may be measured as about 3.1 microns or much more depending on interpretation of the data.

When analyzing the explosive bond between the silver and the 304L stainless steel, scans were made using spectrometers set to identify Ag and Fe, and only Fe. A typical Ag/Fe scan appears in Figure 75 and shows about 2.0 microns of diffusion. The peak that is seen in both traces prior to reaching the interface is probably the effect caused by one of the trapped pockets of material created by the jetting action during explosive welding. Figure 76 is typical of a Fe only scan where none of the trapped pockets were crossed during scanning and shows diffusion of about 3.6 microns.

From evaluation of the ARL data it is apparent the inertia welded interfaces are very consistent and are diffused to about 4.0 microns. The diffusion is visually observable at the 6061 to 2219 bond but not at the 304L to 6061 bond during microscopic examination of prepared specimens. The interface consistency, however is very apparent from a visual inspection of either of the bonds. The explosive welded microsecions, on the other hand, show consistent patterns of radically differing conditions. This was readily apparent because of the non-repeatability of the ARL data which indicated very altered results for each new scanning path. While the diffusion level in the bond appears to be about 3.0 microns, the areas indicating this diffusion level were those which had fairly straight-forward ARL traces and therefore are not really representative of the total surface contact areas. Both the inertia welded and explosive welded interfaces appear to be geniune metallurgical bonds.

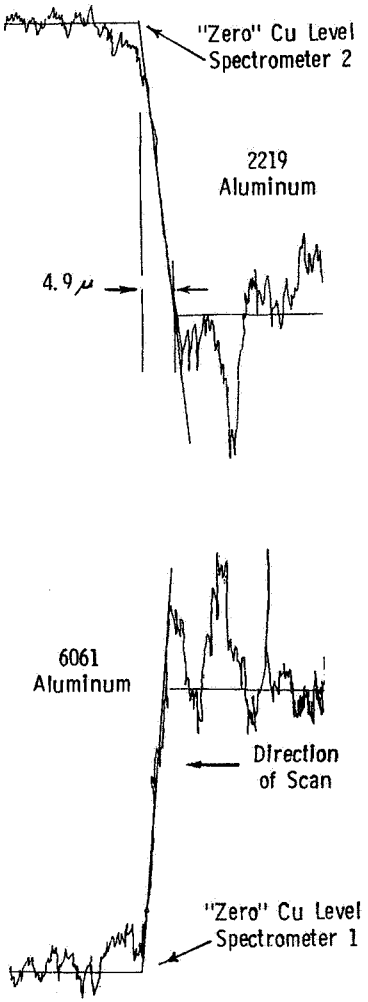

Figure 70
Electron Microprobe Scan
of 6061/2219 Inertia Weld

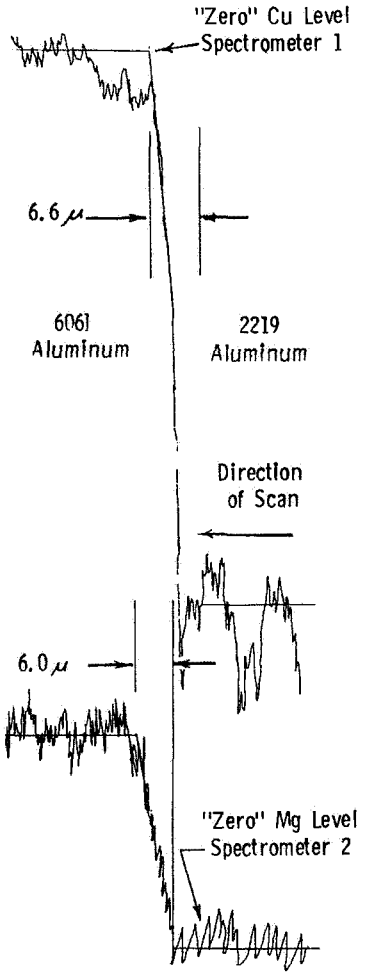

Figure 71
Electron Microprobe Scan
of 6061/2219 Inertia Weld

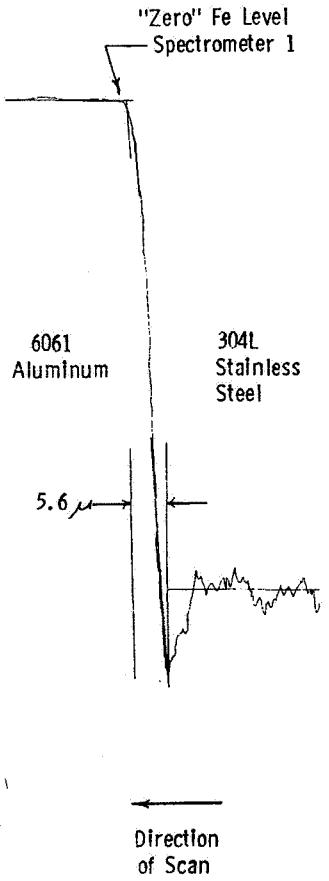

Figure 72
Electron Microprobe Scan
of 304L/6061 Inertia Weld

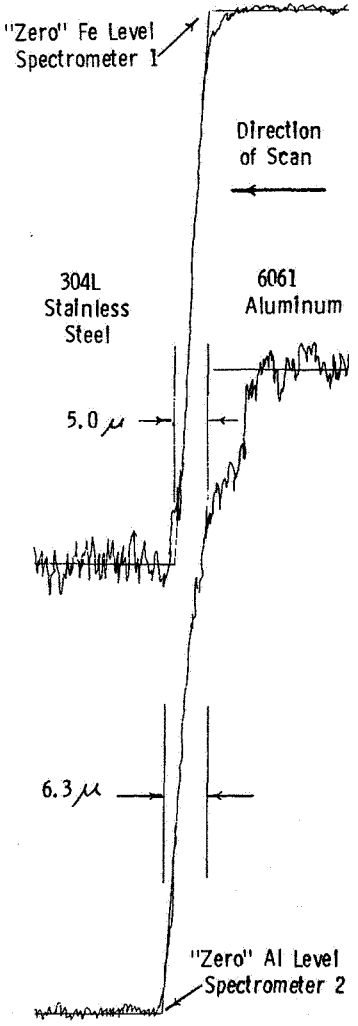

Figure 73
Electron Microprobe Scan
of 304L/6061 Inertia Weld

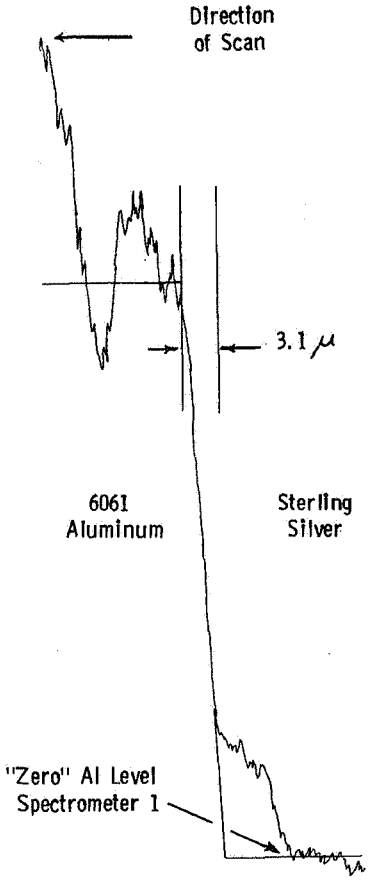

Figure 74
Electron Microprobe Scan
of 6061/Ag Explosive Bond

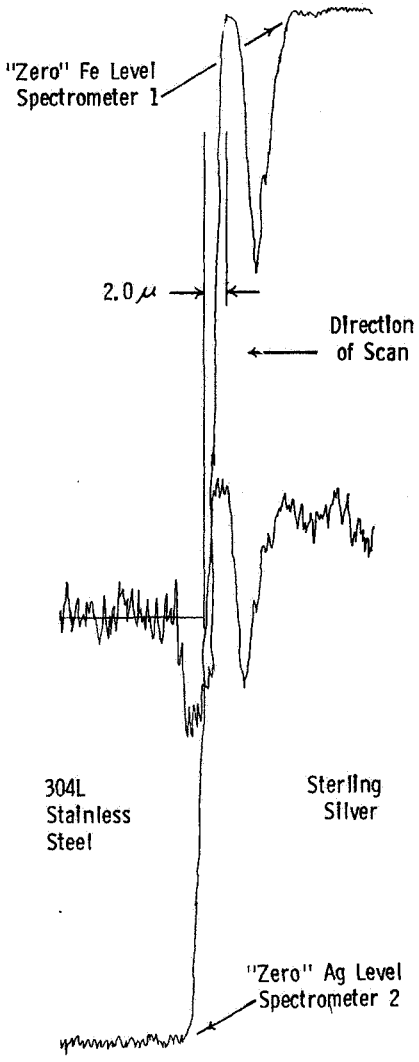

Figure 75
Electron Microprobe Scan
of 304L/Ag Explosive Bond

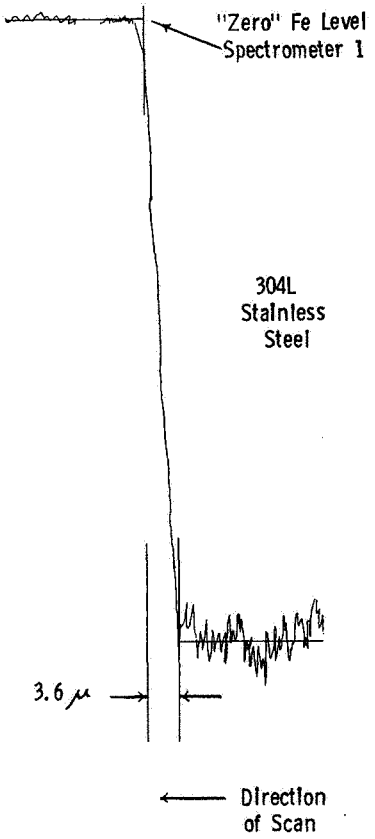

Figure 76
Electron Microprobe Scan
of 304L/Ag Explosive Bond

LARGE JOINT EVALUATION

Applications exist for dissimilar metals joints of much larger sizes than those used for this development program. Estimates have been made of the fabrication techniques, feasibility, and costs of producing larger joints. Sizes which were chosen for evaluation were based on tubing diameter requirements presently indicated on Shuttle Orbiter. These include:

Line Size	Corresponding Orbiter Line
20 cm (8 in.) diameter	Fill and Drain, LOX & LH_2
30 cm (12 in.) diameter	MPS Engine Feedline Section, LOX & LH_2
43 cm (17 in.) diameter	MPS Manifold Feedline Section, LOX & LH_2

The configuration established for the evaluation is shown in Figure 77. The wall thickness shown is 0.33 cm (0.13 in.), since the feasibility of fabricating joints of this thickness has been demonstrated in the 6.4 cm (2.5 in.) diameter joints. The desirability of fabricating joints having a wall as thin as 0.10 cm (0.040 in.) for some aerospace applications is recognized; but, in most cases this thin wall will affect only the final machining and not the fabrication technique. The aluminum end of the joint is shown having a welding boss similar to that of the 6.4 cm (2.5 in.) O.D. joints and is left adequately long to assure adaptability to any foreseeable welding technique. The welding boss may not be necessary and the aluminum (or stainless steel) length may be excessive (depending on the application of the joint), but these are relatively minor modifications of the baseline configuration.

The estimated costs and other appropriate information are treated separately for each joint type in the following sections. The estimated costs shown assume that each manufacturer provides joints directly to NASA or other users for evaluation or use, and include each manufacturer's overhead and profit charges.

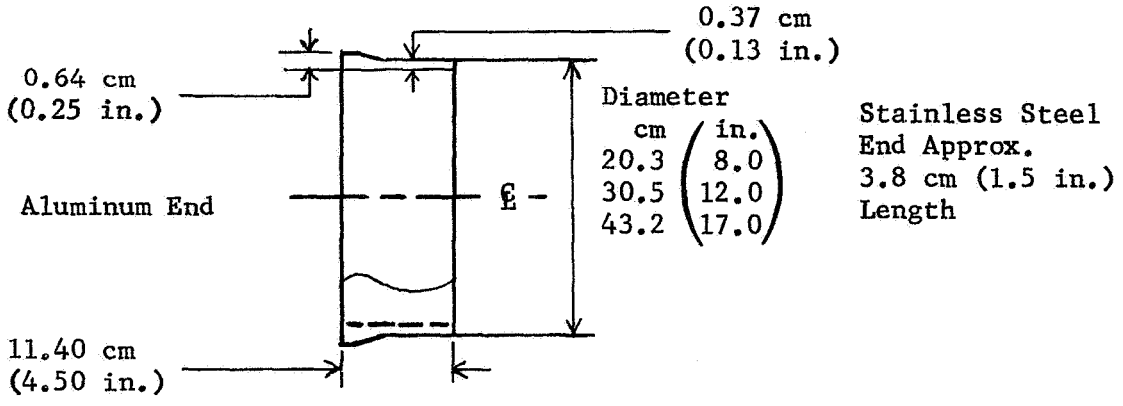

Figure 77.- Baseline Joint Configuration - Large Joint Evaluation

Inertia Welded Large Joints

Based on the results of the 6.4 cm (2.5 in.) diameter joint development and test, the production of 20, 30, and 43 cm (8, 12 and 17 in.) diameter joints by inertia welding should require a minimum of development. As the areas to be welded increase the required energy capacity of the inertia welding machine also increases. The stainless to aluminum weld requires about 25%

more energy than a corresponding steel to steel weld; but the 0.33 cm (0.13 in.) wall of the proposed 43 cm (17 in.) diameter joint still falls well within the energy capacity of a Caterpillar model 250. Use of this machine, at a cost of $100 per hour including operator, is the basis for the estimated welding cost. An additional requirement for the larger size joint is a tool necessary for adapting this joint to the smaller size collets available as a part of the welder. Because this collet size varies depending on the optional equipment obtained with each welder, this estimate is based upon the assumption that these adapters will be needed for all three sizes of joint. Also, while less powerful inertia welders are available which could produce the 20 cm (8 in.) diameter joint, use of the Model 250 is planned for all three fabrication sizes.

The fabrication technique chosen involves rolling and welding sheet aluminum to form cylinders for inertia welding, rather than using tubing, which is not readily available in these large sizes, or machining the parts from thick plates, which is expensive and leaves an undesirable grain orientation in the aluminum part. The primary disadvantage of rolled and welded cylinders lies with the aluminum strength degradation in the welded area. In order to counteract this, the aluminum welding boss (which is left thickened for installation of the complete joint) would be left longer than otherwise needed in order to prevent the aluminum portion of the joint from being subjected to the full effect of hoop stress at the 0.32 cm (0.13 in.) thick portion during pressurization. Where full weight reduction potential is required, tubing of proper size would need to be purchased to eliminate any axial welds. If a thinner joint wall is required than is established in the baseline, it would still be necessary for the inertia welding to be performed using baseline thickness in order to provide the necessary strength to resist buckling during welding. The technique of rolling and welding the stainless steel portion of the joint would have little effect on the integrity of the completed joint.

The manufacturing plan consists of the following:

1. Fabricate adaption tools to mate joints with inertia welding machine.

2. Produce 6 development joints by the following sequence:

    a. Roll and weld the two aluminum and one stainless steel portion to be inertia welded.

    b. Machine the parts to rough dimensions and establish the proper part geometry at the welding interface.

    c. Inertia weld the 2219 aluminum to the 6061 aluminum, and machine the 6061 to proper dimensions for final inertia welding.

    d. Inertia weld the 2219/6061 aluminum sandwich to the stainless steel portion.

    e. Artifically age the joint to improve aluminum strength in the inertia welded areas.

    f. Perform appropriate NDT or other tests. (This phase is not priced, as intended service conditions will vary).

3. Produce the required number of production joints by this same method for submittal to qualification or other testing as necessary.

Inertia Welded Large Joint Cost Evaluation

Facility Costs

Costs are based on fabrication of four holding jigs to adapt joint parts to be welded to the smaller machine collets. Two jigs will support parts for the 20 cm (8 in.) joints and two jigs will support parts for the 30 cm (12 in.) and 43 cm (17 in.) joints.

Facility Cost	20 cm (8 in.)	30 cm (12 in.)	43 cm (17 in.)
	$3000	$5500	

Development Costs

Costs are based on production of six joints and include the following items:

Design and coordinate

Roll and weld stainless steel

Machine stainless steel

Roll and weld 2219 aluminum

Machine 2219 aluminum

Roll and weld 6061 aluminum

Machine 6061 aluminum

Inertia weld 6061 to 2219

Face machine 6061

Inertia weld stainless steel to aluminum

Artifically age

Final machine

Material: stainless steel, aluminum

	20 cm (8 in.)	30 cm (12 in.)	43 cm (17 in.)
Development Cost	$6000	$7000	$9000

Production Costs

Costs shown are per joint and assume production of 10 to 25 joints of each size. Detail steps are similar to those shown in development.

	20 cm (8 in.)	30 cm (12 in.)	43 cm (17 in.)
Production Cost Per Joint	$800	$900	$1200

Explosive Welded Large Joint

In order to eliminate some of the conditions which were difficult to correct during fabrication of the 6.4 cm (2.5 in.) diameter joints, plans for assembly of the larger diameter joints have included design changes to eliminate these conditions. First, the silver thickness has been increased from 0.025 cm (.010 in.) to 0.076 cm (.030 in.) to simplify the explosive welding of the silver to itself when forming the cone. Second, provisions have been made to better secure and seal the edges of the silver for the silver to aluminum bond. Third, provisions for evacuation of the volume between the stainless and the silver pieces during this bonding step have been made. Fourth, the potential for a shock front occuring during bonding of the stainless to the silver has been eliminated by planning the use of line wave generators to initiate the explosive charge. This technique would be used on the silver to aluminum bond, as well, if a shock front problem became evident due to the larger joint diameters.

The manufacturing plan consists of the following steps:

1. Fabricate the necessary tooling, including the mandrel with removable section shown in Figure 78 and the aluminum clamp ring shown in later sketches. The mandrel will support the joint during each of the explosive steps.

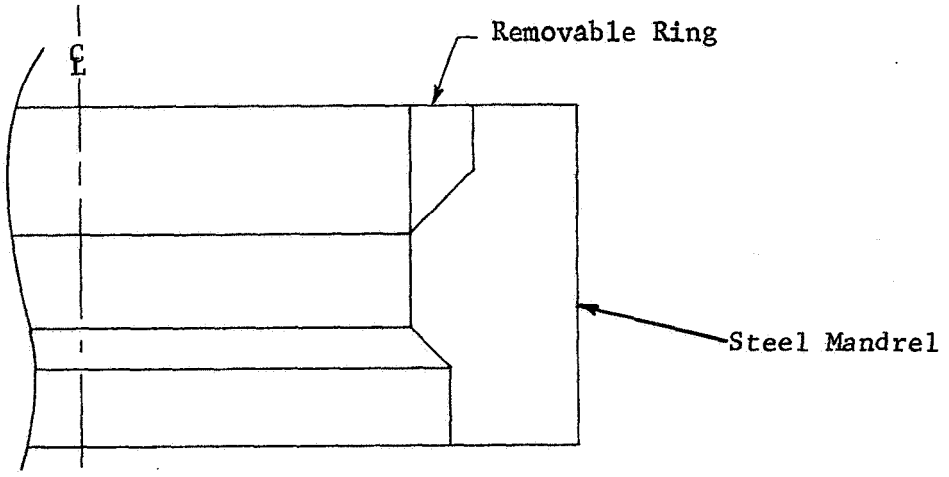

Figure 78. - Large Explosive Joint Mandrel

2. Produce six development joints by the following sequence:

2a. Fabricate a silver cone and bond to the aluminum portion of the joint as shown in Figure 79.

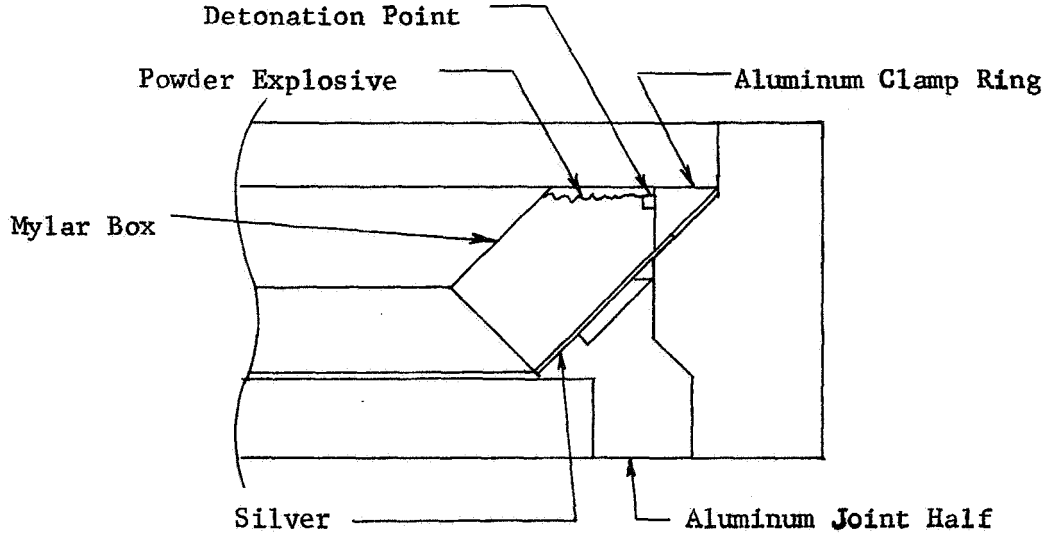

Figure 79. - Large Explosive Joint Silver Bond Concept

2b. Bond the stainless portion to the silver/aluminum sandwich as shown in Figure 80.

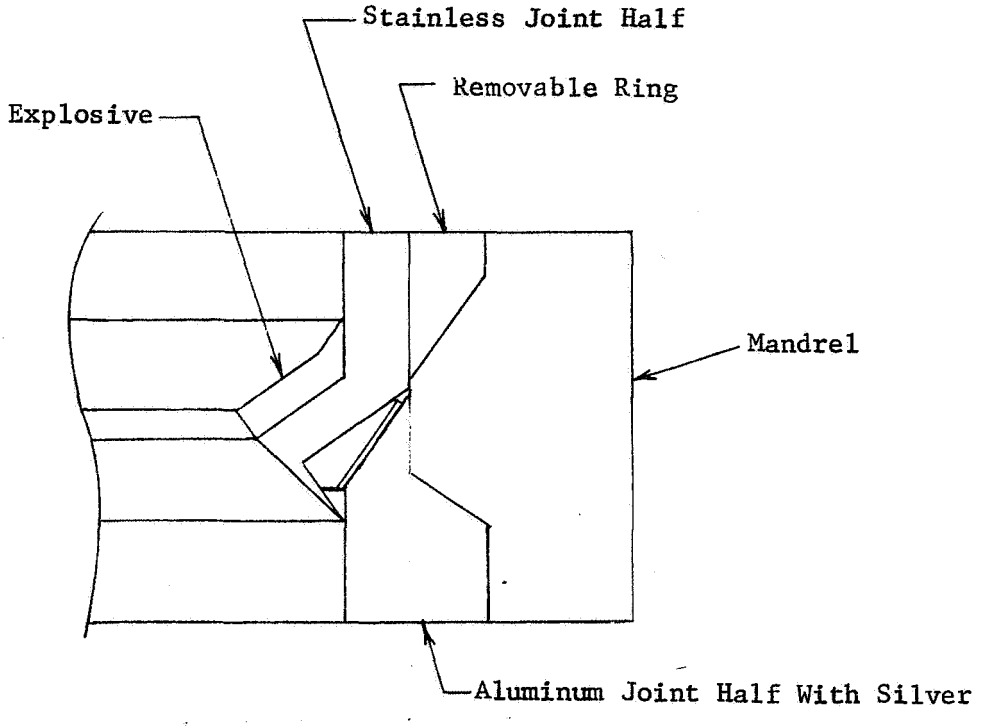

Figure 80. - Large Explosive Joint Stainless Bond Concept

2c. Machine the joint to its final configuration as shown in Figure 77.

2d. Perform appropriate NDT or other tests. (This phase is not priced, as intended service conditions will vary.)

3. Produce the required number of production joints by the same method.

Explosive Welded Large Joint Cost Evaluation

Facility Costs

Costs are based on fabrication of two mandrels with removable rings as are shown in Figure 78, and include the following items:

Design

Fabrication

Material

Facility Cost	20 cm (8 in.)	30 cm (12 in.)	43 cm (17 in.)
	$1800	$2300	$2900

Development Costs

Costs are based on producing six joints, and include the following items:

Design and Coordinate

Fabricate silver cone

Roll and weld aluminum half

Machine aluminum half

Machine aluminum clamp ring

Fabricate mylar box

Bond silver to aluminum

Roll and weld stainless half

Machine stainless half

Bond stainless to silver/aluminum sandwich

Final machine

Material: stainless steel, silver, aluminum, explosive

	20 cm (8 in.)	30 cm (12 in.)	43 cm (17 in.)
Development Cost	$12,000	$12,000	$16,000

Production Costs

Costs shown are per joint and assume production of 10 to 25 joints of each size. Detail steps are similar to those shown in development.

	20 cm (8 in.)	30 cm (12 in.)	43 cm (17 in.)
Production Cost Per Joint	$1500	$1700	$1900

Swaged Construction Large Joints

Ferrules for assembly of swaged joints composed of 6061 or other more common aluminum alloys are presently catalog listed in sizes up to 17.8 cm (7.0 in.) in diameter. As sizes exceed these dimensions, additional tooling would be required which would represent significant production complexity and cost. For instance, the installation tool shown in Figure 21 has three rollers and is intended to be reasonably portable; while the tool envisioned for stretching the 43 cm (17 in.) joints to the accuracy needed would have seventeen rollers, would be heavy, and would require a hydraulic system for operation. The problems encountered with bond leakage of the 6.4 cm (2.5 in.) joints tested are considered solvable, and may be traced both to the haste with which they were prepared and the relative uncertainty of the behavior of the 2219-T851 aluminum when subjected to this swaging operation. The swaging process should be capable of producing a leak-free joint whenever opposing materials have a yield strength or an elastic modulus which differ to any degree. By stretching the materials only the required amounts and by arranging for the proper material to be on the outside, a permanent tensile stress may be induced into the outer material and a compressive stress may be induced into the inner material thus assuring high unit stress at the serrations, even under cryogenic conditions.

For an example of successful applications of these swaged transition joints in aircraft and spacecraft development, refer to Appendix A. It should be noted that a recent joint application has been for glycol and water coolant lines in the Lunar Excursion Module.

Since the method of construction requires one of the materials to yield this material must be homogeneous. If the aluminum is to yield, it should be composed of extruded tubing rather than rolled and welded sheet material. Plate could also be used, but would require considerable machining, and the resultant grain orientation would be less desirable. If the stainless is to yield, it may be rolled and welded sheet material, but should be annealed.

The facility costs shown are affected by the 0.33 cm (0.13 in.) wall thickness of the baseline configuration. Reduction of the wall thickness would lower the swaging forces required, and therefore lower the tooling costs significantly.

Swaged Construction Large Joint Cost Evaluation

Facility Costs

Costs are based on fabrication of tooling in three sizes with some common equipment. The prices include the following:

Design

Fabrication

Materials

	20 cm (8 in.)	30 cm (12 in.)	43 cm (17 in.)
Facility Cost			
Common Equipment Cost		$30,000	
Tooling Cost	$10,000	$20,000	$30,000

Development Costs

Costs are based on production of six joints, and include the following items:

Design and coordinate

Roll and weld stainless steel

Machine stainless steel

Machine aluminum

Swage

Material: stainless steel, aluminum

	20 cm (8 in.)	30 cm (12 in.)	43 cm (17 in.)
Development Cost	$3,000	$4,000	$6,000

Production Costs

Costs are per joint, based on production of 10 to 25 joints of each size. Detail steps are similar to those shown in development.

Design and Coordinate

	20 cm (8 in.)	30 cm (12 in.)	43 cm (17 in.)
Production Cost Per Joint	$360	$530	$920

Coextruded Large Joints

The problems encountered during heat treatment of the 6.4 cm (2.5 in.) joints were not resolved to the extent necessary for extrapolation of this production process to larger sizes with confidence. Therefore, no estimate is included for larger joints produced by this method. If the aluminum alloy was changed, or if joints for specific applications could be made using 2219 aluminum in a non heat-treated temper, then production of larger joints is feasible. Lowering of the aluminum strength requirement is a reasonable design alternative where propellant line wall thickness is determined by structural loading (since strength is a function of moment of inertia and modulus of elasticity) rather than by internal pressure alone, where only material strength is of prime importance.

Heavy presses are available at various locations within the United States that are capable of extruding very large diameters. Billets could be prepared for extrusion and shipped to the appropriate facility. The Air Force has a 4.45×10^8 N (1.00×10^8 lb) press at Curtis Wright in Buffalo, New York, which is easily capable of handling extrusions of the size necessary for the 43 cm (17 in.) diameter joints proposed.

JOINT TYPE SUITABILITY

One of the results of the program was an evaluation of the strengths and weaknesses of each type of joint as referenced to service requirements. This evaluation is based on information gained in selecting venders for each production type, on information developed during the course of each development and manufacture, on the results of the test program performed, and on the results of the Large Joint Evaluation.

The information has been put into matrix form for ease of interpretation. A joint preference was not made as the relative weight used for each evaluation parameter would be difficult to establish, and the selection of one joint type over another is often a function of intended service conditions.

TABLE 13. - JOINT TYPE SUITABILITY

		INERTIA WELDING	COEXTRUSION	EXPLOSIVE WELDING	SWAGED
1. Cost		Low cost after development, all sizes.	Higher cost after development, small size only.	Moderate cost after development, all sizes.	Low cost after development, all sizes.
2. Availability		Most available, many potential suppliers.	Few suppliers	Few suppliers	Single supplier
3. Test Item Consistency		Most consistent test evaluation results. Good process control.	Unknown - only 2 specimens evaluated.	Consistency involves craftsmanship and explosive characteristics, and both are variable.	Fair consistency in this evaluation; should be very consistent with more development.
4. Thermal Tolerance		Minimal effect, 373K to 78K (+212°F to -320 °F) cycles.	Minimal effect, 373K to 78K (+212°F to -320°F) cycles (one joint only.) Survives solutionizing and quench during manufacture.	Minimal effect, 373K to 78K (+212°F to -320°F) cycles.	Minimal effect, 373K to 78K (+212°F to -320°F) cycles.
5. Joint Length		May be short due to butt joint.	Scarf joint requires more length than butt joint.	Scarf joint requires more length than butt joint.	Multiple serrations require more length than other types.
6. Weight		May be same thickness as basic tube.	May be same thickness as basic tube.	May be same thickness as basic tube.	Must be heaviest due to necessary thicker section in serrated area.
7. Loads	A. Pressure Cycle	Near 100% of parent metal tolerance.	Not tested.	20% of parent metal tolerance.	40% of parent metal tolerance.
	B. Bending C. Torsion D. Vibration	These were not tested but will need evaluation prior to firm commitment to larger size use.			

TABLE 13. - JOINT TYPE SUITABILITY (Continued)

	INERTIA WELDING	COEXTRUSION	EXPLOSIVE WELDING	SWAGED
8. Leakage A. Vacuum	No helium leak at 1×10^{-5} torr internal (15 of 15 specimens)	No helium leak at 1×10^{-5} torr internal (2 of 2 specimens)	No helium leak at 1×10^{-5} torr internal (10 of 15 specimens)	No helium leak at 1×10^{-5} torr internal (10 of 15 specimens).
B. Pressure	Less than 3×10^{-10} scc/sec GHe at operating pressure (15 of 15 specimens)	Less than 3×10^{-10} scc/sec GHe at operating pressure (2 of 2 specimens)	Less than 3×10^{-10} scc/sec GHe at operating pressure (7 of 13 specimens).	All units leaked 1×10^{-5} scc/sec GHe minimum (off scale on MSLD).
9. Repairability	Not repairable.	Not repairable.	Not repairable.	Not repairable.
10. Replaceability	Replaceable by cutting out old joint and welding in new if adjacent heat treat requirements are not violated.	Replaceable by cutting out old joint and welding in new if adjacent heat treat requirements are not violated.	Replaceable by cutting out old joint and welding in new if adjacent heat treat requirements are not violated.	Replaceable by cutting out old joint and welding in new if adjacent heat treat requirements are not violated. Possibly swaged in field.
11. Corrosion Resistance (without protection)	Poor in $NaCl/H_2O$	Not tested	Fair Resistance to $NaCl/H_2O$ solution	Process allows use of anodized aluminum interface. Good Resistance
12. Growth Potential (See Large Joint Evaluation for Details)	Excellent potential for high quality large joints.	Good potential if non-heat treated 2219, or another alloy.	Good potential for high quality large joints.	Good potential for high quality large joints.
13. Failure Mode	11 of 11 6.4 cm (2.5 in.) specimens separated into two pieces when hydroburst.	2 of 2 6.4 cm (2.5 in.) specimens separated into two pieces when hydroburst.	7 of 8 6.4 cm (2.5 in.) specimens failed axially in and near the bond; 1 of 8 failed in hoop mode : when hydroburst.	8 of 9 6.4 cm (2.5 in.) specimens failed by axial slip and leakage; 1 of 9 failed in axial stainless shear: when hydroburst

APPENDIX A

COMMERCIAL APPLICATIONS OF METAL BELLOWS CORPORATION

SWAGED TRANSITION JOINTS

VEHICLE	APPLICATION	COMPANY
(LEM) LUNAR EXCURSION MODULE	GLYCOL & WATER COOLANT LINES	GRUMMAN
E-2A AIRCRAFT	FUEL SYSTEM LINES (JP-4)	GRUMMAN
AWACS, 727, 737 ACFT	AIR CONDITIONING/PNEUMATIC LINES	BOEING/SEATTLE
HELICOPTERS	PNEUMATIC LINES	BOEING/VERTOL
B-52 ACFT	FUEL SYSTEM LINES (JP-4)	BOEING/WICHITA
DC-9 ACFT	PNEUMATIC LINES	MCDONNELL DOUGLAS
ATLAS MISSILE	HIGH PRESSURE-PRESSURIZATION LINES	GENERAL DYNAMICS/ CONVAIR

APPENDIX B

Pressure/Stress Chart for 6.4 cm (2.5 in.) OD x 0.32 cm (0.13 in.) Wall Tube

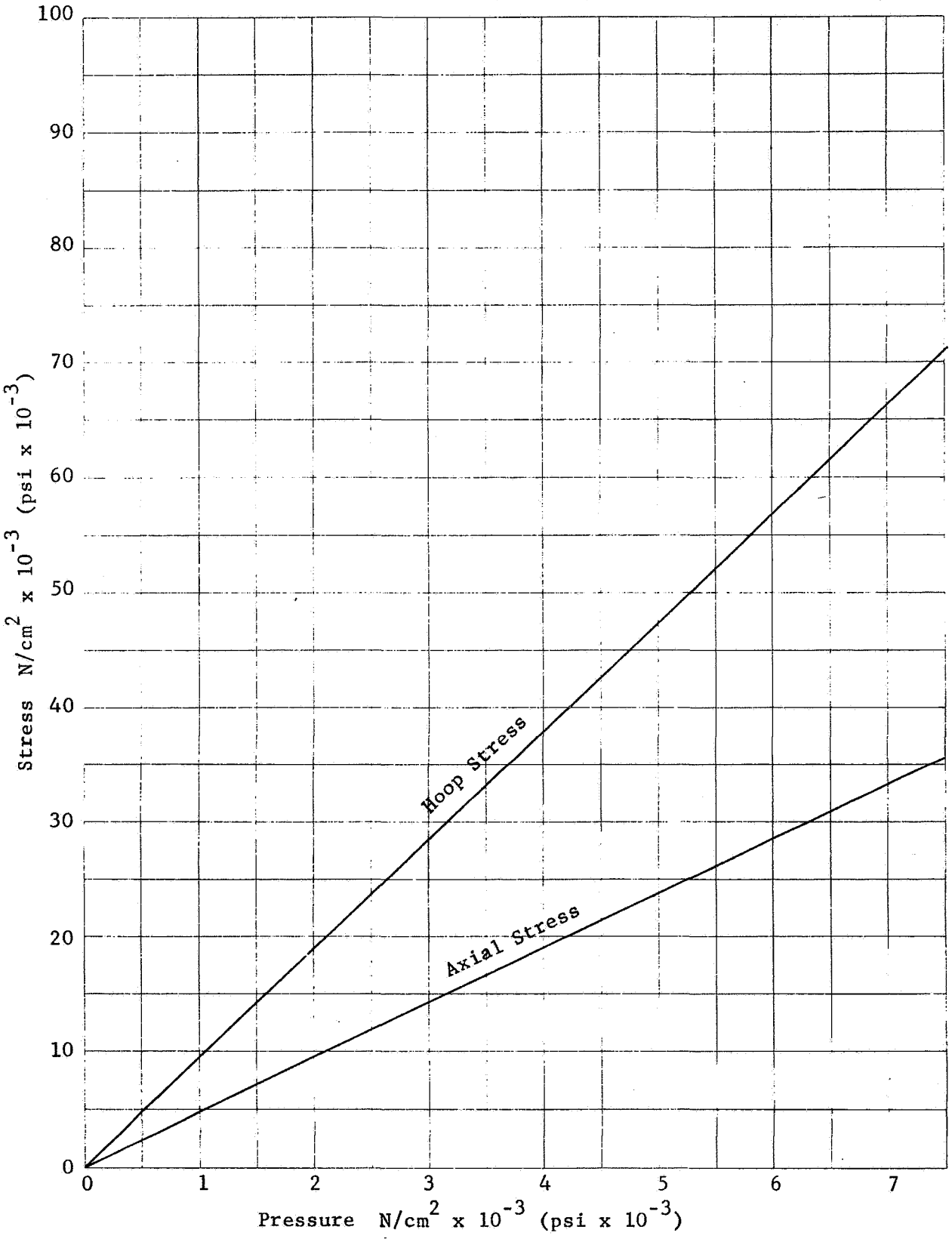

APPENDIX C PROPERTIES OF MATERIALS

	304L (annealed)	Silver Sterling (hard)	2219-T851 (extruded)	6061-T6 (extruded)
Modulus of Elasticity N/cm^2 (psi)	19×10^6 (28×10^6)	7.6×10^6 (11.0×10^6) (Pure)	7.3×10^6 (10.6×10^6)	6.9×10^6 (10.0×10^6)
Tensile Strength N/cm^2 (Ksi)	55,800 (81) (Plate)	48,000 (70)	40,000 (58)	26,000 (38)
Yield Strength N/cm^2 (Ksi)	22,700 (33) (Plate)	37,900 (55) (0.5%)	29,000 (42)	24,100 (35)
Elongation, %	60 (Plate)	6	6	8
Hardness, RB	79 (Sheet)	80	75 (T87)	58
EMF Potential, Volts	-3.5	+0.8	-1.7	-1.7
Thermal Coeff., per K (per ^oF)	17.3×10^{-6} (9.6×10^{-6})	19.6×10^{-6} (10.9×10^{-6}) (Pure)	22.3×10^{-6} (12.4×10^{-6})	23.4×10^{-6} (13.0×10^{-6})

APPENDIX D

TEST PROCEDURE

DISSIMILAR METALS
JOINT EVALUATION
NAS9-13570

1.0 Introduction

The objective of this test is to evaluate four types of dissimilar metals tubular transition joints.

The joints are designed to be leak-tight under operating conditions. The test matrices, 4.0 and 5.0, describe the series of tests which these joints will undergo. The test sequence will be as indicated.

2.0 Photographs

Photographs will be taken of each test setup, joints prior to testing, and typical joint failures.

3.0 Quality Control

The program manager is responsible for quality control on this program. Test agency and Air Force Quality are not required.

4.0 Test Matrix (Appears as Table 4)

Inertia Welded Joints
Coextrusion Bonded Joints
Explosive Welded Joints

5.0 Test Matrix (Appears as Table 5)

Swaged Joints

6.0 Specimen Log Book

Establish a log book listing each joint separately. The history of test activities is to be maintained in this book during the test program. Each entry is to specify date, activity, pertinent observations and data, and technician.

7.0 Receiving Inspection

Identify the 15 joints of each configuration using the typed stencil etching tool. Select the joints at random to number from 1 through 15 in each configuration. Identify as follows on the stainless steel and aluminum portions, beginning 1/4 inch from, and parallel to, the bond line.

NAS9-13570

X-Y

X = I.W. for Inertia Welded Joints
X = COX for Coextrusion Bonded Joints
X = EXP for Explosive Welded Joints
X = SWG for Swaged Joints
Y = 1 through 15, as appropriate

Measure the dimensions of each joint. Weigh all joints, photograph them, note any irregularities. Enter all data in the Specimen Log Book.

8.0 Penetrant Inspection

8.1 Perform penetrant inspection per standard procedure. Ultilize Uresco P151 penetrant. Record results in Specimen Log Book.

9.0 Ultrasonic Inspection

9.1 Prepare a reference joint by machining EDM flaws in joint no. 15. Flaws are to be in the plane of the bond line, approximately 5-10% of bond depth, and will serve as a known flaw size when compared to the other test joints ultrasonically.

9.2 Evaluate the program joint(s) using joint No. 15 as a reference. If all joints of a configuration pass helium leakage test at operating pressure, use joint No. 3 for ultrasonic. If one or more joints of a configuration fail helium leak test at operating pressure, submit the joint(s) with least helium leakage to ultrasonic. Record results in Specimen Log Book.

10.0 Leakage Test - One Atmosphere

10.1 Seal the joint ends using flat plate ends and Apiezon. Evacuate the joint using a CEC Mass Spectrometer Leak Detector.

10.2 "Wash" the joint with helium, and record the net leakage in the Specimen Log Book. If leakage is noted, assure that possible leak sources other than the bond have been eliminated by isolation or by flooding with nitrogen.

11.0 Specimen End Closure

11.1 Weld the prepared end closures on each joint, welding the aluminum end first, where applicable. Monitor the aluminum temperature at the bond line, and do not allow it to exceed 390K (250°F) during welding, using the chill ring, EPL 6200605.

12.0 Proof Pressure Test

12.1 Install the joint in the fixture per Figure D-1.

12.2 Place the test cell in a RED condition.

12.3 Increase nitrogen pressure in the joint to 690 ± 30 N/cm^2 (1000 ± 50 psig), then reduce to 340 ± 30 N/cm^2 (500 ± 50 psig) and perform a bubble leak check of fittings, and the joint.

NOTE

The proof pressure will be 90% of the apparent yield pressure for each joint style, as determined in Section 17.0.

12.4 Increase nitrogen pressure in the joint to 2200 ± 30 N/cm^2 (3200 ± 50 psig), and maintain for 5 minutes).

12.5 Vent the joint, inspect it for visible defects, and record all observations and data in the Specimen Log Book.

13.0 Leakage Test - Operating Pressure

13.1 Wrap a polyethylene bag around the joint and tape securely around the barrel section of the joint to prevent H_e background from affecting the leak check of the bonded area.

13.2 Install the joint in the fixture per Figure D-1.

13.3 Penetrate the poly bag and insert a CEC probe tip. Tape the probe/poly bag opening. Obtain leak rate vs. time for the standard leak. (Leak should continuously increase).

NOTE

The leakage test pressure will be 60% of the apparent yield pressure for each joint style, as determined in Section 17.0.

13.4 Increase helium pressure in the joint to 1450 ± 30 N/cm^2 (2100 ± 50 psig), and obtain leak rate vs time. If leakage is too excessive for CEC measurement, use water displacement method.

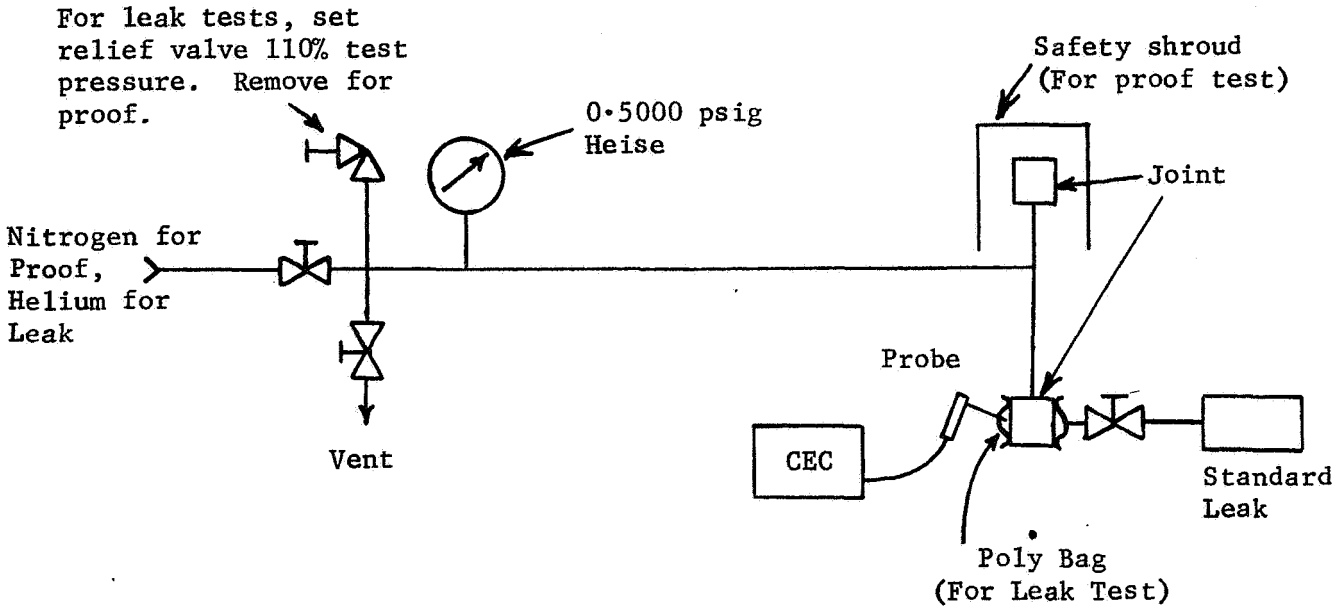

Figure D-1

Proof and Leak Test Fixture Schematic

13.5 Vent the joint and record all observations and data in the Specimen Log Book.

14.0 Thermal Cycle Test

NOTE

Perform thermal cycle on half of the joints of each style designated for this test simultaneously. This will alow evaluation prior to cycling the remainder.

14.1 Manifold the joints to a gage and supply, per Figure D-2, on joints with both ends welded. Pressurize to 31 ± 1.4 N/cm^2 (45 ± 2 psig) and lock off. Assure fittings are bubble tight. Maintain the pressure during subsequent cycling. Mechanical end fittings are not to be fitted to joints without welded aluminum end.

14.2 Place the joints in the 375K (215°F) ethylene glycol/water solution. After an immersion time of 5 minutes remove the joints from the solution and immediately place them in the LN_2.

14.3 After an immersion time of 5 minutes remove the joints from the LN_2 and immediately return them to the ethylene glycol water solution.

14.4 Repeat steps 14.2 and 14.3 for a total of 100 times.

14.5 After returning to ambient temperature, vent the pressure from the joint(s) and record all observations and data in the Specimen Log Book.

15.0 Pressure Cycle Test

NOTE

Perform pressure cycling on half of the joints of each style designated for this test simultaneously. This will allow evaluation prior to cycling the remainder.

15.1 Install the joints as shown in EPL 63001017B, EPL 6301136, and Figure D-3. Install mechanical end fittings on the aluminum ends.

15.2 Using Test Procedure H40519, cycle the joints from 430 ± 60 N/cm^2 (620 ± 100) psig to 2140 ± 70 N/cm^2 (3100 ± 100) psig at 5 cycles/second until all joints fail.

15.3 Record all observations and data in the Specimen Log Book.

16.0 Galvanic Corrosion Test

16.1 Prepare the joints per Figure D-4.

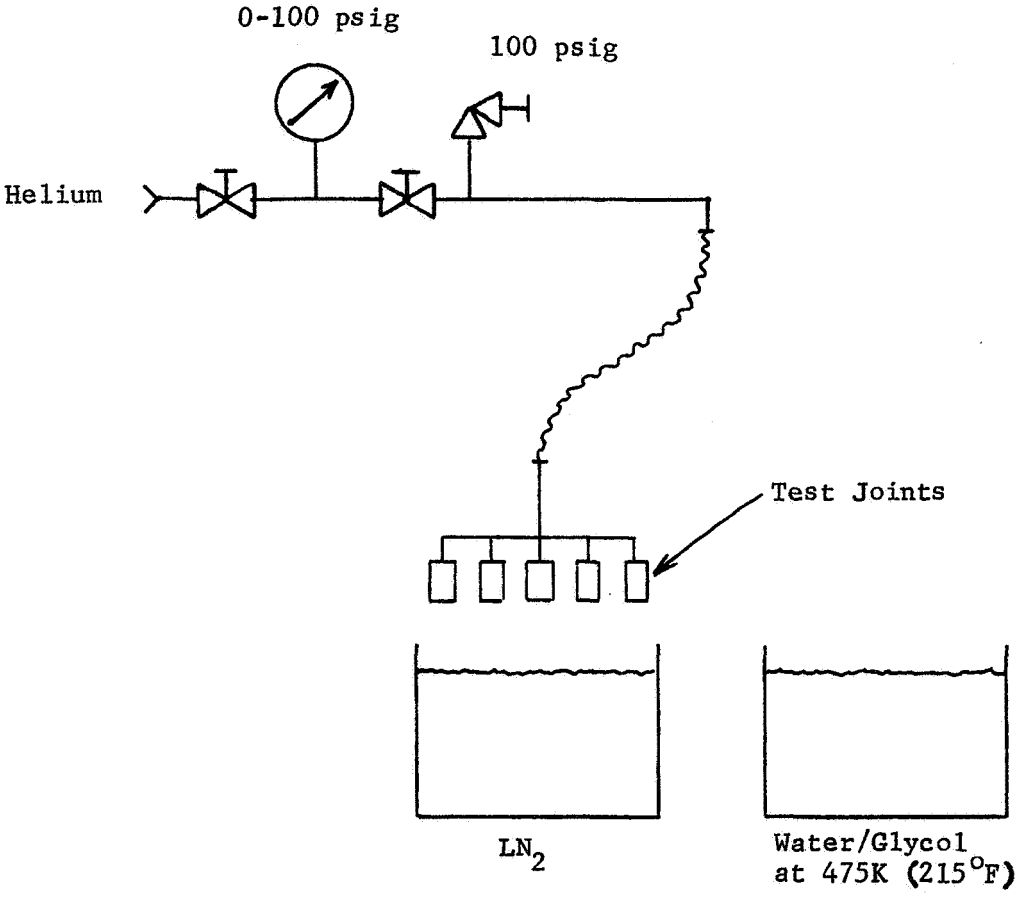

Figure D-2

Thermal Cycle Test Fixture Schematic

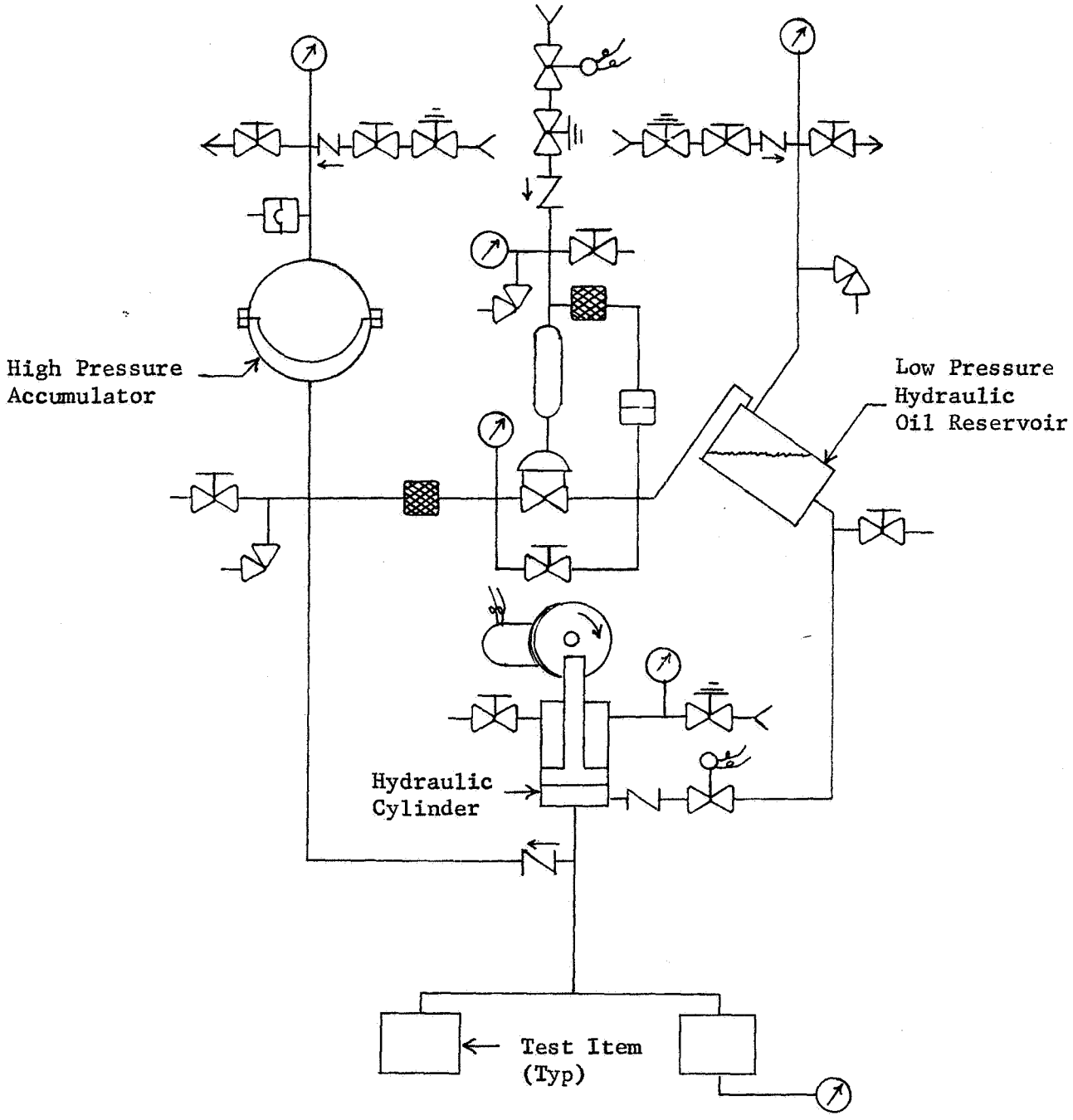

Figure D-3. -Pressure Cycle Test Fixture Schematic

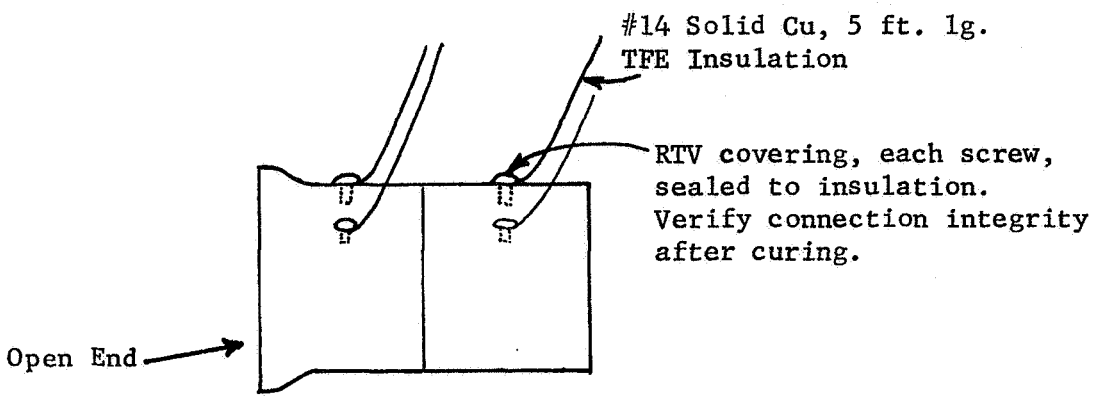

JOINT PREPARATION

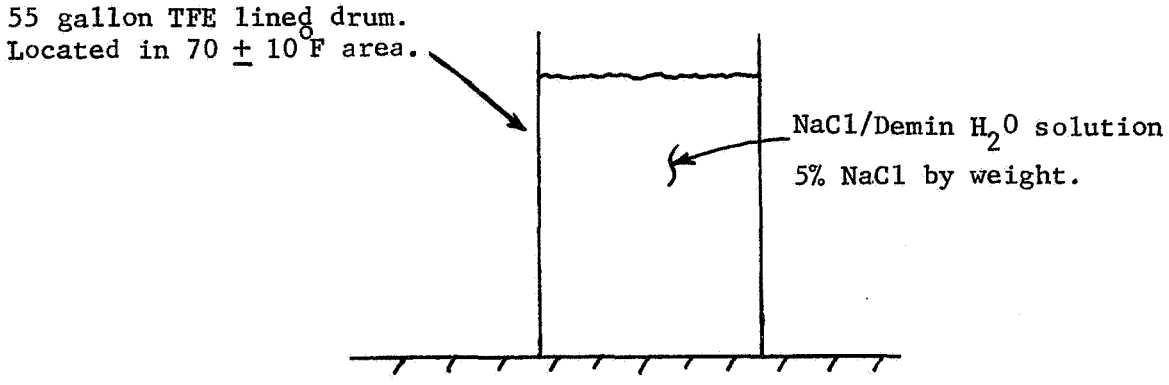

Test Bath

Figure D-4

Corrosion Test Fixture Schematic

16.2 Using the L&N 4735-1 Bridge, measure the electrical resistance of each joint across the bond, and across the common lead wires.

16.3 Submerge the joints in the NaCl bath.

16.4 Remove, clean, dry and repeat electrical resistance measurements of each joint at 2 week intervals, until data indicates the relative resistance of each type of joint to the solution, or until additional test time is not available. Exposure time will be four weeks minimum. Record all observations and data in the Specimen Log Book.

17.0 Yield Determination and Burst Test

17.1 Install joint per Figure D-5. Install mechanical end fittings on the aluminum ends. Thoroughly bleed-in the water system from the hydrostat pump and to the burette. Allow temperature to stabilize.

17.2 Place the test cell in RED condition.

17.3 Pressurize the joint to 700 $\pm$ 30 N/cm^2 (1000 $\pm$ 50 psig). Verify operation of the burette system. Maintain pressure for 5 minutes to verify absence of leakage in either system.

17.4 Increase the joint pressure at a slow rate, reading and recording burette level at 350 N/cm^2 (500 psi) increments. Continue until joint failure. Calculate the yield pressure and record all observations and data in the Specimen Log Book.

18.0 Burst Test

18.1 Install the joint per Figure D-5, except that the volumetric expansion system will not be used. Install mechanical end fittings on the aluminum ends, where required. Thoroughly bleed-in the water system from the hydrostat pump.

18.2 Place the test cell in RED condition.

18.3 Pressurize the joint to 690 $\pm$ 30 N/cm^2 (1000 $\pm$ 50 psig). Maintain pressure for 1 minute to verify absence of system leakage.

18.4 Increase the joint pressure at a slow rate until joint failure. Record all observations and data in the Specimen Log Book.

19.0 Metallographic Inspection

19.1 Prepare a specimen section of the bond area in one or more planes, as appropriate.

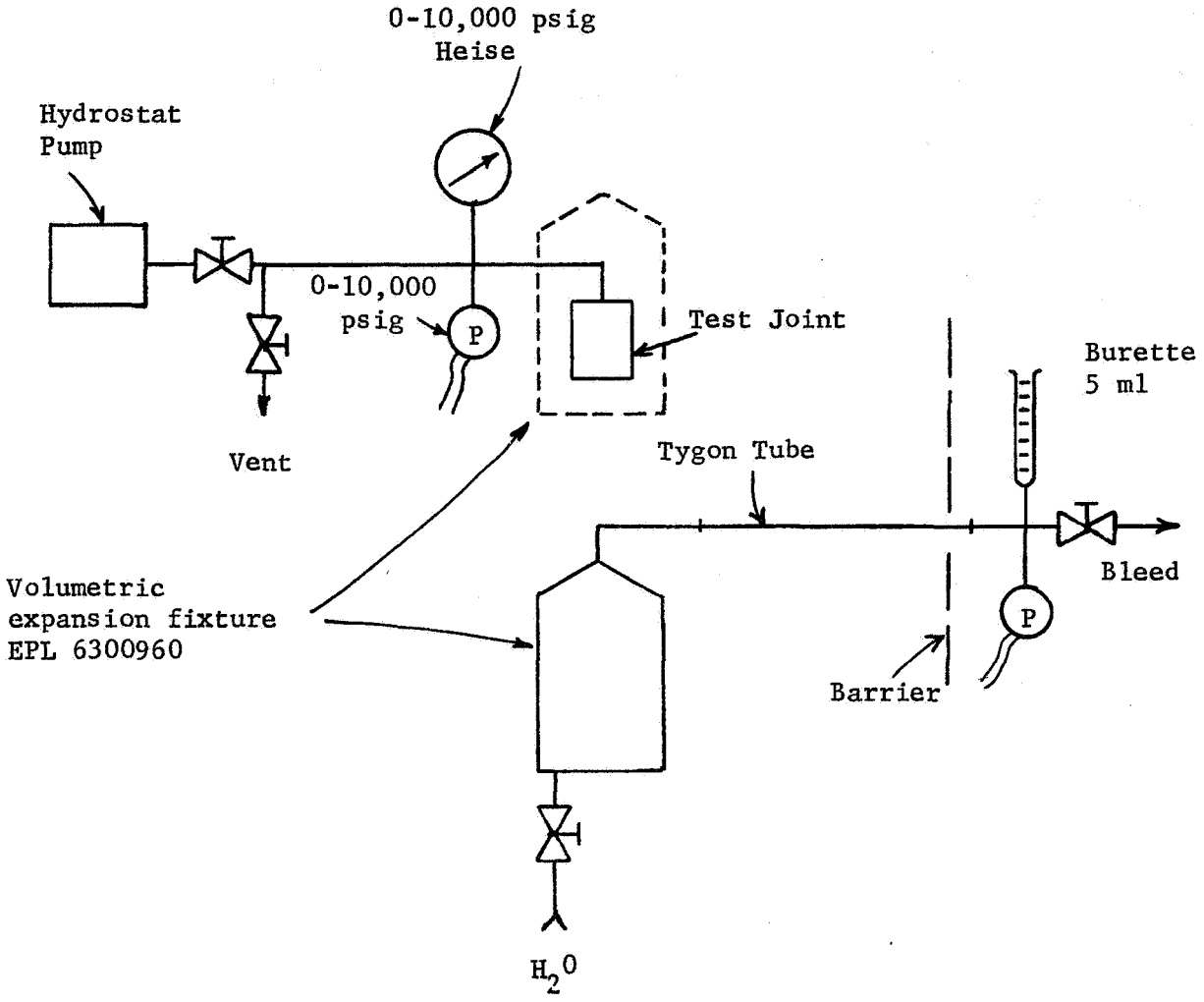

FIGURE D-5

Yield Determination and Burst Test
Fixture Schematic

19.2 Inspect the specimens at various magnification levels, observations to include but not be limited to physical geometry at bond, aluminum grain structure compaction and size, areas of possible aluminum alloy alteration, inclusions in the bond area, and uniformity of the bonded region. Prepare a photomicrograph of pertinent observations. Record observations and data in the Specimen Log Book.

20.0 Interface Constituent Identification

20.1 Prepare a 3.18 cm (1.25 in.) diameter specimen section of the bond area.

20.2 Submit to inspection by the ARL Electron Microprobe for determination of the various metallurgical constituents in or near the bond area. Record observations and data in the Specimen Log Book.